

Light in correlated disordered media

Kevin Vynck*

*Univ. Bordeaux,
Institut d'Optique Graduate School, CNRS,
Laboratoire Photonique Numérique et Nanosciences (LP2N),
F-33400 Talence,
France
Univ. Claude Bernard Lyon 1, CNRS,
Institut Lumière Matière (iLM),
F-69622 Villeurbanne,
France*

Romain Pierrat and Rémi Carminati†

*ESPCI Paris, PSL University, CNRS,
Institut Langevin, F-75005 Paris,
France*

Luis S. Froufe-Pérez and Frank Scheffold‡

*Physics Department,
University of Fribourg,
CH-1700 Fribourg,
Switzerland*

Riccardo Sapienza

*Imperial College London,
Blackett Laboratory,
London, SW7 2AZ,
United Kingdom*

Silvia Vignolini

*Department of Chemistry,
University of Cambridge,
Lensfield Road, Cambridge, CB2 1EW,
United Kingdom*

Juan José Sáenz

*Donostia International Physics Center (DIPC),
20018 Donostia-San Sebastian,
Spain
IKERBASQUE, Basque Foundation for Science, 48013 Bilbao,
Spain*

(Dated: June 29, 2021)

The optics of correlated disordered media is a fascinating research topic emerging at the interface between the physics of waves in complex media and nanophotonics. Inspired by photonic structures in nature and enabled by advances in nanofabrication processes, recent investigations have unveiled how the design of structural correlations down to the subwavelength scale could be exploited to control the scattering, transport and localization of light in matter. From optical transparency to superdiffusive light transport to photonic gaps, the optics of correlated disordered media challenges our physical intuition and offers new perspectives for applications. This article reviews the theoretical foundations, state-of-the-art experimental techniques and major achievements in the study of light interaction with correlated disorder, covering a wide range of systems – from short-range correlated photonic liquids, to Lévy glasses containing fractal heterogeneities, to hyperuniform disordered photonic materials. The mechanisms underlying light scattering and transport phenomena are elucidated on the basis of rigorous theoretical arguments. We overview the exciting ongoing research on mesoscopic phenomena, such as transport phase transitions and speckle statistics, and the current development of disorder engineering for applications such as light-energy management and visual appearance design. Special efforts are finally made to identify the main theoretical and experimental challenges to address in the near future.

CONTENTS

I. Introduction	2	V. Mesoscopic and near-field effects	31
II. Theory of multiple light scattering by correlated disordered media	5	A. Photonic gaps in disordered media	32
A. Theoretical framework	5	1. Definition and identification of photonic gaps in disordered media	32
1. Average field and self-energy	5	2. Competing viewpoints on the origin of photonic gaps	33
2. Refractive index and extinction mean free path	6	3. Reports of photonic gaps in the literature	34
3. Multiple-scattering expansion	6	B. Mesoscopic transport and light localization	35
4. Average intensity and four-point irreducible vertex	7	C. Near-field speckles on correlated materials	36
5. Radiative transfer limit and scattering mean free path	8	1. Intensity and field correlations in bulk speckle patterns	37
6. Transport mean free path and diffusion approximation	9	2. Near-field speckles on dielectrics	38
B. Media with fluctuating continuous permittivity	10	D. Local density of states fluctuations	38
1. First insights on structural correlations	10	VI. Photonics applications	40
2. Lorentz local fields	10	A. Light trapping in layered media	40
3. Average exciting field	11	B. Random lasing	41
4. Long-wavelength solutions for strongly fluctuating media: Bruggeman versus Maxwell-Garnett	12	C. Visual appearance	42
5. Expressions for the scattering and transport mean free paths from the average intensity	13	1. Photonic structures in nature	42
C. Particulate media	13	2. Synthetic structural colors	44
1. Expansion for identical scatterers	13	VII. Summary and perspectives	45
2. Extinction mean free path and effective medium theories	14	A. Near-field-mediated mesoscopic transport in 3D high-index correlated media	45
3. Scattering and transport mean free paths for resonant scatterers	16	B. Mesoscopic optics in fractal and long-range correlated media	46
D. Summary and further remarks	16	C. Towards novel applications	46
III. Structural properties of correlated disordered media	17	Acknowledgments	47
A. Continuous permittivity versus particulate models in practice	17	A. Green functions in Fourier space	47
B. Fluctuation-correlation relation	18	1. Dyadic Green tensor	47
C. Classes of correlated disordered media	18	2. Dressed Green tensor	47
1. Short-range correlated disordered structures	18	B. Derivation of Eq. (26)	48
2. Polycrystalline structures	19	C. Configurational average for statistically homogeneous systems	48
3. Imperfect ordered structures	20	1. Particle correlation functions	48
4. Disordered hyperuniform structures	21	2. Fluctuations of the number of particles in a volume	49
5. Disordered fractal structures	21	D. Local density of states and quasinormal modes	49
D. Numerical construction of correlated disordered media	21	References	50
E. Fabrication of correlated disordered media	22		
1. Jammed colloidal packing	23		
2. Thermodynamically-driven self-assembly	24		
3. Optical and e-beam lithography	25		
F. Measuring structural correlations	25		
IV. Modified transport parameters	26		
A. Light scattering and transport in colloids and photonic materials	26		
1. Impact of short-range correlations: first insights	26		
2. Enhanced optical transparency	27		
3. Tunable light transport in photonic liquids	28		
4. Resonant effects in photonic glasses	28		
5. Modified diffusion in imperfect photonic crystals	29		
B. Anomalous transport in media with large-scale heterogeneity	29		
1. Radiative transfer with non-exponential extinction	29		
2. From normal to super-diffusion	31		

* kevin.vynck@univ-lyon1.fr

† remi.carminati@espci.psl.eu

‡ frank.scheffold@unifr.ch

I. INTRODUCTION

Correlated disordered media are non-crystalline heterogeneous materials exhibiting pronounced spatial correlations in their structure and morphology. The topic has bloomed in the context of optics and photonics, gradually unveiling the considerable impact of structural correlations on the scattering, transport, and localization of light in matter. These findings let us envision novel types of materials with unprecedented optical functionalities and raise a number of challenges in theoretical modelling, material fabrication and optical spectroscopy. This article aims to provide an overview of this emerging research field, starting from the basic principles of light interaction with heterogeneous media to the most recent and still actively debated topics.

The scattering of light by heterogeneous media has a long and venerable history, which started more than a century ago with pioneering studies on the refractive index of fluids of atoms or molecules (Lorentz, 1880;

Lorenz, 1880), the electromagnetic scattering by particles (Maxwell Garnett, 1904; Mie, 1908; Rayleigh, 1899), and the phenomenon of critical opalescence in binary fluid mixtures (Einstein, 1910; Ornstein and Zernike, 1914; Smoluchowski, 1908). The foundations of a rigorous theoretical treatment of multiple light scattering were built in the 1930s (Kirkwood, 1936; Yvon, 1937) to take its full dimension a few decades later with various important contributions (Foldy, 1945; Keller, 1964; Lax, 1951, 1952; Twersky, 1964). These early works already pointed out the key role played by structural correlations on light scattering, a nice illustration of this being the transparency of the cornea resulting from short-range correlations in ensembles of discrete scatterers (Benedek, 1971; Hart and Farrell, 1969; Maurice, 1957; Twersky, 1975).

A new branch of research exploiting light waves to study mesoscopic phenomena in disordered systems emerged in the 1980s, prompted by experimental demonstrations of weak localization (Tsang and Ishimaru, 1984; Van Albada and Lagendijk, 1985; Wolf and Maret, 1985) and theoretical predictions for the three-dimensional Anderson localization of light (Anderson, 1985; John, 1984). The advent of photonic crystals (John, 1987; Yablonovitch, 1987), wherein photonic band gaps are created by a periodic modulation of the refractive index in two or three dimensions, gave additional momentum to research by greatly stimulating the development of nanofabrication techniques for high-index dielectrics (López, 2003). The following decade witnessed a flourishing of studies on periodic dielectric nanostructures (Joannopoulos *et al.*, 2011) and disordered media made of resonant (Mie) scatterers (van Albada *et al.*, 1991; Busch and Soukoulis, 1995; Fraden and Maret, 1990; Lagendijk and Van Tiggelen, 1996; Saulnier *et al.*, 1990) from two overlapping communities (Soukoulis, 2012).

The importance of short-range structural correlations on light transport in disordered systems (Fraden and Maret, 1990; Saulnier *et al.*, 1990) and of random imperfections on light propagation in periodic systems (Asatryan *et al.*, 1999; Sigalas *et al.*, 1996; Vlasov *et al.*, 2000) was recognized quite early. Research on correlated disordered media in optics however really took off in the mid-2000s with experimental studies showing that disorder could be *engineered* to harness light transport (Barthelemy *et al.*, 2008; García *et al.*, 2007; Rojas-Ochoa *et al.*, 2004). The surprising observation of photonic gaps in disordered structures with short-range correlations (Edagawa *et al.*, 2008; Florescu *et al.*, 2009; Liew *et al.*, 2011), reports of mesoscopic phenomena in imperfect photonic crystals (Conti and Fratalocchi, 2008; Garcia *et al.*, 2012; Toninelli *et al.*, 2008) and the prospects of new generations of photonic devices like random lasers (Gottardo *et al.*, 2008), thin-film solar cells (Martins *et al.*, 2013; Oskooi *et al.*, 2012;

Vynck *et al.*, 2012) and integrated spectrometers (Redding *et al.*, 2013), greatly contributed to the emergence of the research field. Figure 1 illustrates some of the key achievements and applications of correlated disordered media in optics and photonics.

Important efforts have been made in recent years to elucidate the role of structural correlations on the emergence of photonic gaps and on Anderson localization in two-dimensional (Conley *et al.*, 2014; Florescu *et al.*, 2009; Froufe-Pérez *et al.*, 2016, 2017) and three-dimensional disordered systems (Aubry *et al.*, 2020; Haberko *et al.*, 2020; Klatt *et al.*, 2019; Ricouvier *et al.*, 2019). Near-field interaction and light polarization considerably complexify theoretical modelling (Escalante and Skipetrov, 2017; Vynck *et al.*, 2016), explaining the widespread use of full-wave numerical methods to address this issue, alongside phenomenological models (Naraghi *et al.*, 2015). The so-called hyperuniform disordered structures (Torquato and Stillinger, 2003) have received considerable attention in this context, leading to a wider exploration of their optical properties (Bigourdan *et al.*, 2019; Leseur *et al.*, 2016; Sheremet *et al.*, 2020) and advances on top-down and bottom-up fabrication techniques (Maimouni *et al.*, 2020; Muller *et al.*, 2017; Ricouvier *et al.*, 2017; Weijs *et al.*, 2015).

In a different context, the interplay of order and disorder appeared quite early as an essential ingredient to explain the colored appearance of certain plants and animals (Kinoshita and Yoshioka, 2005). Research on natural photonic structures continued at a fast pace with important findings, such as the ubiquity of correlated disorder in animals exhibiting vivid diffuse blue colors (Johansen *et al.*, 2017; Magkiriadou *et al.*, 2012; Moyroud *et al.*, 2017; Noh *et al.*, 2010; Yin *et al.*, 2012), the use of short-range correlations to reduce light reflectance (Deparis *et al.*, 2009; Siddique *et al.*, 2015) or structural anisotropy to enhance whiteness (Burresi *et al.*, 2014). Efforts are nowadays made to realize artificial materials exhibiting correlated disorder to create materials with versatile visual appearances (Chan *et al.*, 2019; Forster *et al.*, 2010; Goerlitzer *et al.*, 2018; Jacucci *et al.*, 2020a; Park *et al.*, 2014; Schertel *et al.*, 2019a; Shang *et al.*, 2018; Takeoka, 2012).

In this review, we will introduce the key concepts and techniques in the study of light in correlated disordered media, assess the current state of knowledge on the topic, and define the main challenges that lie ahead of us. Compared to existing reviews on correlated disorder and disorder engineering in optics and photonics (Shi *et al.*, 2013a; Wang and Zhao, 2020; Wiersma, 2013; Yu *et al.*, 2020), we provide here a broader view on the field and sufficient technical details for the readers who wish dive into it, be it from the theoretical or experimental side. This article is also an attempt to bridge the gap between different research fields for which excellent textbooks already exist, namely on ran-

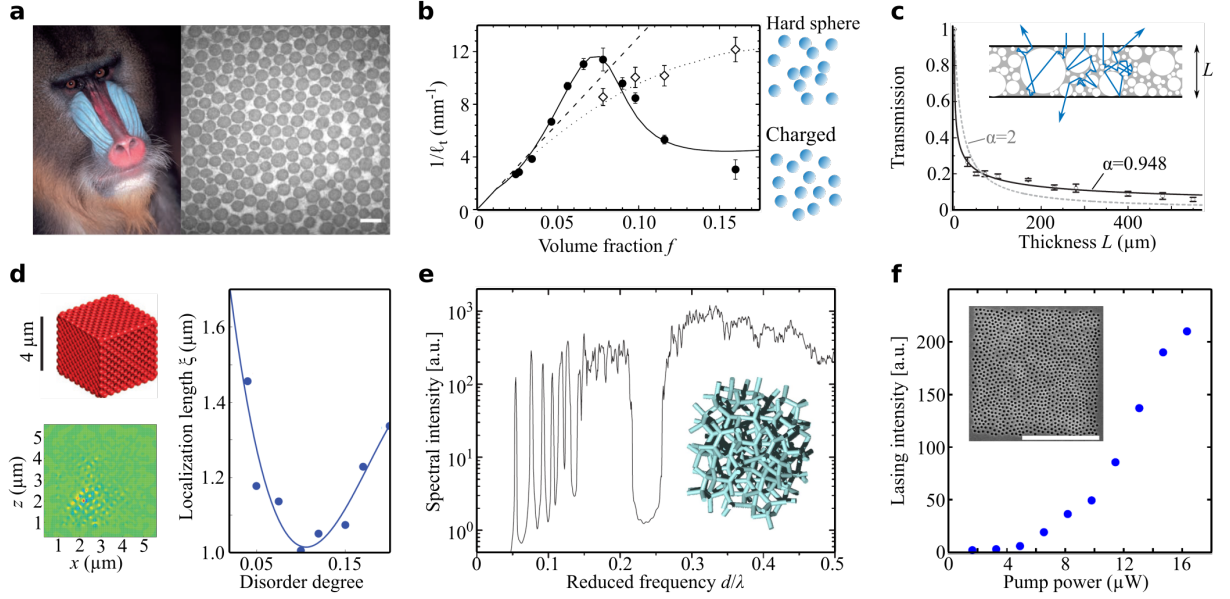


FIG. 1 Early achievements and applications of correlated disordered media in optics and photonics. (a) Male mandrill (*Mandrillus sphinx*) blue facial skin and cross-section of its dermis in the structurally colored area (blue) that reveals parallel collagen fibres organised in a correlated array. Adapted with permission from (Prum and Torres, 2004). (b) Modified light transport (described by the inverse transport mean free path ℓ_t) by engineering short-range structural correlations thanks to Coulomb repulsion between charged particles (filled symbols and solid line). Hard sphere systems (open symbols and dotted line) exhibit weaker correlations. The dashed line is a model neglecting completely structural correlations. Adapted with permission from (Rojas-Ochoa *et al.*, 2004). (c) Anomalous light transport in Lévy glasses. A fractal heterogeneity is engineered by adding transparent spheres with sizes varying over orders of magnitude in a host matrix. Transport can be modelled by a truncated Lévy walk. On finite size samples, this leads to an anomalous scaling of the total transmittance $T \sim L^{\alpha/2}$ (experiments shown as symbols, lines are fits). Adapted with permission from (Barthelemy *et al.*, 2008). (d) Light localization in randomly perturbed inverse opal photonic crystals (upper left inset). Spatially-localized modes are observed near the photonic band edge (lower left inset). Their typical spatial extent (the localization length ξ) depends strongly on the degree of disorder. Adapted with permission from (Conti and Fratallocchi, 2008). (e) Existence of photonic gaps in amorphous photonic materials. Simulations of the spectral density - a quantity proportional to the density of states - in a connected amorphous diamond structure exhibiting short-range order shows a photonic gap near $d/\lambda \simeq 0.23$, where d is the average bond length. Adapted with permission from (Edagawa *et al.*, 2008). (f) Random lasing in two-dimensional photonic structures with correlated disorder. Short-range correlations are shown to increase the lasing efficiency at certain frequencies due to enhanced optical confinement. Adapted with permission from (Noh *et al.*, 2011).

dom heterogeneous materials (Torquato, 2013), multiple light scattering in complex media (Akkermans and Montambaux, 2007; Carminati and Schotland, 2021; Sheng, 2006; Tsang and Kong, 2001) and periodic photonic crystals (Joannopoulos *et al.*, 2011), and which may serve as complementary literature. We focus on two and three-dimensional dielectric materials, intentionally leaving aside one-dimensional dielectric structures (i.e., layered media) (Izrailev *et al.*, 2012) and metallic nanostructures (Shalaev, 2002). We also do not discuss the very fertile fields of metamaterials and metasurfaces, which show some apparent similarities with the present topic in terms of theoretical models and concepts (Mackay and Lakhtakia, 2015), yet with different scopes of application.

The remainder of the article is structured as follows. Section II introduces the basic concepts and important quantities for light scattering and transport in correlated disordered media, namely the extinction, scattering and

transport mean free paths. We derive mathematically explicit results, as a function of the degree of structural correlations, from rigorous multiple scattering theories for both continuous permittivity media and discrete particulate media, emphasizing conceptual similarities between these two viewpoints. Section III addresses the statistical description of the structural properties of correlated disordered media. Different classes of correlated systems are discussed, together with numerical and experimental techniques to realize and characterize them. Section IV reviews experimental and theoretical studies wherein structural correlations yield dramatic variations of light transport parameters, including enhanced scattering in colloidal suspensions of particles, optical transparency in hyperuniform systems and anomalous diffusion in media with large-scale (fractal) heterogeneities. Section V is concerned with emergent mesoscopic phenomena relying on an interplay of order and disorder,

most of which are not yet fully understood. This includes the formation of photonic gaps and localized states in disordered systems, and the statistical properties of near-field speckles and local density of states. Section VI describes various applications of correlated disordered media in optics and photonics, namely light management in thin films, random lasing and visual appearance design. Section VII concludes the review with a discussion on the open challenges in the field.

II. THEORY OF MULTIPLE LIGHT SCATTERING BY CORRELATED DISORDERED MEDIA

The theoretical study of light propagation in disordered media is a notoriously difficult problem that has experienced many developments for more than a century. In this section, we introduce the basic concepts of multiple light scattering by heterogeneities with the aim to give a solid theoretical ground to the role of structural correlations on light scattering and transport.

In Sec. II.A, we first focus on the “constitutive” linear relation between the average electric field and the average polarization density in disordered media, which allows us to introduce the notions of effective permittivity tensor and extinction mean free path. Many of the derived results have been used in the study of the effective optical response and homogenization processes of periodic and amorphous dielectrics (Mackay and Lakhtakia, 2015; Van Kranendonk and Sipe, 1977). We then derive the main equations that govern the propagation of the average intensity and introduce the scattering and transport mean free paths, two experimentally measurable quantities that form the backbone of radiative transfer theory (Chandrasekhar, 1960).

Within this unique theoretical framework, we then address the light scattering problem for systems described by either a continuous permittivity that fluctuates in space [Sec. II.B] or discrete particles correlated in their position [Sec. II.C], see Fig. 2. We derive analytical expressions for the characteristic lengths, allowing us to show, on rigorous grounds, how structural correlations impact scattering and transport.

We summarize the main outcomes of the theoretical analysis in Sec. II.D, for the readers who wish to skip mathematical details.

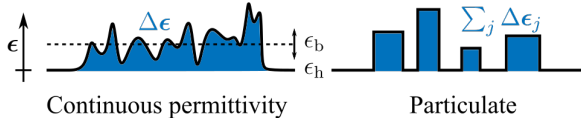


FIG. 2 Disordered media may be described by a continuous permittivity model (left) in the most general case, or by a particulate model (right) in the case where the permittivity variation is compact.

A. Theoretical framework

1. Average field and self-energy

We consider a region of space filled with a non-magnetic, isotropic material (relative permeability, $\mu(\mathbf{r}) = 1$), described by a scalar spatially-varying relative permittivity $\epsilon(\mathbf{r})$ in a uniform *host* medium with relative permittivity ϵ_h . Throughout this review, we consider harmonic fields at frequency ω with the $e^{-i\omega t}$ convention and drop the explicit dependence in the permittivities, fields, etc. for clarity. In absence of charge and currents, the electric field $\mathbf{E}(\mathbf{r})$ at frequency ω satisfies a vector wave propagation equation

$$\nabla \times \nabla \times \mathbf{E}(\mathbf{r}) - k_0^2 \epsilon_h \mathbf{E}(\mathbf{r}) = k_0^2 \mathbf{P}(\mathbf{r}) / \epsilon_0, \quad (1)$$

where $k_0 = \omega/c$ is the vacuum wave number and $\mathbf{P}(\mathbf{r}) = \epsilon_0(\epsilon(\mathbf{r}) - \epsilon_h)\mathbf{E}(\mathbf{r})$ is the polarization density (electric dipole moment per unit volume). The permittivity variation $\Delta\epsilon(\mathbf{r}) = \epsilon(\mathbf{r}) - \epsilon_h$ readily appears as the source of light scattering in the system.

Upon statistical average over disorder realizations, denoted here as $\langle \dots \rangle$, Eq. (1) describes the propagation of the average field $\langle \mathbf{E}(\mathbf{r}) \rangle$ with the average polarization density $\langle \mathbf{P}(\mathbf{r}) \rangle$ as a source term. The difficulty to solve this general problem essentially comes from the fact that the fluctuations of the electric field and of the permittivity are not statistically-independent, i.e., $\langle \Delta\epsilon(\mathbf{r})\mathbf{E}(\mathbf{r}) \rangle \neq \langle \Delta\epsilon(\mathbf{r}) \rangle \langle \mathbf{E}(\mathbf{r}) \rangle$. The standard approach to solve this problem is to make a preliminary ansatz about the effective permittivity of the medium, thereby establishing a constitutive linear relation between the average field and the average polarization density, and then perturbatively calculate correlations in orders the statistical cumulants of the permittivity spatial fluctuations around it.

Let us then rewrite Eq. (1) as (Ryzhov *et al.*, 1965)

$$\nabla \times \nabla \times \mathbf{E}(\mathbf{r}) - k_0^2 \epsilon_b \mathbf{E}(\mathbf{r}) = \mathcal{X}(\mathbf{r})\mathbf{E}(\mathbf{r}), \quad (2)$$

where ϵ_b is a constant, auxiliary, background permittivity that can differ from the permittivity of the host medium ϵ_h , and \mathcal{X} is an effective scattering potential (or electric susceptibility) defined as

$$\mathcal{X}(\mathbf{r}) = k_0^2 (\epsilon(\mathbf{r}) - \epsilon_b) \mathbf{1}, \quad (3)$$

with $\mathbf{1}$ the unit tensor. The average field $\langle \mathbf{E} \rangle$ then fulfills the vector wave equation

$$\nabla \times \nabla \times \langle \mathbf{E} \rangle(\mathbf{r}) - k_b^2 \langle \mathbf{E} \rangle(\mathbf{r}) = \langle \mathcal{X}(\mathbf{r})\mathbf{E}(\mathbf{r}) \rangle, \quad (4)$$

where $k_b^2 = k_0^2 \epsilon_b$. We now introduce the susceptibility tensor Σ , usually called “self-energy” or “mass operator”, following the language of many-body scattering

theory (Dyson, 1949a), as

$$\langle \mathcal{X}(\mathbf{r}) \mathbf{E}(\mathbf{r}) \rangle \equiv \int \Sigma(\mathbf{r}, \mathbf{r}') \langle \mathbf{E} \rangle(\mathbf{r}') d\mathbf{r}', \quad (5)$$

with

$$\Sigma(\mathbf{r}, \mathbf{r}') = k_0^2 (\epsilon_{\text{eff}}(\mathbf{r}, \mathbf{r}') - \epsilon_b \mathbf{1} \delta(\mathbf{r} - \mathbf{r}')). \quad (6)$$

The self-energy depends on the non-local effective permittivity tensor that results from multiple scattering in the disordered medium. Hereafter, we assume that the system has a proper thermodynamic limit in which it becomes spatially homogeneous and translationally invariant on average, i.e. $\epsilon_{\text{eff}}(\mathbf{r}, \mathbf{r}') = \epsilon_{\text{eff}}(\mathbf{r} - \mathbf{r}')$. Aspects related to the effective medium description in large but finite systems and the deep connection with the Ewald-Oseen extinction theorem (Hynne and Bullough, 1987; Van Kranendonk and Sipe, 1977) will thus not be discussed here. In Fourier space, the self-energy is given by

$$\Sigma(\mathbf{k}, \mathbf{k}') = \iint e^{-i\mathbf{k} \cdot \mathbf{r}} \Sigma(\mathbf{r} - \mathbf{r}') e^{i\mathbf{k}' \cdot \mathbf{r}'} d\mathbf{r} d\mathbf{r}' \quad (7)$$

$$= (2\pi)^3 \Sigma(\mathbf{k}) \delta(\mathbf{k} - \mathbf{k}'). \quad (8)$$

It is further convenient to decompose $\Sigma(\mathbf{k})$ into its transverse (\perp) and longitudinal (\parallel) components as

$$\Sigma(\mathbf{k}) = \Sigma_{\perp}(\mathbf{k}) (\mathbf{1} - \mathbf{u} \otimes \mathbf{u}) + \Sigma_{\parallel}(\mathbf{k}) \mathbf{u} \otimes \mathbf{u}, \quad (9)$$

where $\mathbf{u} = \mathbf{k}/|\mathbf{k}|$ and $\mathbf{u} \otimes \mathbf{u}$ is the outer tensor product between \mathbf{u} and itself. Defining \mathbf{e} as the unit polarization vector with $\mathbf{e} \cdot \mathbf{u} = 0$, the transverse component of the self-energy reads

$$\Sigma_{\perp}(\mathbf{k}) = \mathbf{e} \cdot \Sigma(\mathbf{k}) \mathbf{e}. \quad (10)$$

2. Refractive index and extinction mean free path

To understand the role played by the self-energy in wave propagation and scattering, we can seek for transversal solutions of the vector wave propagation equation of the form

$$\langle \mathbf{E} \rangle(\mathbf{r}) = E_0 \mathbf{e} e^{i\mathbf{k}_{\text{eff}} \cdot \mathbf{r}}, \quad (11)$$

with $\mathbf{k}_{\text{eff}} = k_0 n_{\text{eff}} \mathbf{u}$ the wavevector describing propagation in a homogeneous medium with effective refractive index n_{eff} . Assuming a statistically isotropic system, substituting Eq. (11) in Eq. (4) with Eq. (5) and following the decomposition in Eq. (9) with Eq. (10) leads to a transcendental equation for the effective wave number

$$\begin{aligned} k_{\text{eff}} &= k_0 n_{\text{eff}} = \sqrt{k_b^2 + \Sigma_{\perp}(k_{\text{eff}})}, \\ &\equiv k_r + i \frac{1}{2\ell_e}. \end{aligned} \quad (12)$$

The real part of the effective index $\text{Re}[n_{\text{eff}}] = k_r/k_0$ describes the phase velocity of the average field (often called “coherent” or “ballistic” component) in the material, while the imaginary part $\text{Im}[n_{\text{eff}}] = (2k_0\ell_e)^{-1}$ describes its exponential decay with propagation due to absorption and/or scattering on a characteristic length scale that is the extinction mean free path, ℓ_e . In the weak extinction regime, i.e. $\text{Im}\Sigma_{\perp}(k_{\text{eff}}) \ll k_b^2 + \text{Re}\Sigma_{\perp}(k_{\text{eff}})$ and $k_r\ell_e \gg 1$, Eq. (12) leads to

$$\frac{1}{\ell_e} \simeq \frac{\text{Im}\Sigma_{\perp}(k_r)}{k_r}. \quad (13)$$

In non-absorbing dielectric materials, extinction is purely driven by scattering ($\ell_e = \ell_s$ with ℓ_s the scattering mean free path). The problem of light scattering by correlated disordered media can therefore be apprehended by determining the self-energy of the system.

3. Multiple-scattering expansion

A key ingredient in solving multiple light scattering problems is the electromagnetic dyadic Green tensor $\mathbf{G}_b(\mathbf{r}, \mathbf{r}')$, that is the solution of Eq. (2) describing the electric field produced at a point \mathbf{r} by a radiating point electric dipole at \mathbf{r}' in a homogenous medium with permittivity ϵ_b , and is given by

$$\begin{aligned} \mathbf{G}_b(\mathbf{r}, \mathbf{r}') &= -\frac{1}{3k_b^2} \delta(\mathbf{r} - \mathbf{r}') \\ &+ \lim_{a \rightarrow 0} \Theta(|\mathbf{r} - \mathbf{r}'| - a) \left\{ \left(\mathbf{1} + \frac{\nabla \otimes \nabla}{k_b^2} \right) \frac{e^{ik_b|\mathbf{r} - \mathbf{r}'|}}{4\pi|\mathbf{r} - \mathbf{r}'|} \right\}, \end{aligned} \quad (14)$$

where Θ is the Heaviside step function. The Dirac delta function in the right hand side of Eq. (14) gives the well-known singularity in the source region while the second term corresponds to the non-singular, *principal value* of the Green function, $\text{PV}\{\mathbf{G}_0\}$ (Van Bladel and Van Bladel, 1991; Yaghjian, 1980). The Green function enables writing a general solution of the wave equation as a Lippmann-Schwinger equation

$$\mathbf{E}(\mathbf{r}) = \mathbf{E}_b(\mathbf{r}) + \int \mathbf{G}_b(\mathbf{r}, \mathbf{r}') \mathcal{X}(\mathbf{r}') \mathbf{E}(\mathbf{r}') d\mathbf{r}', \quad (15)$$

where $\mathbf{E}_b(\mathbf{r})$ is the solution of the homogeneous problem, which can be seen as a background (incident) field with wave number k_b . Equation (15) can conveniently be written in operator form as

$$\mathbf{E} = \mathbf{E}_b + \mathcal{G}_b \mathcal{X} \mathbf{E}, \quad (16)$$

where \mathcal{G}_b is an integral operator. Equation (16) can be formally solved by successive iterations, leading to a multiple-scattering expansion on orders of \mathcal{X} (i.e., single scattering, double scattering, etc.). Eventually,

all multiple-scattering orders are taken into account by defining a transition operator \mathcal{T} relating the polarization induced in the medium to the *background* field, as (Mesiah, 1999)

$$\mathbf{E} = \mathbf{E}_b + \mathcal{G}_b \mathcal{T} \mathbf{E}_b, \quad (17)$$

with

$$\begin{aligned} \mathcal{T} &= \mathcal{X} + \mathcal{X} \mathcal{G}_b \mathcal{X} + \dots \\ &= [\mathbf{1} - \mathcal{X} \mathcal{G}_b]^{-1} \mathcal{X}. \end{aligned} \quad (18)$$

Keeping only the lowest order of the expansion, $\mathcal{T} = \mathcal{X}$, is known as the Born approximation, wherein one neglects the contribution of the field scattered by neighboring permittivity fluctuations, resulting in a local, single-scattering process. In the general case, multiple scattering occurs leading to a transition operator \mathcal{T} that is spatially non-local, $\mathcal{T} \mathbf{E}_b \equiv \int \mathbf{T}(\mathbf{r}, \mathbf{r}') \mathbf{E}_b(\mathbf{r}') d\mathbf{r}'$.

Upon statistical average of Eqs. (16) and (17), and having Eq. (5), we finally reach a general expression for the average field as a function of the self-energy operator Σ , known as the Dyson equation (Dyson, 1949a,b; Rytov *et al.*, 1989; Yvon, 1937)

$$\langle \mathbf{E} \rangle = \mathbf{E}_b + \mathcal{G}_b \Sigma \langle \mathbf{E} \rangle, \quad (19)$$

with

$$\Sigma = \langle \mathcal{T} \rangle [\mathbf{1} + \mathcal{G}_b \langle \mathcal{T} \rangle]^{-1}. \quad (20)$$

In summary, the disordered medium is described as a permittivity that fluctuates around an auxiliary background permittivity ϵ_b via the scattering potential \mathcal{X} [Eq. (3)]. The field propagates from fluctuation to fluctuation via the dyadic Green tensor \mathcal{G}_b in the homogeneous background with wave number k_b [Eq. (14)]. The multiple scattering process on the scattering potential \mathcal{X} is described (to infinite order) via the transition operator \mathcal{T} of the entire system [Eq. (18)]. The average transition operator $\langle \mathcal{T} \rangle$ finally defines the self-energy Σ [Eq. (20)], which describes the propagation of the average field $\langle \mathbf{E} \rangle$ in the disordered medium, and therefore the extinction (i.e., scattering and absorption) efficiency of the system [Eq. (12)].

4. Average intensity and four-point irreducible vertex

The theory above describes how an incident wave gets attenuated by scattering and absorption in a heterogeneous medium, but not how the light intensity (or energy density) propagates in the medium. Indeed, the energy that is removed by scattering from the average field intensity $|\langle \mathbf{E}(\mathbf{r}) \rangle|^2$, also known as coherent intensity, is redistributed along different directions to form, upon sequences of scattering events, a spatial distribution for the average intensity $\langle |\mathbf{E}(\mathbf{r})|^2 \rangle$ that can strongly

differ from a simple exponentially-decaying profile. The formalism used for the average field will now be applied to the average intensity. This will lead to the definition of the scattering and transport mean free paths, two additional typical lengths at the root of light propagation in disordered media (Apresyan and Kravtsov, 1996; van Rossum and Nieuwenhuizen, 1999; Rytov *et al.*, 1989).

Let us then consider the spatial correlation function of the electric field, or “coherence matrix” (Mandel and Wolf, 1995), $\mathbf{C}(\mathbf{r}, \mathbf{r}') \equiv \langle \mathbf{E}(\mathbf{r}) \otimes \mathbf{E}^*(\mathbf{r}') \rangle$, with $*$ denoting complex conjugate. Starting from the Lippmann-Schwinger equation [Eq. (16)], one can easily show that \mathbf{C} depends on the spatial correlation of the polarization density in the effective scattering potential $\langle (\mathcal{X}(\mathbf{r}) \mathbf{E}(\mathbf{r})) \otimes (\mathcal{X}^*(\mathbf{r}') \mathbf{E}^*(\mathbf{r}')) \rangle$. Similarly to the self-energy that allowed us to relate the average polarization to the average field [Eq. (5)] eventually leading to the Dyson equation [Eq. (19)], we can introduce here an operator Γ known as the “four-point irreducible vertex” – or intensity vertex – that relates the effective polarization density correlation to the electric field correlation. This eventually leads to a closed-form and exact equation, known as the Bethe-Salpeter equation (Salpeter and Bethe, 1951), which reads

$$\begin{aligned} \mathbf{C}(\mathbf{r}, \mathbf{r}') &= \langle \mathbf{E}(\mathbf{r}) \rangle \otimes \langle \mathbf{E}^*(\mathbf{r}') \rangle + \int \langle \mathbf{G}(\mathbf{r}, \mathbf{r}_1) \rangle \otimes \langle \mathbf{G}^*(\mathbf{r}', \mathbf{r}'_1) \rangle \\ &\quad \cdot \Gamma(\mathbf{r}_1, \mathbf{r}_2, \mathbf{r}'_1, \mathbf{r}'_2) \cdot \mathbf{C}(\mathbf{r}_2, \mathbf{r}'_2) d\mathbf{r}_1 d\mathbf{r}'_1 d\mathbf{r}_2 d\mathbf{r}'_2, \end{aligned} \quad (21)$$

where the average Green function $\langle \mathbf{G} \rangle$ is given by the Dyson equation [Eq. (19)],

$$\langle \mathcal{G} \rangle = \mathcal{G}_b + \mathcal{G}_b \Sigma \langle \mathcal{G} \rangle. \quad (22)$$

The symbol \cdot denotes here a tensor contraction, defined such that $(\mathbf{A} \otimes \mathbf{B}) \cdot (\mathbf{e} \otimes \mathbf{f}) = (\mathbf{A}\mathbf{e}) \otimes (\mathbf{B}\mathbf{f})$ and $(\mathbf{A} \otimes \mathbf{B}) \cdot (\mathbf{C} \otimes \mathbf{D}) = (\mathbf{A}\mathbf{C}) \otimes (\mathbf{B}\mathbf{D})$, where \mathbf{e}, \mathbf{f} are vectors and $\mathbf{A}, \mathbf{B}, \mathbf{C}, \mathbf{D}$ matrices.

The first term in Eq. (21) is the source term, given by the coherent intensity that decays exponentially within the scattering medium. The second term expresses the field correlation as a multiple scattering process, wherein the propagation is described by the average Green tensors and scattering by the vertex Γ that connects two pairs of points (for the field and the complex conjugate). Following similar steps as those leading to Eq. (20), we obtain a completely general and exact expression for Γ (here, in operator notation) as (Carminati and Schotland, 2021)

$$\begin{aligned} \Gamma &= [\mathcal{G}_b \mathcal{G}_b^*]^{-1} \left[\mathbf{1} + \mathcal{G}_b \langle \mathcal{T} \rangle + \mathcal{G}_b^* \langle \mathcal{T}^* \rangle \right. \\ &\quad \left. + \langle \mathcal{T} \rangle \mathcal{G}_b \mathcal{G}_b^* \langle \mathcal{T}^* \rangle \right]^{-1}. \end{aligned} \quad (23)$$

We proceed by establishing a link between Γ and the light scattering and transport properties of the medium. Towards this aim, it is convenient to rewrite the Bethe-Salpeter equation in Fourier space. A closed-form an-

alytical formula can be obtained by assuming that the scattering events take place on distances larger than the wavelength, such that the average Green tensor can be approximated as its transverse component only,

$$\langle \mathbf{G}(\mathbf{k}) \rangle = [k^2 \mathbf{P}(\mathbf{u}) - k_b^2 \mathbf{1} - \Sigma(\mathbf{k})]^{-1}, \quad (24)$$

$$\simeq \langle G_\perp(\mathbf{k}) \rangle \mathbf{P}(\mathbf{u}), \quad (25)$$

where $\mathbf{P}(\mathbf{u}) = \mathbf{1} - \mathbf{u} \otimes \mathbf{u}$ is the transverse projection operator and $\langle G_\perp(\mathbf{k}) \rangle = [k^2 - k_b^2 - \Sigma_\perp(\mathbf{k})]^{-1}$ is the (scalar) transverse component. After some algebra provided in details in Appendix B, we reach

$$\begin{aligned} & \left[\left(\mathbf{k} - \frac{\mathbf{q}}{2} \right)^2 - \left(\mathbf{k} + \frac{\mathbf{q}}{2} \right)^2 - \Sigma_\perp^* \left(\mathbf{k} - \frac{\mathbf{q}}{2} \right) + \Sigma_\perp \left(\mathbf{k} + \frac{\mathbf{q}}{2} \right) \right] \mathbf{L}_\perp(\mathbf{k}, \mathbf{q}) \\ &= \left[\langle G_\perp \left(\mathbf{k} + \frac{\mathbf{q}}{2} \right) \rangle - \langle G_\perp^* \left(\mathbf{k} - \frac{\mathbf{q}}{2} \right) \rangle \right] \int \bar{\Gamma}_\perp \left(\mathbf{k} + \frac{\mathbf{q}}{2}, \mathbf{k}' + \frac{\mathbf{q}}{2}, \mathbf{k} - \frac{\mathbf{q}}{2}, \mathbf{k}' - \frac{\mathbf{q}}{2} \right) \cdot \mathbf{L}_\perp(\mathbf{k}', \mathbf{q}) \frac{d\mathbf{k}'}{(2\pi)^3}, \end{aligned} \quad (26)$$

where we relied on the statistical homogeneity and translational invariance of the medium and neglected the source term. The field correlation, described by a new function

$$\mathbf{L}_\perp(\mathbf{k}, \mathbf{q}) \equiv \mathbf{C}_\perp \left(\mathbf{k} + \frac{\mathbf{q}}{2}, \mathbf{k} - \frac{\mathbf{q}}{2} \right), \quad (27)$$

with

$$\mathbf{C}_\perp(\mathbf{k}, \mathbf{k}') = \mathbf{P}(\mathbf{u}) \otimes \mathbf{P}(\mathbf{u}') \cdot \mathbf{C}(\mathbf{k}, \mathbf{k}'), \quad (28)$$

depends only on the transverse part of the intensity vertex, which is given by

$$\begin{aligned} \Gamma_\perp(\mathbf{k}, \boldsymbol{\kappa}, \mathbf{k}', \boldsymbol{\kappa}') &= \mathbf{P}(\mathbf{u}) \otimes \mathbf{P}(\mathbf{u}') \cdot \Gamma(\mathbf{k}, \boldsymbol{\kappa}, \mathbf{k}', \boldsymbol{\kappa}') \\ &= (2\pi)^3 \delta(\mathbf{k} - \boldsymbol{\kappa} - \mathbf{k}' - \boldsymbol{\kappa}') \bar{\Gamma}_\perp(\mathbf{k}, \boldsymbol{\kappa}, \mathbf{k}', \boldsymbol{\kappa}'). \end{aligned} \quad (29)$$

Equation (26) is very general, as it considers all multiple scattering events within the medium and does not make any explicit assumption on the kind of disorder. Note however that neglecting the longitudinal component of the Green tensor implicitly excludes situations wherein near-field contributions are important (e.g., in dense packings of high-index resonant particles).

5. Radiative transfer limit and scattering mean free path

Further approximations are required to extract analytical expressions for the scattering and transport properties of the medium. First, we take the large-scale approximation $|\mathbf{q}| \ll \{|\mathbf{k}|, |\mathbf{k}'|\}$, also known as the radiative transfer limit (Barabanenkov and Finkel'berg, 1968; Henkel, 1997; Ryzhik *et al.*, 1996), which assumes that the average intensity varies on length scales $2\pi/|\mathbf{q}|$ much larger than the typical wavelength in the medium $2\pi/k_r$. Since the average field and intensity vary on the scale of ℓ_e , this approximation holds in the weak extinction limit,

$k_r \ell_e \gg 1$. Equation (26) thus becomes

$$\begin{aligned} & [-2\mathbf{k} \cdot \mathbf{q} + 2i \text{Im} \Sigma_\perp(\mathbf{k})] \mathbf{L}_\perp(\mathbf{k}, \mathbf{q}) = 2i \text{Im} \langle G_\perp(\mathbf{k}) \rangle \\ & \times \int \bar{\Gamma}_\perp(\mathbf{k}, \mathbf{k}', \mathbf{k}, \mathbf{k}') \cdot \mathbf{L}_\perp(\mathbf{k}', \mathbf{q}) \frac{d\mathbf{k}'}{(2\pi)^3}. \end{aligned} \quad (30)$$

In a dilute material, the scattering correction in the average Green function is considered to be weak, i.e. $|\Sigma_\perp| \ll k_b^2$. Using the relation

$$\lim_{\epsilon \rightarrow 0^+} \frac{1}{x - x_0 - i\epsilon} = \text{PV} \left[\frac{1}{x - x_0} \right] + i\pi \delta(x - x_0), \quad (31)$$

where PV stands for the Cauchy principal value operator, the imaginary part of the average Green function reduces to

$$\text{Im} \langle G_\perp(\mathbf{k}) \rangle = \pi \delta[k^2 - k_b^2 - \text{Re} \Sigma_\perp(\mathbf{k})]. \quad (32)$$

This relation fixes the real part of the effective wavevector $k_r = \text{Re} k_{\text{eff}}$ to

$$k_r = \sqrt{k_b^2 + \text{Re} \Sigma_\perp(k_r)}, \quad (33)$$

which is the so-called ‘‘on-shell approximation’’. Second, we assume that the field is fully depolarized, which is a perfectly acceptable hypothesis after many scattering events (i.e., far from a coherent, polarized source) (Bicout and Brosseau, 1992; Gorodnichev *et al.*, 2014; Vynck *et al.*, 2016). This gives

$$\mathbf{C}(\mathbf{k}, \mathbf{k}') = C(\mathbf{k}, \mathbf{k}') \mathbf{1} \quad (34)$$

leading to

$$\mathbf{L}_\perp(\mathbf{k}, \mathbf{q}) = L(\mathbf{k}, \mathbf{q}) \mathbf{P}(\mathbf{u}) \otimes \mathbf{P}(\mathbf{u}') \cdot \mathbf{1}. \quad (35)$$

An inverse Fourier transform of the trace of Eq. (30) together with Eqs. (32) and (35) eventually leads to the famous Radiative Transfer Equation (RTE) (Chan-

drasekhar, 1960)

$$\left[\mathbf{u} \cdot \nabla_{\mathbf{r}} + \frac{1}{\ell_e} \right] I(\mathbf{r}, \mathbf{u}) = \frac{1}{\ell_s} \int p(\mathbf{u}, \mathbf{u}') I(\mathbf{r}, \mathbf{u}') d\mathbf{u}', \quad (36)$$

I is the specific intensity, which can be interpreted as a local (at position \mathbf{r}) and directional (on direction \mathbf{u}) radiative flux, defined as

$$\delta(k - k_r) I(\mathbf{r}, \mathbf{u}) = L(\mathbf{r}, \mathbf{k}). \quad (37)$$

ℓ_s and $p(\mathbf{u}, \mathbf{u}')$ are the scattering mean free path and the phase function, describing respectively the average distance between two scattering events and the angular diagram for an incident planewave along \mathbf{u}' scattered along direction \mathbf{u} . Both quantities are related to the intensity vertex via the relation

$$\frac{1}{\ell_s} p(\mathbf{u}, \mathbf{u}') = \frac{1}{32\pi^2} \text{Tr} [\mathbf{P}(\mathbf{u}) \otimes \mathbf{P}(\mathbf{u}') \cdot \bar{\mathbf{\Gamma}}(k_r \mathbf{u}, k_r \mathbf{u}', k_r \mathbf{u}, k_r \mathbf{u}') \cdot \mathbf{P}(\mathbf{u}') \otimes \mathbf{P}(\mathbf{u}') \cdot \mathbf{1}], \quad (38)$$

and the phase function is normalized as

$$\int p(\mathbf{u}, \mathbf{u}') d\mathbf{u}' = 1. \quad (39)$$

The trace corresponds to an average over all possible polarization states for the incident and scattered fields. The RTE [Eq. (36)] can be seen as an energy balance (Chandrasekhar, 1960). The spatial variation of the specific intensity (term involving the derivative) is due to the loss induced by extinction along the direction \mathbf{u} [term involving ℓ_e] and the gain from scattering from direction \mathbf{u}' to direction \mathbf{u} [term involving ℓ_s and $p(\mathbf{u}, \mathbf{u}')$]. Equations (38) and (39) show that ℓ_s , the key quantity to describe the scattering strength of a medium, is obtained in the radiative transfer limit from the angular integral of the intensity vertex.

Previously, we showed that the extinction mean free path ℓ_e could be obtained from the self-energy Σ and noted that, in absence of absorption, we should have $\ell_e = \ell_s$, the latter being defined from the intensity vertex $\mathbf{\Gamma}$. It is worth emphasizing at this point that the two operators are indeed formally linked by the Ward identity, which may be seen as a generalization of the extinction (optical) theorem and ensures energy conservation (Apresyan and Kravtsov, 1996; Cherroret *et al.*, 2016; Lagendijk and Van Tiggelen, 1996; Sheng, 2006; Tsang and Kong, 2001).

6. Transport mean free path and diffusion approximation

Many experiments on light in disordered media are performed in situations where light experiences not just a few but many scattering events on average. It turns out that many observables accessible experimentally depend

on yet another length scale, that is the transport mean free path ℓ_t , which we will introduce here.

We start by taking the first moment of Eq. (36) (i.e., multiplying both sides by \mathbf{u} and integrating over \mathbf{u}) which directly leads to

$$\int [\mathbf{u} \cdot \nabla_{\mathbf{r}} I(\mathbf{r}, \mathbf{u})] \mathbf{u} d\mathbf{u} + \frac{1}{\ell_t} \mathbf{j}(\mathbf{r}) = 0, \quad (40)$$

where $\mathbf{j}(\mathbf{r}) = \int I(\mathbf{r}, \mathbf{u}) \mathbf{u} d\mathbf{u}$ is the radiative flux vector and

$$\ell_t \equiv \frac{\ell_s}{1 - g}, \quad (41)$$

is the transport mean free path.

$$g = \int p(\mathbf{u}, \mathbf{u}') \mathbf{u} \cdot \mathbf{u}' d\mathbf{u} \quad (42)$$

is the average cosine of the phase function, or scattering anisotropy factor. It can be interpreted as a renormalization factor of the scattering mean free path due to predominantly forward ($0 < g < 1$) or backward ($-1 < g < 0$) single scattering. Physically, ℓ_t describes the average distance required for light to be fully randomized (e.g., forward scattering increases this distance at constant scattering strength ℓ_s). Structural correlations impact the transport mean free path via both the scattering mean free path ℓ_s and the scattering anisotropy described by g .

After propagation on distances much larger than ℓ_t , the specific intensity becomes quasi-isotropic. Expanding the specific intensity in the RTE [Eq. (36)] on Legendre polynomials to first order in \mathbf{u} , that is the so-called P_1 -approximation (Ishimaru, 1978), leads to the diffusion equation. In the steady-state regime, it reads

$$-\mathcal{D} \Delta u(\mathbf{r}) = s(\mathbf{r}) \quad (43)$$

where $u(\mathbf{r}) = v_E^{-1} \int I(\mathbf{r}, \mathbf{u}) d\mathbf{u}$ is the energy density with v_E the energy velocity (Lagendijk and Van Tiggelen, 1996), $\mathcal{D} = v_E \ell_t / 3$ is the diffusion constant and s is a source term given by the ballistic intensity. Resolving this equation in a slab geometry of thickness L under planewave illumination at normal incidence gives the following asymptotic behavior for the total transmittance

$$T \sim \frac{5}{3} \frac{\ell_t}{L}, \quad (44)$$

also known as Ohm's law. Many transport observations in the diffusive limit depend directly on the transport mean free path, including the linewidth of the coherent backscattering cone (Akkermans *et al.*, 1988, 1986), the time-resolved transmittance and reflectance (Contini *et al.*, 1997), and long-range speckle correlations (Fayard *et al.*, 2015; Scheffold and Maret, 1998; Shapiro, 1999).

In summary, the average transition operator of the medium $\langle \mathcal{T} \rangle$ defines the four-point irreducible vertex $\mathbf{\Gamma}$ [Eq. (23)]. Neglecting near-field interaction between scat-

tering elements, taking the radiative transfer limit, using the on-shell approximation and assuming fully depolarized light allow us to relate the transverse component of $\mathbf{\Gamma}$ to the scattering mean free path ℓ_s and phase function $p(\mathbf{u}, \mathbf{u}')$ [Eq. (38)]. Looking at the radiative flux vector leads to the definition of the transport mean free path ℓ_t [Eq. (41)], related to the intensity vertex via Eqs. (38) and (39).

The theoretical framework described here will now be used to get closed-form expressions for the different optical length scales in the cases of random media described by a continuous permittivity [Sec. II.B] and assemblies of identical particles [Sec. II.C].

B. Media with fluctuating continuous permittivity

1. First insights on structural correlations

We consider a statistically homogeneous and isotropic disordered medium, described by a spatially-dependent permittivity $\epsilon(\mathbf{r}) = \langle \epsilon \rangle + \Delta\epsilon(\mathbf{r})$, where $\Delta\epsilon$ is the fluctuating part with statistics

$$\langle \Delta\epsilon(\mathbf{r}) \rangle = 0, \quad (45)$$

$$\langle \Delta\epsilon(\mathbf{r}) \Delta\epsilon(\mathbf{r}') \rangle = \langle \epsilon \rangle^2 \delta_\epsilon^2 h_\epsilon(|\mathbf{r} - \mathbf{r}'|). \quad (46)$$

Here, $\delta_\epsilon^2 = \langle \Delta\epsilon^2 \rangle / \langle \epsilon \rangle^2$ is the normalized variance of ϵ and $h_\epsilon(|\mathbf{r} - \mathbf{r}'|) = \langle \Delta\epsilon(\mathbf{r}) \Delta\epsilon(\mathbf{r}') \rangle / \langle \Delta\epsilon^2 \rangle$ is the normalized permittivity-permittivity correlation function ($h_\epsilon(0) = 1$). Hereafter, we assume ergodicity, such that the ensemble average is equivalent to a volume average over in the infinite-volume limit, and isotropic permittivity fluctuations, keeping in mind, however, that anisotropic fluctuations may take place even in isotropic materials (Landau *et al.*, 2013).

The statistical properties on $\epsilon(\mathbf{r})$ straightforwardly translate into statistical properties on $\mathcal{X}(\mathbf{r})$ via Eq. (3). The self-energy Σ can be expressed in terms of \mathcal{X} by inserting the expression for the transition operator \mathcal{T} given by Eq. (18) into Eq. (20), leading to

$$\Sigma = \left\langle \mathcal{X} [1 - \mathcal{G}_b \mathcal{X}]^{-1} \right\rangle \left\langle [1 - \mathcal{G}_b \mathcal{X}]^{-1} \right\rangle^{-1}. \quad (47)$$

In the simplest approach, we proceed by assuming that the scattering potential \mathcal{X} weakly fluctuates around its average value $\langle \mathcal{X} \rangle$. Expanding the last expression near $\langle \mathcal{X} \rangle$ leads to

$$\Sigma \sim \langle \mathcal{X} \rangle + \langle (\mathcal{X} - \langle \mathcal{X} \rangle) \mathcal{G}_b (\mathcal{X} - \langle \mathcal{X} \rangle) \rangle + \dots \quad (48)$$

At this stage, we need to define explicitly the constant auxiliary background permittivity ϵ_b , which describes the reference value around which the permittivity fluctuates. A reasonable choice is to set it to the average permittivity, $\epsilon_b = \langle \epsilon \rangle \equiv \epsilon_{av}$, which, for a two-component medium with permittivities ϵ_p and ϵ_h at filling fractions f and

$1 - f$, respectively, would simply be $\epsilon_{av} = f\epsilon_p + (1 - f)\epsilon_h$. Having then $\langle \mathcal{X} \rangle = 0$, the leading term for the self-energy becomes $\langle \mathcal{X} \mathcal{G}_b \mathcal{X} \rangle$, such that

$$\Sigma(\mathbf{r} - \mathbf{r}') = k_{av}^4 \delta_\epsilon^2 h_\epsilon(|\mathbf{r} - \mathbf{r}'|) \mathbf{G}_{av}(\mathbf{r} - \mathbf{r}'), \quad (49)$$

where \mathbf{G}_{av} is the Green tensor in a homogeneous medium with permittivity ϵ_{av} . Correlated permittivity fluctuations mutually interacting via \mathbf{G}_{av} are readily responsible for the non-local character of the self-energy [Eq. (6)]. In Fourier space, Eq. (49) becomes

$$\Sigma(\mathbf{k}) = k_{av}^4 \delta_\epsilon^2 \int h_\epsilon(|\mathbf{k} - \mathbf{k}'|) \mathbf{G}_{av}(\mathbf{k}') \frac{d\mathbf{k}'}{(2\pi)^3}. \quad (50)$$

The extinction mean free path ℓ_e can finally be determined using Eq. (13) with $k_r = k_{av}$. We consider media composed of non-absorbing materials [$\epsilon(\mathbf{r})$ always real], such that $k_{av} = k_0 \sqrt{\epsilon_{av}}$. The imaginary part of the Green tensor is given by

$$\text{Im} \mathbf{G}_{av}(\mathbf{k}) = \pi \delta(k^2 - k_{av}^2) \mathbf{P}(\mathbf{u}). \quad (51)$$

Using Eq. (10) for the transverse component with \mathbf{e} the polarization such that $\mathbf{e} \cdot \mathbf{u} = 0$, we eventually obtain

$$\begin{aligned} \frac{1}{\ell_e} &\simeq \frac{\text{Im} \Sigma_\perp(k_{av})}{k_{av}} \\ &= \frac{k_{av}^4}{16\pi^2} \delta_\epsilon^2 \int h_\epsilon(k_{av}|\mathbf{u} - \mathbf{u}'|) (\mathbf{e} \cdot \mathbf{P}(\mathbf{u}') \mathbf{e}) d\mathbf{u}'. \end{aligned} \quad (52)$$

Introducing the scattering wavenumber $q = k_{av}|\mathbf{u} - \mathbf{u}'|$, we eventually reach

$$\frac{1}{\ell_e} = \frac{k_0^4}{8\pi k_{av}^2} \epsilon_{av}^2 \delta_\epsilon^2 \int_0^{2k_{av}} P\left(\frac{q}{2k_{av}}\right) h_\epsilon(q) q dq, \quad (53)$$

where

$$P(k) \equiv 1 - 2k^2 + 2k^4, \quad (54)$$

is due to the vector nature of light. The integral over q , which corresponds to an integral over the scattering angle, should be made up to twice the wave number in the homogeneous effective background with permittivity ϵ_{av} .

Equation (53), obtained in non-absorbing disordered media with weak permittivity fluctuations, constitute the first analytical expression for the extinction mean free path in correlated media. Very importantly, it shows that spatial correlations, described here by h_ϵ , are as important for light scattering as the amplitude of the permittivity fluctuations, $\epsilon_{av}^2 \delta_\epsilon^2 = \langle \Delta\epsilon^2 \rangle$.

2. Lorentz local fields

The approximation of weak fluctuations is prohibitive in many realistic cases. Fortunately, this constraint

can be eliminated by properly handling the singularity of the dyadic Green function at the origin [Eq. (14)], which constitutes the basis of a strong fluctuation theory (Finkel'berg, 1964; Ryzhov *et al.*, 1965; Tsang and Kong, 1981). Related approaches were introduced by Bedeaux and Mazur (1973) and Felderhof (1974) in the description of the optical response of non-polar fluids, and more recently by Torquato and Kim (2021) in the study of two-phase composite media. Extensions to chiral and anisotropic media have also been proposed (Mackay and Lakhtakia, 2015; Michel and Lakhtakia, 1995; Ryzhov and Tamoikin, 1970), but will not be discussed here.

The singularity of the Green function is handled by considering the scattering medium as being made of infinitesimal volume elements within which the polarization density $\mathbf{P}(\mathbf{r})$ is constant. This physical viewpoint is nothing but the basis of the renowned discrete dipole approximation (Draine and Flatau, 1994; Lakhtakia, 1992). Let us then write the Green function as a sum of two contributions

$$\mathbf{G}_b(\mathbf{r}, \mathbf{r}') = \Theta(|\mathbf{r} - \mathbf{r}'| - a) \tilde{\mathbf{G}}_b(\mathbf{r}, \mathbf{r}') + \Theta(a - |\mathbf{r} - \mathbf{r}'|) \mathbf{g}_b(\mathbf{r}, \mathbf{r}'), \quad (55)$$

where \mathbf{g}_b contains the singular part of the Green function and $\tilde{\mathbf{G}}_b$ is the so-called Lorentz propagator, which is then purely non-local. The contributions are distinguished as belonging or not to a spherical volume of radius a and volume $v = 4\pi a^3/3$ around \mathbf{r}' . Choosing a such that $k_b a \ll 1$, the singular part reads

$$\mathbf{g}_b(\mathbf{r}, \mathbf{r}')|_{k_b a \ll 1} = -\frac{1}{3k_b^2} \delta(\mathbf{r} - \mathbf{r}') \mathbf{1} + i \frac{k_b}{6\pi} \mathbf{1} + \dots \quad (56)$$

Keeping the lowest-order terms in the real and imaginary parts, the Lippmann-Schwinger equation [Eq. (15)] can be rewritten as

$$\mathbf{E}(\mathbf{r}) = \left\{ \mathbf{E}_b(\mathbf{r}) + \left(-\frac{1}{3k_b^2} + i \frac{k_b v}{6\pi} \right) \mathcal{X}(\mathbf{r}) \mathbf{E}(\mathbf{r}) \right\} + \int \tilde{\mathbf{G}}_b(\mathbf{r}, \mathbf{r}') \mathcal{X}(\mathbf{r}') \mathbf{E}(\mathbf{r}') d\mathbf{r}'. \quad (57)$$

The actual field at \mathbf{r} is then given by the sum of the external field $\mathbf{E}_b(\mathbf{r})$ and the *local* contributions (terms in braces), plus the *non-local* contributions coming from neighboring permittivity fluctuations (integral term).

In this framework, the field exciting a small volume element around \mathbf{r} , $\mathbf{E}_{\text{exc}}(\mathbf{r})$, is the sum of the incident (background) field and the field scattered by other permittivity fluctuations. Going back to the operator notation, we thus reach an important set of equalities

$$\begin{aligned} \mathbf{E}_{\text{exc}} &= \mathbf{E}_b + \tilde{\mathbf{G}}_b \mathcal{X} \mathbf{E} = [\mathbf{1} - \mathbf{g}_b \mathcal{X}] \mathbf{E} \\ &= \mathbf{E}_b + \tilde{\mathbf{G}}_b \tilde{\mathcal{T}} \mathbf{E}_{\text{exc}} = [\mathbf{1} + \tilde{\mathbf{G}}_b \tilde{\mathcal{T}}] \mathbf{E}_b. \end{aligned} \quad (58)$$

We have introduced here a new quantity, $\tilde{\mathcal{T}}$, that plays

the role of a *local* transition operator. From Eqs. (58), we straightforwardly obtain

$$\mathcal{T} = \tilde{\mathcal{T}} [\mathbf{1} - \tilde{\mathbf{G}}_b \tilde{\mathcal{T}}]^{-1}. \quad (59)$$

The transition operator of the system is now expressed as a multiple-scattering expansion on small independent scattering elements, connected via the (non-local) Lorentz propagator. Consistently with this picture, from Eqs. (58), we also obtain

$$\tilde{\mathcal{T}} = \mathcal{X} [\mathbf{1} - \mathbf{g}_b \mathcal{X}]^{-1}. \quad (60)$$

For $k_b a \ll 1$, the (local) transition operator $\tilde{\mathcal{T}}$ is directly proportional to the polarizability of the volume element,

$$\tilde{\mathcal{T}}(\mathbf{r}, \mathbf{r}') = k_b^2 \frac{\alpha(\mathbf{r})}{v} \delta(\mathbf{r} - \mathbf{r}') \mathbf{1}, \quad (61)$$

with

$$\alpha(\mathbf{r}) = \frac{\alpha_0(\mathbf{r})}{1 - i \frac{k_b^3}{6\pi} \alpha_0(\mathbf{r})}, \quad \alpha_0(\mathbf{r}) = 3v \frac{\epsilon(\mathbf{r}) - \epsilon_b}{\epsilon(\mathbf{r}) + 2\epsilon_b}, \quad (62)$$

where α_0 is the quasi-static polarizability that depends on space via $\epsilon(\mathbf{r})$.

3. Average exciting field

To determine the self-energy Σ of the system, it is convenient to introduce a self-energy $\tilde{\Sigma}$ for the exciting field defined from a Dyson equation

$$\langle \mathbf{E}_{\text{exc}} \rangle = \mathbf{E}_b + \tilde{\mathbf{G}}_b \tilde{\Sigma} \langle \mathbf{E}_{\text{exc}} \rangle, \quad (63)$$

thereby leading to

$$\tilde{\Sigma} = \left\langle \tilde{\mathcal{T}} [\mathbf{1} - \tilde{\mathbf{G}}_b \tilde{\mathcal{T}}]^{-1} \right\rangle \left\langle [\mathbf{1} - \tilde{\mathbf{G}}_b \tilde{\mathcal{T}}]^{-1} \right\rangle^{-1}. \quad (64)$$

Note the similarity of this expression with Eq. (47), where the self-energy Σ was expressed directly in terms of the scattering potential \mathcal{X} . From Eqs. (20), (59) and (64), one shows that the two self-energies are related as

$$\Sigma = \tilde{\Sigma} [\mathbf{1} + \mathbf{g}_b \tilde{\Sigma}]^{-1}. \quad (65)$$

Let us then expand $\tilde{\Sigma}$ in Eq. (64) near $\langle \tilde{\mathcal{T}} \rangle = \tilde{\mathcal{T}} - \Delta \tilde{\mathcal{T}}$,

$$\tilde{\Sigma} \sim \langle \tilde{\mathcal{T}} \rangle + \langle \Delta \tilde{\mathcal{T}} \hat{\mathbf{G}}_b \Delta \tilde{\mathcal{T}} \rangle + \dots \equiv \tilde{\Sigma}_1 + \tilde{\Sigma}_2 + \dots \quad (66)$$

We have introduced here a new “dressed” propagator,

$$\hat{\mathbf{G}}_b = [\mathbf{1} - \tilde{\mathbf{G}}_b \langle \tilde{\mathcal{T}} \rangle]^{-1} \tilde{\mathbf{G}}_b. \quad (67)$$

Noting that $\langle \tilde{\mathcal{T}} \rangle$ corresponds to an average polarizability of the medium (for $k_b a \ll 1$, see Eqs. (61)), one understands that $\hat{\mathbf{G}}_b$ describes the fact that the fields propa-

gate from fluctuation to fluctuation via a medium with a permittivity that can differ from the background permittivity ϵ_b (Bedeaux and Mazur, 1973; Felderhof, 1974).

The self-energy (for the average exciting field) in Eq. (66) now explicitly depends on the spatial correlations of the fluctuations of $\tilde{\mathcal{T}}$, i.e. of the polarizability of small volume elements. In most practical cases, the expansion is stopped at the second order, corresponding to the so-called “bilocal” approximation (Tsang and Kong, 2001), due to the lack of information on higher-order correlation functions in real systems.

Expanding Σ in Eq. (65) near $\tilde{\Sigma}_1$, we obtain

$$\begin{aligned}\Sigma &\sim \tilde{\Sigma}_1 \left[\mathbf{1} + \mathbf{g}_b \tilde{\Sigma}_1 \right]^{-1} + \tilde{\Sigma}_2 \left[\mathbf{1} + \mathbf{g}_b \tilde{\Sigma}_1 \right]^{-2} + \dots \\ &\equiv \Sigma_1 + \Sigma_2 + \dots\end{aligned}\quad (68)$$

The self-energy is now expressed in terms of the scattering properties of vanishingly small, individual scattering elements.

4. Long-wavelength solutions for strongly fluctuating media: Bruggeman versus Maxwell-Garnett

As in the case of weakly fluctuating media discussed above, we now need to give an explicit definition of the constant auxiliary background permittivity ϵ_b , that describes the homogeneous effective medium in which the permittivity fluctuations scatter light. We will see that this sole parameter constitutes the essential difference between the two most famous “mixing rules” in the literature, due to Bruggeman (Bruggeman, 1935) and Maxwell Garnett (Maxwell Garnett, 1904), presented here in a unique theoretical framework. Despite the arbitrariness in the choice of ϵ_b , it is important to realize that all models would eventually be strictly equivalent when carried out to infinite order. The applicability of a model is thus mainly a question of accuracy at the lowest orders and convergence.

A first possibility for ϵ_b is to set it such that $\langle \tilde{\mathcal{T}} \rangle = 0$. In the limit of small volume elements, this corresponds to having a zero average polarizability, see Eqs. (61)-(62). Considering a two-component medium with relative permittivities ϵ_p (at filling fraction f) and ϵ_h (at filling fraction $1 - f$) in the quasi-static limit ($\alpha = \alpha_0$ in Eq. (62)), one obtains

$$\frac{\epsilon_p - \epsilon_{BG}}{\epsilon_p + 2\epsilon_{BG}} f + \frac{\epsilon_h - \epsilon_{BG}}{\epsilon_h + 2\epsilon_{BG}} (1 - f) = 0 \quad (69)$$

which is nothing but the Bruggeman mixing rule (Bruggeman, 1935) with $\epsilon_b \equiv \epsilon_{BG}$. The generalization to N -component media is straightforward. Having $k_b^2 = k_{BG}^2 = k_0^2 \epsilon_{BG}$, $\hat{\mathcal{G}}_b = \hat{\mathcal{G}}_{BG}$ and $\Sigma \sim \tilde{\Sigma}$ since

$\tilde{\Sigma}_1 = 0$, we eventually arrive to

$$\Sigma(\mathbf{k}) = k_{BG}^4 \delta_\alpha^2 \int h_\alpha(|\mathbf{k} - \mathbf{k}'|) \hat{\mathcal{G}}_{BG}(\mathbf{k}') \frac{d\mathbf{k}'}{(2\pi)^3}, \quad (70)$$

with $\delta_\alpha^2 = \langle \Delta\alpha^2 \rangle / v^2$ a normalized variance of the polarizability and $h_\alpha(|\mathbf{k} - \mathbf{k}'|)$ the Fourier transform of the normalized polarizability-polarizability correlation function $h_\alpha(|\mathbf{r} - \mathbf{r}'|) = \langle \Delta\alpha(\mathbf{r}) \Delta\alpha(\mathbf{r}') \rangle / \langle \Delta\alpha^2 \rangle$. The function h_α therefore plays the role of h_ϵ in the weakly fluctuating permittivity model to describe structural correlations.

Assuming non-absorbing media and following the same steps as those leading to Eq. (53) with $\text{Im} \hat{\mathcal{G}}_{BG}(\mathbf{k}) = \pi \delta(k^2 - k_{BG}^2) \mathbf{P}(\mathbf{u})$, we obtain

$$\frac{1}{\epsilon_e} = \frac{k_0^4}{8\pi k_{BG}^2} \epsilon_{BG}^2 \delta_\alpha^2 \int_0^{2k_{BG}} P\left(\frac{q}{2k_{BG}}\right) h_\alpha(q) q dq, \quad (71)$$

with $q = k_{BG}|\mathbf{u} - \mathbf{u}'|$. Equation (71) is strikingly similar to Eq. (53), the essential differences being (i) on the permittivity of the homogeneous effective medium and (ii) on the description of the system via a local polarizability instead of a local permittivity.

A second possibility for the choice of ϵ_b is to set it to the permittivity of the host medium, i.e. $\epsilon_b = \epsilon_h$, in which case $\langle \tilde{\mathcal{T}} \rangle \neq 0$. Considering again a two-component system for volume elements in the quasi-static limit, we obtain

$$\tilde{\Sigma}_1(\mathbf{r} - \mathbf{r}') = k_h^2 \rho \alpha_0 \delta(\mathbf{r} - \mathbf{r}') \mathbf{1}, \quad (72)$$

with $\rho = f/v$ the average number density of the small volume elements with permittivity ϵ_p , and

$$\tilde{\Sigma}_2(\mathbf{r} - \mathbf{r}') = k_h^4 \delta_\alpha^2 h_\alpha(|\mathbf{r} - \mathbf{r}'|) \hat{\mathcal{G}}_h(\mathbf{r} - \mathbf{r}'). \quad (73)$$

Using Eq. (68), we arrive to an expression for the self-energy in reciprocal space as

$$\begin{aligned}\Sigma(\mathbf{k}) &= k_0^2 (\epsilon_{MG} - \epsilon_h) \mathbf{1} \\ &+ k_h^4 \delta_\alpha^2 f_L \int h_\alpha(|\mathbf{k} - \mathbf{k}'|) \hat{\mathcal{G}}_h(\mathbf{k}') \frac{d\mathbf{k}'}{(2\pi)^3},\end{aligned}\quad (74)$$

where $f_L = (\partial \epsilon_{MG} / \partial \rho) / (\epsilon_h \alpha_0)$ and

$$\epsilon_{MG} = \epsilon_h + \epsilon_h \frac{\rho \alpha_0}{1 - \rho \alpha_0 / 3}, \quad (75)$$

is the Maxwell-Garnett mixing rule (Markel, 2016; Maxwell Garnett, 1904). By contrast with the previous case, the lowest-order term now provides the renormalization of the wave number in the effective medium, structural correlations appearing at the next order. The factor f_L is a local-field correction coming from the fact that the fluctuation of polarizability ($\Delta\alpha$ in δ_α^2) is evaluated with respect to the host medium. Following again the same steps as those leading to Eq. (53), noting that ϵ_{MG} is real in the quasi-static limit for non-absorbing

media, and showing that

$$\text{Im}\hat{\mathbf{G}}_h(\mathbf{k}) = \pi f_L \delta(k^2 - k_{\text{MG}}^2) \mathbf{P}(\mathbf{u}), \quad (76)$$

see Appendix A.2, we eventually obtain

$$\frac{1}{\ell_e} = \frac{k_0^4}{8\pi k_{\text{MG}}^2} f_L^2 \delta_\epsilon^2 \int_0^{2k_{\text{MG}}} P\left(\frac{q}{2k_{\text{MG}}}\right) h_\alpha(q) q dq, \quad (77)$$

with $q = k_{\text{MG}}|\mathbf{u} - \mathbf{u}'|$. The expression for ℓ_e takes the same form as previously with the permittivity of the homogeneous medium around the fluctuations being given by the Maxwell-Garnett mixing rule and a prefactor to account for local-field corrections.

All in all, the similarity between Eqs. (53), (71) and (77) demonstrates the deep physical implication of structural correlations for light scattering, whatever the effective medium approach used.

5. Expressions for the scattering and transport mean free paths from the average intensity

We conclude this part on continuous permittivity media by deriving the expressions for ℓ_s and ℓ_t from the theory for the average intensity. An expansion of the intensity vertex \mathbf{I} in Eq. (23) with \mathcal{T} given by Eq. (18) to the first two orders leads to

$$\mathbf{I} \sim \langle \mathcal{T} \mathcal{T}^* \rangle - \langle \mathcal{T} \rangle \langle \mathcal{T}^* \rangle \sim \langle \mathcal{X} \mathcal{X}^* \rangle - \langle \mathcal{X} \rangle \langle \mathcal{X}^* \rangle. \quad (78)$$

This expansion is valid in the weak extinction limit $k_r \ell_e \gg 1$. Similarly to the case of weakly fluctuating media, we set the auxiliary background permittivity as $\epsilon_b = \langle \epsilon \rangle \equiv \epsilon_{\text{av}}$, such that $\langle \mathcal{X} \rangle = 0$, and assume a non-absorbing material. This leads to

$$\bar{\mathbf{I}}(k_{\text{av}}\mathbf{u}, k_{\text{av}}\mathbf{u}', k_{\text{av}}\mathbf{u}, k_{\text{av}}\mathbf{u}') = k_0^4 \epsilon_{\text{av}}^2 \delta_\epsilon^2 h_\epsilon(k_{\text{av}}|\mathbf{u} - \mathbf{u}'|) \times \mathbf{1} \otimes \mathbf{1}. \quad (79)$$

The scattering mean free path is then obtained by integrating Eq. (38) over \mathbf{u}' , leading to

$$\frac{1}{\ell_s} = \frac{k_0^4}{8\pi k_{\text{av}}^2} \epsilon_{\text{av}}^2 \delta_\epsilon^2 \int_0^{2k_{\text{av}}} P\left(\frac{q}{2k_{\text{av}}}\right) h_\epsilon(q) q dq, \quad (80)$$

with $q = k_{\text{av}}|\mathbf{u} - \mathbf{u}'|$. Similarly, the transport mean free is obtained by calculating the average cosine of Eq. (38) and using Eqs. (41)-(42),

$$\frac{1}{\ell_t} = \frac{k_0^4}{16\pi k_{\text{av}}^4} \epsilon_{\text{av}}^2 \delta_\epsilon^2 \int_0^{2k_{\text{av}}} P\left(\frac{q}{2k_{\text{av}}}\right) h_\epsilon(q) q^3 dq. \quad (81)$$

In absence of absorption, one should have $\ell_s = \ell_e$ which is exactly what we obtain here comparing Eqs. (80) and (53).

C. Particulate media

1. Expansion for identical scatterers

Let us now consider in detail a system whose morphology consists in localized (i.e., compact) permittivity variations in a uniform background. We take the most natural choice for the background permittivity $\epsilon_b = \epsilon_h$ from the start but the theory can also be developed with an arbitrary ϵ_b . We also restrict the discussion to composite media made of *identical* inclusions with relative permittivity ϵ_p circumscribed in a volume v , centered at positions $\mathbf{R} = [\mathbf{R}_1, \mathbf{R}_2, \dots, \mathbf{R}_N]$. The medium permittivity then reads

$$\epsilon(\mathbf{r}) = \sum_j \epsilon_p(\mathbf{r} - \mathbf{R}_j) \Theta(a - |\mathbf{r} - \mathbf{R}_j|). \quad (82)$$

The particle configuration is described statistically by the probability distribution function $p(\mathbf{R})$. Implicitly, we neglect here the possibility to have orientational correlations between particles (otherwise, the distribution should include orientational variables). Under the ergodic hypothesis, defining the statistical average as an average over all possible particle positions as $\langle \mathbf{f}(\mathbf{R}) \rangle = \int \mathbf{f}(\mathbf{R}) p(\mathbf{R}) d\mathbf{R}$, where $\mathbf{f}(\mathbf{R})$ is an arbitrary tensor, the statistical properties of the medium can be described by n -particle probability density functions (Lebowitz and Percus, 1963; Tsang *et al.*, 2004)

$$\rho_n(\mathbf{r}_1, \dots, \mathbf{r}_n) = \left\langle \sum_{j_1 \neq j_2 \dots \neq j_n} \delta(\mathbf{r}_1 - \mathbf{R}_{j_1}) \dots \delta(\mathbf{r}_n - \mathbf{R}_{j_n}) \right\rangle, \quad (83)$$

or equivalently by n -particle correlation functions

$$g_n(\mathbf{r}_1, \dots, \mathbf{r}_n) = \frac{1}{\rho^n} \rho_n(\mathbf{r}_1, \dots, \mathbf{r}_n), \quad (84)$$

where ρ is the constant particle number density reached in the limit of infinite system size ($\rho = \lim_{N, V \rightarrow \infty} N/V$).

Similar to the case of random media described by a continuous permittivity, the first step is to derive an expression for the transition operator \mathcal{T} of the medium. The fact to have a discrete set of identical particles allows us to express the multiple-scattering problem in such a way as to separate the effects associated to (local) particulate resonances and (non-local) structural correlations on light scattering. We start by rewriting the integral equation for the total field, Eq. (16) using integral operators, for particulate media,

$$\mathbf{E} = \mathbf{E}_h + \sum_j \mathcal{G}_h \mathcal{X}_j \mathbf{E}, \quad (85)$$

with the effective scattering potential $\mathcal{X}_j(\mathbf{r} - \mathbf{R}_j) \equiv k_0^2 [\epsilon_p(\mathbf{r} - \mathbf{R}_j) \Theta(a - |\mathbf{r} - \mathbf{R}_j|) - \epsilon_h] \mathbf{1}$. We can then express the polarization induced in particle j in terms of

the polarization induced in all particles as

$$\mathbf{x}_j \mathbf{E} = \mathbf{x}_j \mathbf{E}_h + \mathbf{x}_j \sum_k \mathbf{g}_h \mathbf{x}_k \mathbf{E}, \quad (86)$$

$$= \mathbf{x}_j \mathbf{E}_h + \mathbf{x}_j \mathbf{g}_h \mathbf{x}_j \mathbf{E} + \mathbf{x}_j \sum_{k \neq j} \mathbf{g}_h \mathbf{x}_k \mathbf{E}, \quad (87)$$

$$= \mathcal{T}_j \mathbf{E}_h + \mathcal{T}_j \sum_{k \neq j} \mathbf{g}_h \mathbf{x}_k \mathbf{E}. \quad (88)$$

In the second expression, we separated the contribution from the particle j on itself and the contribution from all other particles. The last expression was obtained by introducing the transition operator \mathcal{T}_j of an individual particle centered at \mathbf{R}_j as

$$\mathcal{T}_j = \mathbf{x}_j [\mathbf{1} - \mathbf{g}_h \mathbf{x}_j]^{-1}. \quad (89)$$

Very importantly, \mathcal{T}_j can be determined for particles of virtually any size, shape and composition, either analytically using Mie theory for simple geometries like spherical particles (Bohren and Huffman, 2008) or numerically by any method for solving Maxwell's equations otherwise (Mishchenko *et al.*, 2000). This allows considering strongly resonant particles exhibiting high-order multipolar resonances as the building blocks of the disordered medium.

Inserting Eq. (88) into Eq. (85) and iterating over scattering sequences, we reach an expression for the transition operator \mathcal{T} of the entire system [Eq. (17)] in terms of the transition operator of the individual particle, as

$$\begin{aligned} \mathcal{T} &= \sum_j \mathcal{T}_j + \sum_j \mathcal{T}_j \sum_{k \neq j} \mathbf{g}_h \mathcal{T}_k \\ &+ \sum_j \mathcal{T}_j \sum_{k \neq j} \mathbf{g}_h \mathcal{T}_k \sum_{l \neq k} \mathbf{g}_h \mathcal{T}_l + \dots \end{aligned} \quad (90)$$

This series expansion is the root of multiple scattering theory for particulate media and was introduced in the pioneering work of Kirkwood and Yvon as early as 1936 (Kirkwood, 1936; Yvon, 1937) to determine the permittivity of molecular liquids. Similar multiple scattering equations were later discussed by Foldy and Lax (Foldy, 1945; Lax, 1951). It is further interesting to note the occurrence of so-called “recurrent scattering”, that is, scattering sequences that involve the same particle multiple times (for instance, l can be equal to j in the last displayed term). The series in Eq. (90) can in fact be rewritten as a “cluster” expansion according to the number of particles involved in each term (Felderhof *et al.*, 1982; Finkel'berg, 1964).

It is interesting to remark that the Green function in Eq. (89) for the transition operator \mathcal{T}_j of a specific particle j always connects two points that belong to the same particle, whereas the Green function in Eq. (90) for the transition operator \mathcal{T} of the entire system always connects two points that belong to different particles. This

is conceptually analogous to Eq. (55) for continuous permittivity media where the Green function was split into local and non-local terms. To determine the self-energy $\tilde{\Sigma}$ in Dyson equation [Eq. (19)], we may then follow the same strategy as done for continuous permittivity media and consider the exciting field \mathbf{E}_{exc} . Let us then write the Green function \mathbf{g}_h as \mathbf{g}_h when connecting two points in the same particle and $\tilde{\mathbf{g}}_h$ otherwise. Removing the local contribution on the induced polarization in Eq. (87) and rewriting $\mathbf{x}_k \mathbf{E}$ in terms of the exciting field leads to

$$\mathbf{x}_j \mathbf{E}_{\text{exc}} = \mathbf{x}_j \mathbf{E}_h + \mathbf{x}_j \sum_k \tilde{\mathbf{g}}_h \tilde{\mathcal{T}}_k \mathbf{E}_{\text{exc}}, \quad (91)$$

with $\tilde{\mathcal{T}}_j = \mathbf{x}_j [\mathbf{1} - \mathbf{g}_h \mathbf{x}_j]^{-1} = \mathcal{T}_j$, see Eq. (89). Note that the sum now runs over all particles k . Further defining $\tilde{\mathcal{T}} \equiv \sum_j \tilde{\mathcal{T}}_j$, we naturally recover Eq. (59) for continuous media,

$$\mathcal{T} = \tilde{\mathcal{T}} [\mathbf{1} - \tilde{\mathbf{g}}_h \tilde{\mathcal{T}}]^{-1}. \quad (92)$$

Expanding the self-energy $\tilde{\Sigma}$ for the average exciting field near $\langle \tilde{\mathcal{T}} \rangle = \tilde{\mathcal{T}} - \Delta \tilde{\mathcal{T}}$ then leads to Eq. (66), and expanding Σ near $\tilde{\Sigma}_1$ to Eq. (68).

The problem of scattering by particulate media is thus described in a strictly similar manner to that of scattering by strongly fluctuating continuous permittivity media (i.e., including local-field corrections). The essential difference is the fact that the volume elements composing the continuous medium are no longer vanishingly small but actual scattering particles of a finite size.

Recall that Eq. (66) is reached by neglecting particle correlations beyond the second order. Higher-order particle correlations may yet be taken into account by treating them as sequences of two-particle correlations (which is formally exact for crystalline media). This is the so-called quasicrystalline approximation (QCA) originally due to Lax (1952), further developed by Fikioris and Waterman (1964) and Tsang and Kong (1980, 1982) among others, and used nowadays in various contexts (Gower *et al.*, 2018; Kristensson, 2015; Tsang *et al.*, 2000; Wang and Zhao, 2018).

2. Extinction mean free path and effective medium theories

Writing the transition operator of an individual particle as $\mathcal{T}_j \equiv \mathbf{T}_0(\mathbf{r} - \mathbf{R}_j, \mathbf{r}' - \mathbf{R}_j)$, we obtain for the lowest order in Eq. (66), $\tilde{\Sigma}_1 \equiv \langle \tilde{\mathcal{T}} \rangle = \langle \sum_j \tilde{\mathcal{T}}_j \rangle$,

$$\tilde{\Sigma}_1(\mathbf{r} - \mathbf{r}') = \rho \int \mathbf{T}_0(\mathbf{r} - \mathbf{r}_p, \mathbf{r}' - \mathbf{r}_p) d\mathbf{r}_p. \quad (93)$$

This term leads to the extinction (optical) theorem for uncorrelated particle assemblies at vanishingly small particle densities, which relates the extinction mean free path to the forward scattering characteristics of the in-

dividual particle, $\ell_e^{-1} \sim \rho (\mathbf{e} \cdot \text{Im}[\mathbf{T}_0(k_h \mathbf{u}, k_h \mathbf{u})\mathbf{e}] / k_h$.

For the second order, $\tilde{\Sigma}_2 \equiv \langle \Delta \tilde{\mathcal{T}} \hat{\mathcal{G}}_h \Delta \tilde{\mathcal{T}} \rangle = \langle \tilde{\mathcal{T}} \hat{\mathcal{G}}_h \tilde{\mathcal{T}} \rangle - \langle \tilde{\mathcal{T}} \rangle \hat{\mathcal{G}}_h \langle \tilde{\mathcal{T}} \rangle$, we get

$$\begin{aligned} \tilde{\Sigma}_2(\mathbf{r} - \mathbf{r}') &= \rho \int [\delta(|\mathbf{r}_p - \mathbf{r}_q|) + \rho h_2(|\mathbf{r}_p - \mathbf{r}_q|)] \\ &\quad \times \mathbf{T}_0(\mathbf{r} - \mathbf{r}_p, \mathbf{r}'' - \mathbf{r}_p) \hat{\mathcal{G}}_h(\mathbf{r}'' - \mathbf{r}''') \\ &\quad \times \mathbf{T}_0(\mathbf{r}''' - \mathbf{r}_q, \mathbf{r}' - \mathbf{r}_q) d\mathbf{r}'' d\mathbf{r}''' d\mathbf{r}_p d\mathbf{r}_q, \end{aligned} \quad (94)$$

where

$$h_2(\mathbf{r}) \equiv g_2(\mathbf{r}) - 1 \quad (95)$$

is the total pair correlation function and g_2 is defined from Eq. (84).

To reach a general expression for the self-energy Σ via Eq. (68), we need to define the operator \mathcal{G}_h that describes the local propagation of radiation within each particle. As first pointed out by Sullivan and Deutch (Sullivan and Deutch, 1976), \mathcal{G}_h may be chosen to obtain different lowest order results for the effective permittivities and refractive index, such as Maxwell-Garnett (Bedeaux and Mazur, 1973; Felderhof, 1974), Onsager-Bütcher (Böttcher *et al.*, 1978; Hynne and Bullough, 1987; Onsager, 1936) or Wertheim (Wertheim, 1973). Differences vanish when all orders of the expansion are taken into account, but the rate of convergence of the different formulations is influenced by the particular choice of the Green function (Bedeaux and Mazur, 1973; Bedeaux *et al.*, 1987; Geigenmüller and Mazur, 1986; Sullivan and Deutch, 1976).

For pedagogical reasons, we restrict ourselves here to the Maxwell-Garnett result obtained in the long-wavelength limit. For some applications dealing with particles with complex shapes and relatively low scattering contrast, one can simplify the problem using the well-known Rayleigh-Gans approximation (Bohren and Huffman, 2008) or subsequent generalizations (Acquista, 1976). In this framework, the transition operator can be written as

$$\mathbf{T}_0(\mathbf{r} - \mathbf{R}_j, \mathbf{r}' - \mathbf{R}_j) = k_h^2 \frac{\alpha_p}{v} \Theta[a - |\mathbf{r} - \mathbf{R}_j|] \delta(\mathbf{r} - \mathbf{r}') \mathbf{1} \quad (96)$$

with α_p the particle polarizability. Inserting this expression in Eqs. (93) and (94) straightforwardly leads to an expression for the self-energy that reads in reciprocal space as

$$\begin{aligned} \Sigma(\mathbf{k}) &= k_0^2 (\epsilon_{\text{MG}} - \epsilon_h) \mathbf{1} + \rho \frac{k_h^4 \alpha_p^2}{\epsilon_h \alpha_p} \frac{\partial \epsilon_{\text{MG}}}{\partial \rho} \\ &\quad \times \int S(|\mathbf{k} - \mathbf{k}'|) \left| \frac{3j_1(|\mathbf{k} - \mathbf{k}'|a)}{|\mathbf{k} - \mathbf{k}'|a} \right|^2 \hat{\mathcal{G}}_h(\mathbf{k}') \frac{d\mathbf{k}'}{(2\pi)^3}. \end{aligned} \quad (97)$$

j_n is the spherical Bessel function of the first kind and order n , ϵ_{MG} is the Maxwell-Garnett permittivity given by Eq. (75) with $\alpha_0 \equiv \alpha_p$, and

$$S(\mathbf{k}) \equiv 1 + \rho h_2(\mathbf{k}), \quad (98)$$

is the *static structure factor*, probably the most famous quantity for light scattering studies in correlated disordered media, as we will see throughout this review.

Following the same steps as those for continuous permittivity random media, assuming non-absorbing materials, we eventually reach a simple expression for the extinction mean free path,

$$\frac{1}{\ell_e} = \frac{2\pi\rho}{k_{\text{MG}}^4} \int_0^{2k_{\text{MG}}} F(q) S(q) q dq, \quad (99)$$

with $q = k_{\text{MG}} |\mathbf{u} - \mathbf{u}'|$. We have defined here the form factor

$$F(q) = k_{\text{MG}}^2 \frac{d\sigma}{d\Omega} \left(\frac{q}{2k_{\text{MG}}} \right) f_L^2 \left| \frac{3j_1(qa)}{qa} \right|^2, \quad (100)$$

and the Rayleigh differential scattering cross-section

$$\frac{d\sigma}{d\Omega}(k) = k_h^4 \frac{\alpha_p^2}{(4\pi)^2} P(k), \quad (101)$$

where $P(k)$ is given by Eq. (54).

Remarkably, the respective contributions of the individual scattering elements, via the form factor $F(q)$, and of their spatial arrangement, via the structure factor $S(q)$, on the extinction (or scattering) strength of the medium are treated independently. Structural correlations act as a weighting function to the optical response of a random (uncorrelated) assembly of identical scatterers, physically due to far-field interference between pairs of particles.

Equation (99) was obtained here in the long-wavelength limit, for small (non-resonant) particles. The more general situation of resonant particles is significantly more difficult to address within the theory for the average field. A heuristic extension of the Maxwell-Garnett approximation to resonant dipolar particles has been proposed by (Doyle, 1989) and further analyzed in (Grimes and Grimes, 1991; Rupp, 2000). The approach provides some understanding to the spectral resonances observed in certain light scattering experiments. A more rigorous framework is given by the so-called Coherent Potential Approximation (CPA) (Tsang and Kong, 2001; Tsang and Kong, 1980), which may be seen as a generalization of the approach leading to the Bruggeman mixing rule for continuous permittivity media, as presented above. Considering scattering elements that are not only the particles but also the host medium, one looks for an auxiliary background permittivity ϵ_b such that the average transition operator vanishes $\langle \mathcal{T} \rangle = 0$, or equivalently that the background Green function \mathcal{G}_b equals the actual

averaged Green function $\langle \mathcal{G} \rangle$. Different CPA-like models have been developed based on different self-consistent conditions (Busch and Soukoulis, 1995; Soukoulis *et al.*, 1994).

3. Scattering and transport mean free paths for resonant scatterers

In this last part, we show that the case of resonant particles can be more easily solved within the theory for the average intensity. For this, we assume that a solution for the real part of the effective index, k_r , exists. In the weak extinction limit (i.e. $k_r \ell_e \gg 1$) and using the expansion of the transition operator \mathcal{T} in Eq. (90), the intensity vertex given by Eq. (23) can be reduced to its lowest order terms as

$$\begin{aligned} \Gamma &\sim \langle \mathcal{T} \mathcal{T}^* \rangle - \langle \mathcal{T} \rangle \langle \mathcal{T}^* \rangle \\ &\sim \left\langle \sum_{i,j} \tau_i \tau_j^* \right\rangle - \left\langle \sum_i \tau_i \right\rangle \left\langle \sum_j \tau_j^* \right\rangle. \end{aligned} \quad (102)$$

In Fourier space, this leads to

$$\bar{\Gamma}(k_r \mathbf{u}, k_r \mathbf{u}', k_r \mathbf{u}, k_r \mathbf{u}') = \rho \mathbf{T}_0(k_r \mathbf{u}, k_r \mathbf{u}') \otimes \mathbf{T}_0^*(k_r \mathbf{u}, k_r \mathbf{u}') \times S(k_r(\mathbf{u} - \mathbf{u}')). \quad (103)$$

In the radiative transfer limit, taking the on-shell approximation and using Eqs. (38)-(39) leads to

$$\frac{1}{\ell_s} = \frac{\rho}{16\pi^2} \int |\mathbf{P}(\mathbf{u}) \mathbf{T}_0(k_r \mathbf{u}, k_r \mathbf{u}') \mathbf{e}'|^2 S(k_r(\mathbf{u} - \mathbf{u}')) d\mathbf{u} \quad (104)$$

where \mathbf{e}' is the polarization vector perpendicular to \mathbf{u}' . This expression is valid for a spherical particle of arbitrary size. Notice also that \mathbf{T}_0 is evaluated for the incident and scattered wavevectors not in the host medium but in the *effective* medium, i.e. with wavenumber k_r . Equation (104) can eventually be reformulated using the form factor

$$F(q) = k_r^2 \frac{d\sigma}{d\Omega}(q), \quad (105)$$

where $q = k_r |\mathbf{u} - \mathbf{u}'|$ and the differential scattering cross-section is now defined as

$$\frac{d\sigma}{d\Omega}(q) = \frac{1}{16\pi^2} |\mathbf{P}(\mathbf{u}) \mathbf{T}_0(k_r |\mathbf{u} - \mathbf{u}'|) \mathbf{e}'|^2. \quad (106)$$

This leads to

$$\frac{1}{\ell_s} = \frac{2\pi\rho}{k_r^4} \int_0^{2k_r} F(q) S(q) q dq, \quad (107)$$

The approaches based on the average field and the average intensity lead to the same final expressions [Eqs. (99) and (107), respectively] for non-absorbing media.

A similar derivation using Eqs. (38), (41) and (42) fi-

nally leads to a closed-form expression of the transport mean free path,

$$\frac{1}{\ell_t} = \frac{\pi\rho}{k_r^6} \int_0^{2k_r} F(q) S(q) q^3 dq. \quad (108)$$

Equations (107) and (108) are surely the most widely-used expressions in the literature on light scattering and transport in correlated disordered media (Fraden and Maret, 1990; Reufer *et al.*, 2007; Rojas-Ochoa *et al.*, 2004). These two expressions, originally derived from phenomenological arguments, have been obtained here within a rigorous theoretical framework.

D. Summary and further remarks

The literature on multiple light scattering theory is vast and many approaches have been developed throughout the years. We adopted here a unique theoretical framework that can handle both families of systems described by a continuous permittivity that fluctuates in space or by a set of identical particles that are randomly arranged in space. This has the great benefit of highlighting the main physical principles behind the role of spatial correlations on light scattering and transport, as well as the underlying approximations. Analytical expressions for the characteristic lengths were obtained in the weak extinction limit ($k_r \ell_e \gg 1$, with k_r the effective wave number and ℓ_e the extinction mean free path), and considering non-absorbing media such that the extinction is only due to scattering ($\ell_e = \ell_s$).

For media described by a continuous permittivity, the scattering mean free path is given by Eq. (71) or Eq. (77). The expression to use depends on the choice of the “reference” homogeneous medium around which the permittivity fluctuates: the former is thus associated to the Bruggeman mixing rule and the latter to the Maxwell-Garnett mixing rule. The common ground that links these two approaches, as discussed for instance by Mackay and Lakhtakia (2015), is often overlooked.

For assemblies of small identical and non-absorbing particles, the scattering mean free path is instead given by Eq. (99). A comparison with Eq. (77) unveils a fundamental concept, namely that a fluid of tiny identical particles with a fluctuating density (e.g., a fluid of molecules) can be assimilated to a continuous medium with a fluctuating permittivity (or polarizability). Indeed, taking the limit $qa \rightarrow 0$ in Eq. (99), one finds the equivalence

$$\langle \Delta\rho(\mathbf{r}) \Delta\rho(\mathbf{r}') \rangle \alpha_p^2 \equiv \langle \Delta\alpha(\mathbf{r}) \Delta\alpha(\mathbf{r}') \rangle / v^2. \quad (109)$$

This is the reason why Rayleigh’s and Einstein’s quantitative results on the mean free paths (explaining the blue color of the sky) were essentially identical (Einstein, 1910; Rayleigh, 1899).

Finally, for assemblies of large, possibly resonant par-

ticles, the scattering and transport mean free paths are respectively given by Eqs. (107) and (108). These expressions were derived from a theory for the average intensity in the large-scale approximation. Their strength lies in the fact that the contributions from the individual particles and from structural correlations are treated separately, thereby providing considerable physical insight.

III. STRUCTURAL PROPERTIES OF CORRELATED DISORDERED MEDIA

Correlated disordered media can exhibit a rich variety of complex morphologies, which will impact light scattering and transport in many different ways. This section is concerned with the statistical description of the structural properties of these materials. For a more complete and thorough description, we recommend the textbook by Torquato (2013). After comparing the quantities describing spatial correlations and derived in the previous section on realistic systems [Sec. III.A] and introducing a fundamental relation between fluctuations of particle number and spatial correlations in point patterns [Sec. III.B], we define the main classes of correlated disordered media according to their pair correlation function $g_2(r)$ and structure factor $S(q)$ [Sec. III.C]. We then review the main techniques to construct numerically [Sec. III.D] and fabricate experimentally [Sec. III.E] such complex materials in practice. The section is concluded with a brief summary of the experimental techniques to characterize structural correlations in real materials [Sec. III.F].

A. Continuous permittivity versus particulate models in practice

As shown in the previous section, light scattering in correlated disordered media can be described either by a continuous permittivity model that relies on a spatial permittivity correlation function or by a particulate model that relies on a two-point correlation function in the specific case of localized permittivity variations. To start this section, it is interesting to compare these two pictures in practical cases.

We consider a classical and very relevant example for photonics, that is a 2D assembly of impenetrable disks (diameter a) at two different packing fractions $p = 0.10$ and 0.50 , see Fig. 3. The disk packings were generated with a compression algorithm (Skoge *et al.*, 2006) that will be briefly described in Sec. III.D. The top-left panel of Fig. 3 shows the permittivity correlation function $g_\epsilon(|\mathbf{r} - \mathbf{r}'|) = h_\epsilon(|\mathbf{r} - \mathbf{r}'|) + 1$ for the disk packings. The function first displays a rapid decrease of correlation followed by regular, vanishing oscillations. The very short-range correlation here is mostly associated to the finite size of the disks and the oscillations, which are

stronger for higher packing fractions, are a signature of correlations between neighboring particles.

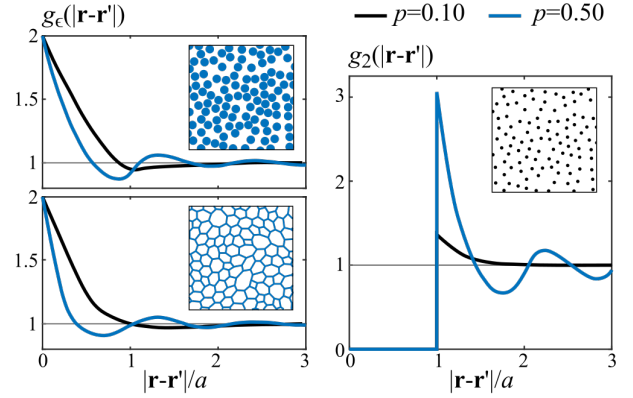


FIG. 3 Description of structural correlations for hard disk (diameter a) packings at packing fractions $p = 10\%$ (black curves) and $p = 50\%$ (blue curves). (Left) Correlation function $g_\epsilon(r) = h_\epsilon(r) + 1$ describing correlations due to the finite-size of the disks and to their positional correlation, for two different topologies: (top) a packing of disks and (bottom) a continuous network. (Right) Pair correlation function $g_2(r) = h_2(r) + 1$, which describe only the positional correlation between the disk centers.

The generated disk positions can also serve as a basis to generate more complex structures. An example often encountered in photonics is based on Delaunay tessellations (described in Sec. III.D). In the bottom-left panel of Fig. 3, we show the permittivity correlation function for these “inverted” structures, as generated from the disk packing above. Strikingly, the behavior of the correlation functions are very similar to those of the disk packing. The major difference is observed at small distances due to a very different morphology, but the curves become indistinguishable for $|\mathbf{r} - \mathbf{r}'| \gtrsim a$.

Finally, we can consider the pair-correlation function $g_2(|\mathbf{r} - \mathbf{r}'|)$. The results are shown in the right panel of Fig. 3. The pair-correlation function for the disk packing is zero for $|\mathbf{r}_a - \mathbf{r}_b|$ between 0 to $2R$ due to the impenetrability of the disks, and exhibits strong oscillations indicating structural correlations in the relative position between particles. Note that the amplitude of the oscillations is much larger than for $g_\epsilon(|\mathbf{r} - \mathbf{r}'|)$.

This simple comparison quite importantly shows that the use of the two-point permittivity correlation is hardly sufficient to distinguish very different disordered media. In fact, the permittivity correlation of the inverted disk structure at $p = 0.50$ would be strictly identical to that of the direct structure by definition, while light scattering would evidently be markedly different. This is a strong indication that scattering is both dramatically affected by the local morphology of the system, which yields optical resonances, and by structural correlations in the relative position between scattering elements. Although the

definition of a “scattering element” is questionable for inverted structures such as connected networks, we will focus on the particulate description of scattering media in the remainder of this section.

B. Fluctuation-correlation relation

The description of point patterns underlying the structure of correlated disordered media is central, and many descriptors may be used in general.

An important attribute of point patterns is the variance of the number N of points contained within windows Ω_i with volume V and shifted by \mathbf{r} . This quantity has a long history, several derivations are found for both continuous and discrete disorder models (de Boer, 1949; Landau and Lifshitz, 1980; Martin and Yalcin, 1980; Ornstein and Zernike, 1914; Torquato and Stillinger, 2003; Van Kranendonk and Sipe, 1977). Probabilistic calculations eventually lead to a closed-form expression for the variance of N

$$\frac{\langle N^2(\mathbf{r}, \Omega) \rangle - \langle N(\mathbf{r}, \Omega) \rangle^2}{\langle N(\mathbf{r}, \Omega) \rangle} = 1 + \rho \int_{\Omega_1 \cap \Omega_2} h_2(\mathbf{r}) d\mathbf{r} \quad (110)$$

where $h_2(\mathbf{r}) = g_2(\mathbf{r}) - 1$ is again the total correlation function and the integral is performed over the intersection volume between the two shifted windows (Torquato and Stillinger, 2003). Equation (110) requires $h_2(\mathbf{r})$ to be integrable on the intersection volume and go to 0 at large distances r . Interestingly, in the limit of large windows, one finds that (Torquato and Stillinger, 2003)

$$\lim_{V \rightarrow \infty} \frac{\langle N^2(\mathbf{r}, \Omega) \rangle - \langle N(\mathbf{r}, \Omega) \rangle^2}{\langle N(\mathbf{r}, \Omega) \rangle} = \lim_{|\mathbf{q}| \rightarrow 0} S(\mathbf{q}), \quad (111)$$

which corresponds to the simplified definition given in Appendix C.2.

Equations (110) and (111) are remarkable in that they describe the spatial fluctuations in the number of points in the pattern from its pair correlation between points – or equivalently, its structure factor near 0, which is a measurable quantity (e.g., by small-angle scattering, see Sec. III.F). A Poisson point pattern $p_N = \langle N \rangle^N \exp[-\langle N \rangle]/N!$ yields $\langle N^2 \rangle = \langle N \rangle + \langle N \rangle^2$, which, as expected, corresponds to a fully uncorrelated system with $h_2(\mathbf{r}) = 0$ or $\lim_{|\mathbf{q}| \rightarrow 0} S(\mathbf{q}) = 1$. Implementing structural correlations at constant density ρ therefore results into weaker or stronger point density fluctuations. Negative correlations are obtained when $\rho \int_{\Omega_1 \cap \Omega_2} h_2(\mathbf{r}) d\mathbf{r} < 0$, leading to a sub-Poissonian fluctuations, while positive correlations are obtained when $\rho \int_{\Omega_1 \cap \Omega_2} h_2(\mathbf{r}) d\mathbf{r} > 0$, leading to a super-Poissonian fluctuations. In the literature, such structures are sometimes denoted as negatively- and positively-correlated, respectively (Davis and Mineev, 2008). As illustrated in Fig. 4, they correspond to situations in which the points either

repel or attract themselves. As we will see in Sec. IV, the impact of negative and positive correlations on optical transport are markedly different.

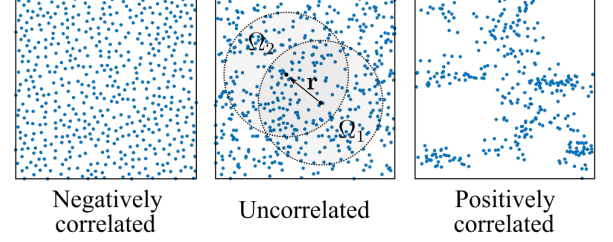


FIG. 4 Illustration of the fluctuation-correlation relation with three point patterns: (left) A negatively-correlated disordered medium, where points tend to repel themselves; (middle) A Poisson point pattern, that is uncorrelated; (right) A positively-correlated disordered medium, wherein clustering is present. Two windows denoted as Ω_1 and Ω_2 in which a number of points is counted are shifted by \mathbf{r} .

C. Classes of correlated disordered media

Figure 5 summarizes the most important classes of correlated disordered media and their properties, that we will now describe specifically.

1. Short-range correlated disordered structures

Consider a volume containing a disordered ensemble of mobile, impenetrable particles – i.e. a fluid of hard particles – at a low density. With increasing particle density, the particles tend to organize themselves to fill space. In this regime of low to moderate densities, the system exhibits no structural correlation in the long range yet the impenetrability of the particles impose a short-range correlation that increases with the packing fraction (Hansen and McDonald, 1990). As shown in Fig. 5 (1st column), short-range structural correlations give rise to decaying oscillations in the pair correlation function g_2 . The most likely distance to find a neighboring particle is given by the position of the first peak and the decay of the higher-order peaks, which is generally rapid, allows defining a correlation length. In reciprocal space, such oscillations are also observed. When increasing short-range correlations, the structure factor goes from a flat response around 1 to sharper peaks whose amplitudes decrease with increasing q . Short-range structural correlations can be described, for instance, by analytical or semi-analytical solutions of the Ornstein-Zernike equation using the so-called Percus-Yevick approximation (Percus and Yevick, 1958; Wertheim, 1963) in three dimensions and the Baus-Colot approximation in two dimensions (Baus and Colot, 1987), respectively. At higher

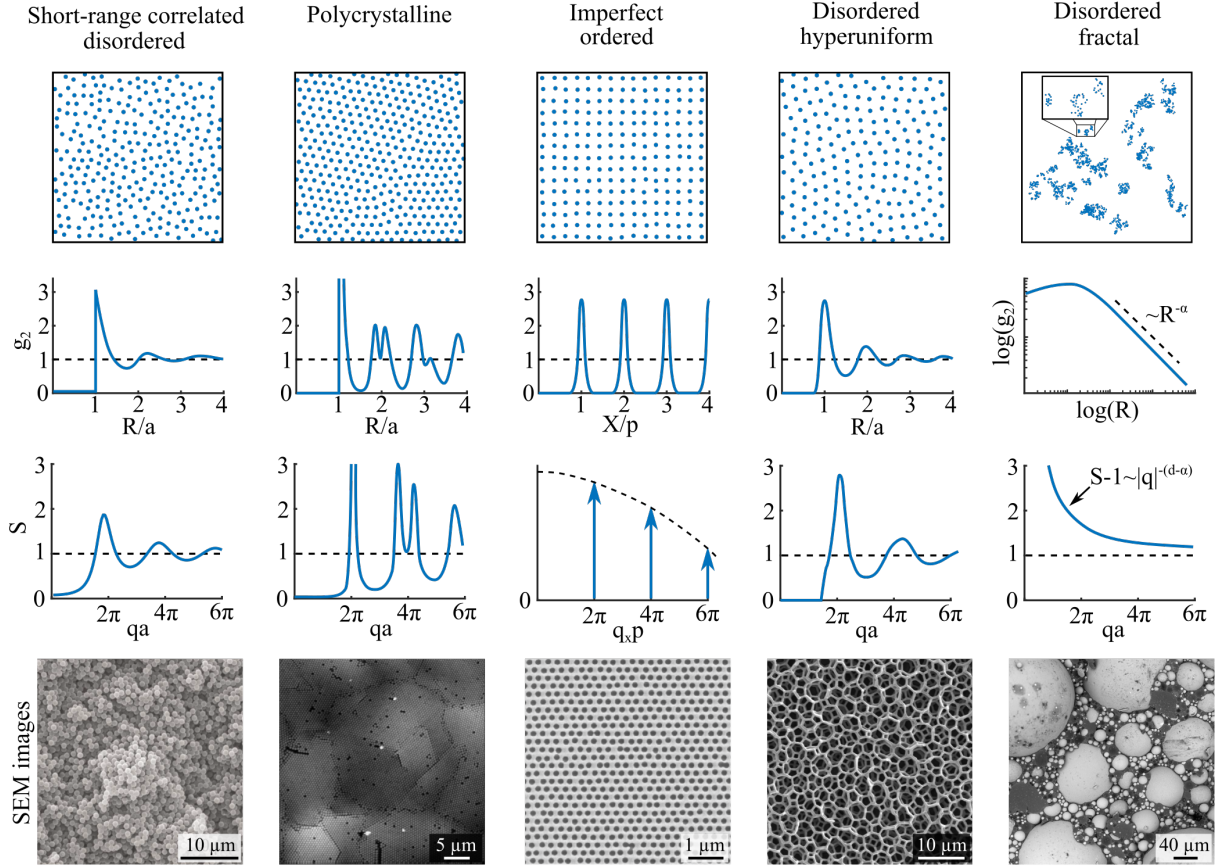


FIG. 5 Classes of correlated disordered media. (From top to bottom) Illustration of a correlated disordered medium; Pair correlation function; Structure factor; SEM image of a fabricated correlated disordered structure. (From left to right) Disordered short-range correlated structures, SEM image Adapted with permission from (García *et al.*, 2008); Polycrystalline structure, SEM image Adapted with permission from (Salvarezza *et al.*, 1996); Imperfect ordered structures, SEM image Adapted with permission from (García *et al.*, 2012); Disordered hyperuniform structures, SEM image Adapted with permission from (Haberkorn and Scheffold, 2013); Disordered hierarchical structures, SEM image Adapted with permission from (Burrelli *et al.*, 2012).

densities, these models become less accurate, although, for slightly polydisperse systems, errors appear to cancel, and predictions by Percus-Yevick approximation can describe experimental data up to random close packing or jamming (Frenkel *et al.*, 1986; Scheffold and Mason, 2009).

Short-range correlated disordered systems constitute the primary class found in colloidal systems with isotropic interactions, since short-range correlations stem from the impenetrability of particles in suspension. Interestingly, densely packed sphere assemblies are also hyperuniform, but not stealthy (Zachary *et al.*, 2011), for details see section III.C.4. The behavior of other repulsive particles, such as charge-stabilized particles, can often be mapped onto the isotropic hard-sphere case (Gast and Russel, 1998; Pusey and Van Megen, 1986). The recent advent of colloids interacting via sticky patches could open a pathway towards more complex structures through self-assembly (He *et al.*, 2020).

In general, short-range structural correlations are not

limited to sphere assemblies but can also be encoded in connected networks (Florescu *et al.*, 2009; Liew *et al.*, 2011; Muller *et al.*, 2013), in which case the individual scattering centers are more difficult to identify. This form of correlated structure is widespread in natural photonic structures such as bird feathers (Saranathan *et al.*, 2012) and very popular in artificial photonic structures fabricated by top-down techniques (Liew *et al.*, 2011; Riboli *et al.*, 2014). Dry foams are promising candidates for correlated network structures that can be made by self-assembly (Ricouvier *et al.*, 2019).

2. Polycrystalline structures

For a disordered ensemble of identical hard particles, one reaches a liquid-crystal coexistence at about 49% and a purely crystalline phase for concentrations above 54.5% (Gast and Russel, 1998; Pusey and Van Megen, 1986; Pusey, 1991; Zhu *et al.*, 1997). The equilibrium

structure appears to be face-centered-cubic but hexagonal close packed structures are also observed and are found to be at least meta-stable (Pusey *et al.*, 1989). This liquid to crystal phase transition, also known as the Kirkwood-Alder transition (Gast and Russel, 1998), is purely driven by the higher entropy of the crystalline phase compared to the liquid phase. The densest packing of monodisperse spheres in three dimensions is approximately 74%, also referred to as the close-packing of equal spheres. Monodisperse particles usually assemble in finite-sized crystal clusters. These clusters are randomly arranged and form a polycrystalline materials (Astratov *et al.*, 2002; Yang *et al.*, 2010b), see Fig. 5 (2nd column). In the bulk, crystallites are formed by homogeneous nucleation throughout the sample (Pusey *et al.*, 1989). The size of the crystal clusters is then typically several tens of μm , much larger than the particle diameter $\sim \lambda$ but smaller than the usual sample size, which is typically in the millimeter to centimeter range. The radially-averaged pair correlation function exhibits peaks indicating the position of the n th-order neighboring particles, as well as minima approaching zero. Positional correlations vanish for distances exceeding the size of the crystal clusters. Similarly, the structure factor shows well-defined Debye-Scherrer rings due to Bragg scattering from randomly oriented crystal planes, that can be identified in light scattering (Pusey *et al.*, 1989), similarly to powder diffraction in X-ray crystallography.

The formation of clusters of regular arrays in fluids of hard particles is strongly influenced by the polydispersity of the particles, since particles of very different sizes do not naturally arrange in a crystal. Indeed, for hard sphere fluids with a polydispersity larger than 6-12%, crystallization is avoided in three dimensions (Pusey, 1987). The spheres remain disordered and particles enter a solid glass phase at about 58%. The glass can be further compressed until the spheres ‘jam’ forming what is known as a “randomly closed packed” or “maximally jammed structure” in the literature (Torquato *et al.*, 2000). The presence of some hidden structural order, crystalline precursors or locally favoured structures in the glass and jammed phase is still being discussed (Zhang *et al.*, 2016).

Due to the unavoidable finite polydispersity, experimental realizations of crystalline photonic structures based on colloidal suspensions are the exception rather than the rule even at high packing fractions. By careful synthesis of colloidal particles made from polystyrene or silica (SiO_2), it is however possible to induce crystallization rather easily (Salvarezza *et al.*, 1996). These materials are usually polycrystalline and display some defects and stacking faults to a varying degree. Polycrystalline structures are also observed in natural photonic structures, such as opals. Interestingly, relatively little is known about the comparison of scattering and light transport between random-close-packed assemblies of spheres and polycrystalline materials (Yang *et al.*,

2010b), in particular when the size of crystallites is gradually reduced to smaller length scales.

3. Imperfect ordered structures

The two previous classes of correlated disorder were obtained by “adding order” into a fully-disordered (uncorrelated) system. Materials with correlated disorder can also be obtained starting from the other limit, that is a periodic system with random perturbations, see Fig. 5 (3rd column). In systems of infinite size, both the pair-correlation function g_2 and the structure factor S are characterized by a series of Dirac peaks located at $\mathbf{r} - \mathbf{r}' = u_1 \mathbf{a}_1 + u_2 \mathbf{a}_2 + u_3 \mathbf{a}_3$ with $u_i \in \mathbb{Z}$ and \mathbf{a}_i the lattice vectors, and $\mathbf{G} = v_1 \mathbf{b}_1 + v_2 \mathbf{b}_2 + v_3 \mathbf{b}_3$ with $v_i \in \mathbb{Z}$ and \mathbf{b}_i the reciprocal lattice vectors, respectively (Joannopoulos *et al.*, 2011; Kittel, 1976). If the position of a point of the lattice is randomly shifted (e.g., with normal distribution) around its nominal position, this results in a broadening of the Dirac peaks with a width that depends on the disorder amplitude. By contrast with the previous classes of disordered systems, disorder in such a periodic-on-average structure does not impact the correlation length, which remains infinite. The striking consequence of this is that the structure factor remains characterized by Dirac peaks of vanishing width (for systems of infinite size) yet with an amplitude that decays with q . This reasoning does not only hold for periodic media but also for quasiperiodic systems (e.g. Fibonacci structures, Penrose tiles, etc.), which also exhibit a discrete pattern in reciprocal space - meaning structural order and long-range correlation. Real systems are however never exactly periodic, due to fabrication imperfections and in practice this also leads to a finite correlation length (Koenderink *et al.*, 2005; López, 2003; Meseguer *et al.*, 2002; Nelson *et al.*, 2011).

A plethora of studies of ordered photonic crystal structures with imperfections, both numerical and experimental, can be found in the literature (Soukoulis, 2012). Defects were also added intentionally, either at random or selected positions, to study the interplay between defect states, density of states, wave tunneling and percolation, random diffuse scattering, and directed Bragg scattering of light (Aeby *et al.*, 2020; Fernandes *et al.*, 2013; Florescu *et al.*, 2010; García *et al.*, 2009). Moreover, the interaction between the band structures and defect scattering is fascinating, since it might lead to other critical coherent transport phenomena such as Anderson localization of light (John, 1987). Defect states can also be introduced in a photonic crystal to deliberately implement a particular function, such as optical sensing applications, lasing, or optical circuitry (Joannopoulos *et al.*, 2011; Nelson *et al.*, 2011; Soukoulis, 2012).

4. Disordered hyperuniform structures

One of the important characteristics of point patterns is how the number of points contained in a given volume fluctuate with various disorder realizations (Torquato, 2013). This quantity is related to the notion of spatial uniformity. For a Poisson point process, one shows from Eq. (110) that the variance in the number of points N contained in a d -dimensional sphere of radius R grows as the sphere volume, i.e. $\langle N^2 \rangle - \langle N \rangle^2 = \langle N \rangle \sim R^d$. This result holds for many disordered point patterns. By contrast, the same analysis performed on a periodic pattern shows that the variance grows with the surface of the sphere, $\langle N^2 \rangle - \langle N \rangle^2 \sim R^{d-1}$. In a founding work, Torquato and Stillinger (2003) proposed to define a general class of point patterns, dubbed “hyperuniform”, the property of which is to exhibit point number fluctuations scaling as the surface of the window, that is slower than expected for usual disordered media. Hyperuniformity encompasses periodic, quasi-periodic but also – very interestingly in the framework of this review – a subclass of disordered systems, see Fig. 5 (4th column) for an illustration and (Torquato, 2018) for a recent review. It was observed numerically that maximally jammed packings of spheres and platonic solids tend to a hyperuniform structure (Jiao and Torquato, 2011). While such long-range fluctuations can hardly be observed on the pair-correlation function, hyperuniform point patterns can be recognized from the behavior of the structure factor at low values

$$\lim_{\mathbf{q} \rightarrow 0} S(\mathbf{q}) = 0. \quad (112)$$

Of particular interest in photonics are so-called “stealthy” hyperuniform structures, for which $S(\mathbf{q}) = 0$ for $0 < q \leq q_{\max}$, where q_{\max} may be set to an arbitrary value. The region of zero structure factor is often followed by oscillations similar to those found in short-range disordered correlated media (Froufe-Pérez *et al.*, 2016).

The concept of hyperuniformity in photonics has first been introduced in a numerical study by Florescu *et al.* (2009). Important efforts have been put since then on the fabrication of hyperuniform disordered systems, which could be achieved so far by lithography in 2D (Man *et al.*, 2013) and 3D (Muller *et al.*, 2013), block copolymer assembly (Zito *et al.*, 2015), emulsion routes (Piechulla *et al.*, 2018; Ricouvier *et al.*, 2017; Weijs *et al.*, 2015), and spinodal solid-state dewetting (Salvalaglio *et al.*, 2020).

5. Disordered fractal structures

In all classes of disordered point patterns discussed above, the average number of points N contained in a d -dimensional sphere of radius R is expected to grow as

$\langle N \rangle \propto R^d$ - by doubling the observation radius for a 3D point pattern, the number of points increases by a factor $2^3 = 8$. This scaling is however not a general rule. Introduced by Mandelbrot (1967), the concept of fractals encompasses systems for which the power-law scaling of the mass with the system size does not have the Euclidean dimension as an exponent. More specifically, for fractal point patterns, we have $\langle N \rangle \propto R^{d_f}$, where d_f is a non-integer fractal dimension. Fractality has a dramatic impact on the structure, as illustrated in Fig. 5 (5th column). First, it is statistically self-similar, meaning that the structure is statistically identical whatever the scale on which it is looked at (though lower and upper bounds are always met in practice). Second, it exhibits enormous local density fluctuations and high lacunarity (Allain and Cloitre, 1991), meaning that both very dense and very empty regions are found. As a result, the pair correlation function can be shown to decay as a power-law as $g_2(R) \sim R^{-\alpha}$ and similarly for the structure factor, $S(q) - 1 \sim |q|^{-(d-\alpha)}$ assuming that $0 < \alpha < d$. Depending on the process of structure formation, one can directly relate the exponent α with the fractal dimension d_f . For instance, clustering described by the Soneira-Peebles model gives $\alpha = d - d_f$, leading to $S(q) - 1 \sim |q|^{-d_f}$ (Soneira and Peebles, 1977). It is important to note that real systems generally exhibit lower and upper bounds in their fractal nature. This implies that the power-law decays are observed on finite range ($g_2(R)$ eventually goes to 1 at large R).

Fractal disordered optical materials are encountered in a wide variety of colloidal aggregates that form naturally for certain charged particles (Meakin, 1987) as well as in certain emulsions (Bibette *et al.*, 1993). They can also be designed in a laboratory by inserting spacing particles with a size distribution that covers several orders of magnitude in a statistically-homogeneous disordered medium (Barthelemy *et al.*, 2008; Bertolotti *et al.*, 2010a).

D. Numerical construction of correlated disordered media

Numerical simulations of the complex heterogeneous morphologies play a key role in colloidal chemistry and soft matter physics. For light scattering studies, modelled structured materials are taken as input data for solving Maxwell’s equations. Here, we present some standard numerical approaches that have been used in the literature to generate correlated disordered structures.

Random packings of hard spheres in different dimensions is of great interest due to their structural and thermodynamic properties. The numerical generation of such ensembles plays a key role in research, especially in the case of random close packings (RCP) (Song *et al.*, 2008). When the packing fraction of the system is kept below a few tens of percent, a random sequential absorption

model (RSA) model (Widom, 1966) is suitable to generate large (non-equilibrium) ensembles in any dimensionality. In the RSA model, new points are randomly added to the system following a uniform distribution. The new point is rejected if closer than a given distance to any of the previous points in the pattern. A careful management of the coordinates storage in appropriate structures lead to very efficient algorithms. However, the former algorithms become dramatically inefficient when the rejection rate is high, the maximum filling fraction being $\phi \simeq 54\%$ in 2D (Wang, 2000) and $\phi \simeq 38\%$ in 3D (Meakin and Jullien, 1992).

In order to achieve larger packing fractions up to the jamming packing (at a filling fraction $\phi \simeq 64\%$ in 3D) several approaches leading to efficient algorithms have been developed. The Lubachevsky-Stillinger (or compression) algorithm (Lubachevsky and Stillinger, 1990) generates random packings of any physically-realistic ϕ by placing a set of N particles of vanishingly small size in a closed or periodic domain at random, and then letting the particles grow at a given rate, move and collide (elastically), until the desired ϕ is reached. This algorithm has been successfully used in the study of sphere packings in any dimensionality (Skoge *et al.*, 2006) and is largely used in photonics (Conley *et al.*, 2014; Froufe-Pérez *et al.*, 2016). An approach named “ideal amorphous solids” was also proposed by Lee *et al.* (2010) to realize maximally random jammed packings of polydisperse particles. The method relies on building aggregates of touching spheres by placing spheres one by one around a center of mass.

Enlarging the kind of correlations encountered in sphere packings requires the use of interaction potentials beyond the hard sphere model. Simple two-body interaction potentials such as Lennard-Jones together with standard Monte-Carlo techniques have been used to generate assemblies of scatterers in different phases (De Sousa *et al.*, 2016). Two and three-body interaction models like the Stillinger-Weber model (Stillinger and Weber, 1985) can be used to generate fully connected dielectric networks showing the same statistical structural properties (coordination and angle statistics) as amorphous silicon or diamond. Stealthy hyperuniform point patterns have been generated numerically using a suitable pairwise, long-range potential in the real space (Froufe-Pérez *et al.*, 2016). Quite often, the structures are generated using molecular dynamics. Being a very vast and mature field, various softwares are nowadays available, including NAMD (Phillips *et al.*, 2005) and CHARMM (Brooks *et al.*, 2009), which are both extensively used in the field of chemistry and biochemistry. Other software packages include HOOMD-blue (Anderson *et al.*, 2008), which is implemented for GPU, and LAMMPS (LAMMPS, 2019), which exploits massive parallelization (Plimpton, 1995).

Instead of using constraints in real space as in the case of hard spheres, targeted interaction potentials can be obtained by imposing constraints on the structure factor in

reciprocal space (Uche *et al.*, 2004), which allowed realizing, e.g., stealthy hyperuniform structures (Batten *et al.*, 2008; Florescu *et al.*, 2009). A more general approach to the problem is obtained using constrained Fourier transforms as collective coordinates (Kim *et al.*, 2018).

Materials forming a continuous correlated disordered network are very relevant on different levels (Wright and Thorpe, 2013). On the one hand, a network presents the necessary structural stability required by different fabrication methods (Gaio *et al.*, 2019). On the other hand, the topology of the network apparently plays an important role in the emergence of different optical properties such as photonic gaps in disordered networks (Florescu *et al.*, 2009; Weaire, 1971). Besides the Stillinger-Weber model considered above, there are different protocols described in the literature to generate continuous random networks. The Wooten-Winer-Weaire (WWW) algorithm (Wooten *et al.*, 1985) considers a collection of points and bonds connecting pairs of points. The initial network, that can be ordered, is randomized after a number of bond reassignments followed by a relaxation of the structure (for instance following the Stillinger-Weber interaction potential). In this way, accurate predictions of the electronic structure, bond geometry statistics and atomic structure of amorphous semiconductors are obtained (Barkema and Mousseau, 2000). Replacing the chemical bonds by dielectric rods leads to amorphous dielectric materials (Edagawa, 2014).

A protocol to generate strongly correlated continuous random networks was first proposed by Florescu *et al.* (2009) in two dimensions and used by Liew *et al.* (2011) in three dimensions. The idea is to create a uniform topology network starting from an arbitrary point pattern. The Delaunay tessellation (Watson, 1981) is constructed from the seed point pattern. By definition each Delaunay cell is surrounded by 3 (in 2D) or 4 (in 3D) neighbors. The protocol indicates that the centroids of neighboring triangles (2D) or tetrahedrons (3D) are linked. This connected network shows a uniform connectivity since each node of the network is linked to the same number of neighbors. When the seed pattern is strongly correlated, for instance using random closed or stealthy hyperuniform packings, the resulting dielectric network presents interesting photonic properties, for instance complete gaps in its density of states (Florescu *et al.*, 2009; Froufe-Pérez *et al.*, 2016; Liew *et al.*, 2011) in 2D and 3D. The optical aspects of these structures will further be discussed in Sec. V.

E. Fabrication of correlated disordered media

Here, we present an overview of the different strategies and important design parameters for the experimental fabrication of strongly scattering correlated disordered media. We mainly focus on the fabrication of 3D materi-

als but note that many of the concepts discussed here also hold for 2D materials. We will illustrate the fabrication concepts with a few examples but will not attempt to provide a comprehensive overview of this field of materials research, which is beyond the scope of our work. We note that the fabrication of disordered correlated photonic materials faces the same challenges than other optical metamaterials such as photonic crystal circuits or other 3D arrangements of structural units (Soukoulis and Wegener, 2011). The trade-offs one needs to consider are simplicity, freedom of design, speed or throughput, accuracy and resolution. Those parameters vary enormously and therefore no *one-method-fits-all* fabrication route can be singled out.

The range of interest to observe strong scattering and coherent phenomena due to structural correlations is when typical length scales of the structure are on the order of the wavelength (typically half a wavelength) in the medium. This mandates, first of all, the sub-micron structuring of dielectric materials on length scales comparable to the wavelength of light with a refractive index contrast $(n/n_h) - 1 \gg 0.1$. In practice, finding the optical material properties is also influenced by the fact that the effective refractive index n_{eff} is often higher than the nominal background material index n_h which reduces the transport coefficient $1/\ell_t$ (Naraghi *et al.*, 2015; Reufer *et al.*, 2007; Schertel *et al.*, 2019b). As a general rule, the higher the space filling fraction of the scattering material the higher $n_{\text{eff}} \geq n_h$ and the stronger this effect. The optimum space filling fraction is often found around $\phi \sim 0.3$ which is much lower than the space filling fraction obtained naturally by randomly packing spheres $\phi \sim 0.64$. In addition to these fundamental scattering parameters, structural correlations are key for the design and fabrication of optimally white materials.

In general we can distinguish global structural properties, i.e. properties that can be expressed by statistical averages and a corresponding structure factor $S(q)$, and local properties related the local topology, filling fraction and the scatterer morphology. In the following, we describe different approaches that have been used to fabricate disordered and strongly scattering media. Structural correlations then appear naturally or by design.

Figure 6 summarizes the most important fabrication methods of correlated disordered media, that we will describe consecutively in detail below. Thermal or assisted self-assembly are bottom-up processes driven by a combination of entropy and external forces, such as gravity. Equilibrium and non-equilibrium self-assembly design routes following predefined pathways are frequently found in nature but are also increasingly considered as alternatives in the laboratory. Top-down approaches based on lithography come in many flavors and take advantage of powerful technology at hand. Lithography is very powerful for structuring two dimensional materials but only more recently significant progress has been made to fabri-

cate 3D structured materials on submicron length scales. We will discuss some of the strengths and limitations of the different methods.

1. Jammed colloidal packing

Dispersing submicron sized colloidal particles in a solvent phase with a lower index of refraction is the most common and most simple way to fabricate a strongly scattering, disordered medium. Ubiquitous examples are white paints, often based on a dispersion of submicron TiO_2 or polymer latex particles, or milk. For uniform suspensions of spherical particles, structural correlations appear naturally owing to the interactions between the particles which can be longer range DLVO-type double-layer repulsion or short-range excluded volume interactions. The preparation is fairly simple and only requires some command over the stability of the suspension to avoid the formation of very large aggregates or flocks (Galisteo-López *et al.*, 2011). The degree of structural correlations can be controlled by the composition in particle volume fraction, electrolyte and type of solvent.

Colloidal particles can also be processed as powders which provides a higher refractive index contrast to air ($n_h^{\text{air}} = 1$), as compared to solvent based dispersions (e.g. $n_h^{\text{water}} = 1.33$), but offers less control over the microstructure. The statistically well defined structure in a liquid can be transferred to a solid film by film drying often preceded by sedimentation or centrifugation, see Fig. 6 (left column, top) (Reufer *et al.*, 2007). Such a colloidal film has the structural properties of a frozen colloidal liquid at random close packing conditions. For identical spheres, this results in pronounced short-range correlations. It is however often difficult to avoid crystallization. To avoid the formation of crystallites one can employ size polydispersity, the pre-formation of aggregates or the use of non-spherical particles, but this usually leads to a reduction of structural correlations. Photonic crystals with controlled disorder can also be fabricated by combining spherical colloids of two different polymers, and to selectively etch one after the crystal deposition. In this way, controlled defects in an otherwise periodic lattice are formed (García *et al.*, 2009). Optimizing this fabrication process has been subject of active research (García *et al.*, 2007).

Finally, densely-packed colloidal aggregates, typically of micron-sized spherical shapes, can be realized by selective solvent evaporation or spray-drying (Manoharan *et al.*, 2003; Moon *et al.*, 2004; Vogel *et al.*, 2015; Yazhgur *et al.*, 2021; Yi *et al.*, 2003), see Fig. 6 (left column, bottom). These so-called “photonic balls”, which may be composed of dielectric or metallic particles and be suspended in air or in a solvent, have been used to realize angle-independent structural colors (Park *et al.*, 2014), artificial (meta) materials (Dintinger *et al.*, 2012)

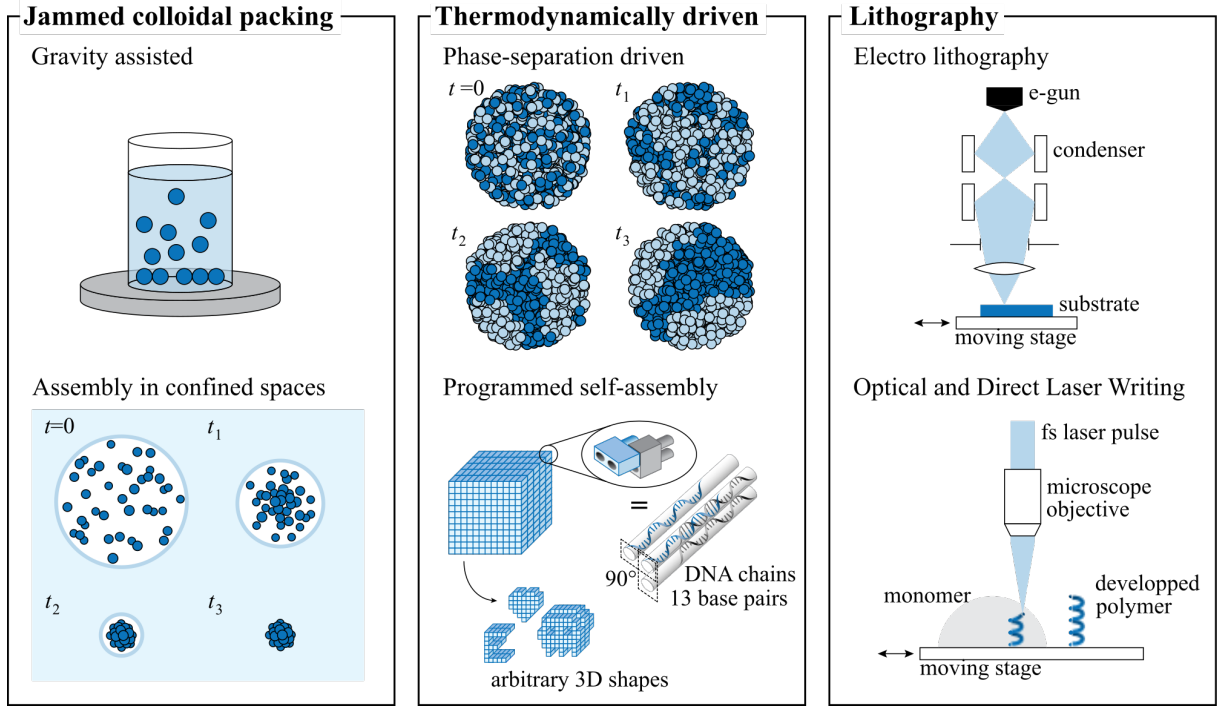


FIG. 6 Overview of fabrication methods. (From left to right) *Jammed colloidal packing*, where the colloids deposit via gravity assisted methods, or where they assemble in confined spaces due to local interactions. *Thermodynamically driven assembly*, where the system goes through a phase-separation and rearrangement, driven by entropy or by pre-programmed interactions as for example using DNA strands. *Optical and electron lithography*, where samples are fabricated by direct sculpturing of a material, using optical or electron beams to modify the local physical and chemical properties (subtractive) or where material is locally added to the structure via selective polymerisation or deposition (additive). Courtesy from Mélanie M. Bay (University of Cambridge, UK).

or micron-sized random lasers (Ta *et al.*, 2021). The finite size of the photonic balls breaks the translational invariance and, for small photonic balls, this leads to additional metaball-scattering contribution. Structural correlations within the balls are likely to depend on the size of the aggregate and the quenching rate. Crystallisation of the surface layer is often observed.

2. Thermodynamically-driven self-assembly

Colloidal self-assembly proceeds via a random process that arranges prefabricated scatterer of a given size a in space. The fabrication process is stochastic and driven by thermal motion or external fields such as gravity and the resulting structures are relatively simple. In contrast, biology and recent DNA based nano-fabrication processes rely on well defined fabrication pathways or cascades that can be programmed which leads to beautiful and complex optical materials in nature (Prum *et al.*, 1998; Vignolini *et al.*, 2012). In biology, it is known that many species are able to produce optical materials that show color or whiteness with optimal morphology and structural correlations, short or long ranged (Burrese *et al.*, 2014; Luke *et al.*, 2010; Prum *et al.*, 2009). The physical mecha-

nisms that underlies the assembly of photonic structures in living organism is still not understood (Dufresne *et al.*, 2009; Onelli *et al.*, 2017; Prum *et al.*, 2009; Wilts *et al.*, 2019). Even without a complete understanding of the biological processes, it is possible to use such architectures as materials for biotemplating. To this end, the biological material is used as a template or cast for a synthetic material with a high refractive index such as TiO_2 (Galusha *et al.*, 2010). Analogous three-dimensional architectures have been produced on the tens of nanometer-scale via block-copolymers self-assembly (Stefik *et al.*, 2015), and the interplay between order and disorder on a slightly larger-scale (few hundreds of nanometers) have been shown to be controllable via block-copolymers brush systems (Song *et al.*, 2018), see Fig. 6 (middle column, top).

Another very promising route is based on DNA-nanotechnology (He *et al.*, 2020). DNA-origami techniques, invented a decade ago (Rothemund, 2006), are considered one of the breakthroughs in nanotechnology. Recently, methods for making micrometre-scale DNA-Origami objects have been developed (Zhang and Yan, 2017), see Fig. 6 (middle column, bottom). The use of DNA-origami or bioinspired assembly techniques is still in its infancy. It is however the only fabrication route

that may possibly allow the design of complex, correlated disordered three-dimensional optical materials in the visible range owing to the nanoscale control over the fabrication process.

3. Optical and e-beam lithography

Despite the rapid advances in nano-assembly, such as DNA origami, it is still difficult and often impossible to fabricate tailored disordered optical materials at will. In particular optimized structures designed *in silico* cannot be readily transferred into real materials yet using such approaches. Lithography is an established and powerful alternative to self-assembly. Its leading performance is unchallenged in the fabrication of two dimensional materials, such as silicon, owing to the decades of optimization in the semiconductor industry. The resolution of deep UV based optical lithography is now at 10 – 20 nm (Sanders, 2010). The use of a predefined photographic mask means that this is a highly parallelized method and the resolution can be reached over a large area, such as entire 30 cm silicon wafers. High resolution optical lithography however has a very high start-up cost for instrumentation and for the fabrication of individual photo masks. E-beam lithography is a serial fabrication tool with similar resolution capacity. It is versatile and can fabricate any 2D structure but it is much slower and thus not suited for high-output volumes (Altissimo, 2010). Early attempts in the late 1990s focused on the fabrication of structured photonic materials in 2D for visible and near-infrared wavelengths using lithographic patterning followed by reactive ion etching to produce long air holes in high index materials (Krauss *et al.*, 1996; Zoorob *et al.*, 2000). It is very challenging to generalize the use of these powerful 2D methods for the fabrication of 3D materials. Small sized three-dimensional infrared photonic crystal on a silicon wafer were reported based on stacking several layers of 2D structures, fabricated with fairly standard microelectronics fabrication technology (Lin *et al.*, 1998). In principle, this approach can also be applied to correlated disordered materials but owing to its extreme cost and complexity as well as limitations in size it has not been widely used. More recently, the etching of air rods has been applied to fabricate 3D hole-arrays using 3D masks (Grishina *et al.*, 2015). This method is in an early stage of development and the evaluation of the optical performance of the materials obtained is still in progress, nonetheless, it offers potential also for the template-free, direct fabrication of correlated disordered 3D photonic materials with a very high refractive index contrast.

The inherent limitations of conventional colloidal self-assembly strategies have led to the development of a class of 3D high resolution lithography tools in the late 1990s and the early 2000s known as direct laser writing

(DLW) (Deubel *et al.*, 2004; Sun *et al.*, 1999). The most popular implementation of direct laser writing is based upon the development of the two-photon microscope in 1990 by Denk *et al.* (1990). Using a focused femtosecond pulsed laser two photons are absorbed simultaneously in the focal spot, but not elsewhere, owing to the highly nonlinear absorption cross section. In microscopy, the re-emission of a photon is used for imaging, in direct laser writing the absorbed energy is used to initiate a chemical reaction in the photoresist. By scanning a near infrared fs-pulsed laser beam in 3D, a polymeric structure can be written with a resolution of approximately 200nm laterally and 500nm axially. The resolution is limited by the point spread function of the microscope objective and the two photon cross section as well as the photoresist. Recently, it was shown that the resolution can be further enhanced using a stimulated-emission-depletion (STED) microscopy inspired approach (Fischer and Wegener, 2011; Klar *et al.*, 2014). DLW has been used to fabricate polymer templates for a variety of optical metamaterials such as woodpile photonic crystals, quasicrystals and polarizers (Deubel *et al.*, 2004; Gansel *et al.*, 2009; Ledermann *et al.*, 2006; Soukoulis and Wegener, 2011). It has also been instrumental for the experimental realization of 3D correlated disordered network materials, based on hyperuniform point patterns or other types of disordered correlated photonic materials (Renner and Von Freymann, 2015). Despite its power and versatility, the DLW method also suffers from imperfections due to shrinkage of the polymer structure during development and deformations (Deubel *et al.*, 2004; Haberkorn *et al.*, 2013; Renner and Von Freymann, 2015). Moreover, due to the relatively low refractive index of the polymer photoresist ($n \simeq 1.5$), it is usually necessary to transfer the cast or template into another, higher index, material such as TiO_2 or silicon. This can be done using single or double inversion protocols which can be parallelized (Marichy *et al.*, 2016; Muller *et al.*, 2013, 2017; Staude *et al.*, 2010; Tétreault *et al.*, 2006). Therefore, such single or double inversion of the template is, in principle, not a time limiting step in the fabrication protocol. However, the complex chemical and etching procedures needed often lead to an incomplete infiltration (and thus a lower refractive index) (Marichy *et al.*, 2016; Staude *et al.*, 2010), a general deterioration of the quality of the structure and additional surface roughness (Muller *et al.*, 2017).

F. Measuring structural correlations

Structural correlations in disordered photonic media can be measured using microscopy, tomography and scattering. Scattering can only be employed if the materials structure is translationally invariant and isotropic or aligned in a well-defined direction. This is the case for

colloidal photonic liquids and glasses or randomly close packed particles or rods which are correlated on short length scale but on large length scales are statistically uncorrelated (at least asymptotically) (García *et al.*, 2007; Reufer *et al.*, 2007; Rojas-Ochoa *et al.*, 2004). A challenge is the fact that the material has to be fairly transparent to the used radiation and therefore light is not a suitable probe, unless some form of refractive index matching or clearing is possible. In the latter case, confocal microscopy has also been applied successfully (Haberkorn *et al.*, 2013). Optical materials are usually fairly transparent to neutrons or x-rays. Ultra Small Angle Neutron and X-Ray scattering instruments are in principle suitable for this task and available at large scale facilities (Bahadur *et al.*, 2015) but these experiments are difficult and time-consuming and they are thus not routinely carried out to measure structural correlations in complex photonic media. Small angle neutron scattering (SANS) has been used successfully to measure the structure factor of photonic liquids composed of relatively small colloids in suspension (Rojas-Ochoa *et al.*, 2004). The direct visualization of the materials local and global structure is often more useful or, for many novel systems, even required. To this end, electron microscopy is routinely applied often in tandem with focused ion beam milling and cutting. More recently, X-ray imaging and X-ray tomography have been developed as non-invasive tools for the real space characterization of correlated photonic materials (Grishina *et al.*, 2018; Wilts *et al.*, 2018a). Another promising route to study the internal structure of 3D photonic materials is destructive tomography using ion beam milling or etching techniques in conjunction with electron or atomic force microscopy (Buresi *et al.*, 2014; Magerle, 2000).

IV. MODIFIED TRANSPORT PARAMETERS

The primary effect of structural correlations is to modify the light scattering and transport parameters. This section offers a survey of the theoretical predictions and experimental observations of modified transport properties due to structural correlations. We first focus on colloidal systems and photonic materials, typically characterized by short-range correlations (i.e., negatively-correlated) [Sec. IV.A]. We discuss optical transparency and enhanced single backscattering phenomena on the basis of the theory developed in Sec. II, and survey progress on resonant and Bloch-mediated scattering. In a second part, we describe the markedly different transport properties of materials with large-scale heterogeneities (i.e., positively-correlated) [Sec. IV.B]. Transport in such systems requires a generalization of the radiative transfer equation and can become anomalous in presence of a fractal heterogeneity.

A. Light scattering and transport in colloids and photonic materials

1. Impact of short-range correlations: first insights

Let us start this section by examining the expressions derived for the scattering and transport mean free paths for assemblies of spherical particles, Eqs. (107) and (108). In deriving these expressions, we have assumed that an effective permittivity ϵ_{eff} for the system can be defined, leading to an effective wavenumber $k_r = k_0 \text{Re}[n_{\text{eff}}]$ and a scattering wavevector $q = k_r |\mathbf{u} - \mathbf{u}'|$, where \mathbf{u} and \mathbf{u}' are the scattered and incident directions. The form factor is given by $F(q) = k_r^2 \frac{d\sigma}{d\Omega}(q)$ [Eq. (105)], where $\frac{d\sigma}{d\Omega}$ is the differential scattering cross-section of the individual particle in the host medium evaluated at the wavenumber k_r . The structure factor $S(q)$ is the key quantity describing structural correlations for particulate media. Figure 7(a) shows the structure factor predicted within the Percus-Yevick approximation for hard spherical particles (Wertheim, 1963) at different filling or packing fractions $p = (\pi/6)a^3\rho$, where a is the particle diameter and ρ is the particle density. Increasing the density and/or the particle diameter leads to short-range correlations characterized by a reduction of S at small values of q (gray-shaded area), the emergence of a peak near $qa = 2\pi$, and oscillations with a decaying amplitude at larger values of qa .

The effect of these short-range correlations on light scattering can be apprehended by rewriting the scattering wavevector as $q = 2k_r \sin \theta/2$ with θ the scattering angle. Insightful expressions for the scattering and transport mean free paths can in fact be derived from this change of variables, leading to

$$\frac{1}{\ell_s} = \rho \int_{4\pi} \frac{d\sigma}{d\Omega}(\theta) S(\theta) d\Omega, \quad (113)$$

and

$$\frac{1}{\ell_t} = \rho \int_{4\pi} \frac{d\sigma}{d\Omega}(\theta) S(\theta) (1 - \cos \theta) d\Omega. \quad (114)$$

respectively, where Ω is the solid angle. Similarly, the scattering anisotropy parameter is given by

$$g = \frac{\int_{4\pi} \frac{d\sigma}{d\Omega}(\theta) S(\theta) \cos \theta d\Omega}{\int_{4\pi} \frac{d\sigma}{d\Omega}(\theta) S(\theta) d\Omega}. \quad (115)$$

The structure factor can thus be seen as a quantity that modifies the scattering diagram $\frac{d\sigma}{d\Omega}(\theta)$ of the individual particle due to far-field interference. In absence of correlations ($S = 1$), the scattering mean free path is simply given by $\ell_s^0 = (\rho\sigma_s)^{-1}$ with $\sigma_s = \int_{4\pi} \frac{d\sigma}{d\Omega}(\theta) d\Omega$ the scattering cross-section of an individual particle.

Figure 7(b) shows the structure factor for $p = 0.4$ expressed as a function of a/λ_r with $\lambda_r = \lambda/\text{Re}[n_{\text{eff}}]$ and θ . The most remarkable features here are the systematic re-

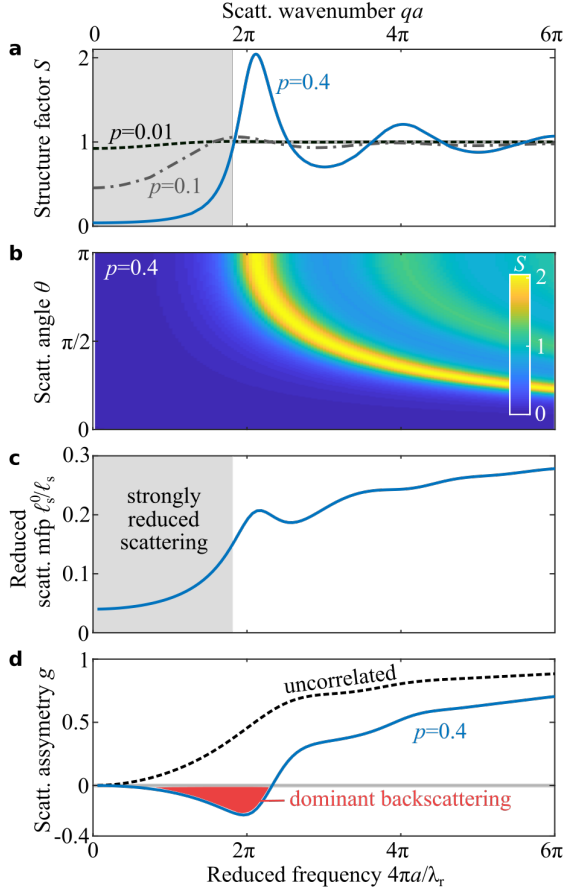


FIG. 7 Impact of structural correlations on light scattering and transport in colloids. (a) Structure factor S of a hard-sphere liquid for three different packing fractions $p = \pi/6a^3\rho$, with a the particle diameter and ρ the particle number density. The gray-shaded area indicates the low scattering wavenumber range where the structure factor is strongly diminished. (b) Angular and spectral response of the structure factor taking $q = 4\pi/\lambda_r \sin \theta/2$ and θ the scattering angle for $p = 0.4$. Exact backscattering ($\theta \rightarrow \pi$) is particularly pronounced when $\lambda_r \approx 2a$. (c) Ratio of the scattering mean free paths neglecting structural correlations (ℓ_s^0) and considering structural correlations (ℓ_s), and (d) scattering anisotropy parameter g without and with structural correlations, obtained in the realistic case of particles of diameter $a = 100$ nm and refractive index $n_p = 1.6$ (e.g., polystyrene) in a host medium with index $n_h = 1.33$ (e.g., water). The observed features are directly linked to the structure factor. The red-shaded area in panel (d) highlights the range where single scattering is dominantly backward, implying $\ell_t < \ell_s$.

duction of scattering around the forward direction $\theta \approx 0$ and strong increases in the backward direction $\theta \approx \pi$ at specific frequencies, especially near $qa = 2\pi$, similarly to the Bragg condition in crystals.

We apply Eqs. (113)-(115) to a practical situation, namely spherical polystyrene particles ($n_p = 1.6$) with diameter 100 nm dispersed in water ($n_h = 1.33$). We use the CPA to get the effective index (Soukoulis *et al.*,

1994), resulting in $n_{\text{eff}} \approx 1.44$ on the entire wavelength range considered here, although the actual choice of the effective medium theory is of little importance for such low-index contrast systems. Figures 7(c)-(d) show the variation of scattering efficiency ℓ_s^0/ℓ_s , and the scattering asymmetry parameter g in the limit of an uncorrelated medium (asymmetric scattering is then entirely due to the particle alone) and for a strongly correlated system, $p = 0.4$. Two main conclusions can be drawn here. First, structural correlations lead to a reduction of the scattering efficiency, that is particularly pronounced in the low frequency range, where the wavelength is much larger than the characteristic length of the system. Thus, an incident wave propagates ballistically on longer distances (on average). Second, the angular dependence up to the first peak in the structure leads to a negative scattering anisotropy parameter g , meaning that light is predominantly scattered backward, leading to $\ell_t < \ell_s$. Both these effects have been observed experimentally, as reported below.

We considered here particles with a fairly low-index contrast to emphasize the role of short-range structural correlations on light scattering and transport. The range of optical properties is significantly enriched when considering the possibility of having spectrally sharp Mie resonances in high-index contrast materials, or longer-range structural correlations.

2. Enhanced optical transparency

The impact of structural correlations on light scattering in colloids emerged in the 1950s when it was noticed that the light intensity scattered either by protein solutions (Doty and Steiner, 1952) or by collagen fibrils in the cornea stroma (Maurice, 1957) was not following the behavior expected for small scattering elements uncorrelated in position. In the celebrated article by Maurice (1957), it was supposed that a periodic organization of the fibrils was at the origin of a surprising optical transparency. Later works shown theoretically that this transparency could be explained by short-range correlated disorder (Benedek, 1971; Hart and Farrell, 1969; Twersky, 1975). More recently, dense nanoemulsions, a kind of synthetic mayonnaise made from smaller than usual oil droplets with a diameter around 50 nm, have been shown to be much more transparent than more dilute suspensions $\phi \sim 0.1$ of the same droplets (Graves and Mason, 2008). A transparency window has been observed in scattering fibrillar collagen matrices as a function of collagen concentration (Salameh *et al.*, 2020). All these observations are explained by the strongly reduced scattering efficiency observed in the long-wavelength regime and shown in Fig. 7(c).

The notion of transparency relies on the proportion of ballistic light after a sample and therefore depends on the

ratio between the extinction mean free path ℓ_e , or scattering mean free path ℓ_s in absence of absorption, and the sample thickness L . Thus, materials exhibiting short-range correlated disorder unavoidably become opaque for very large thicknesses. The question of whether this conclusion holds for stealthy hyperuniform media, for which the structure factor strictly equals 0 on a range of scattering wavevectors q , naturally follows. The perturbative expansion of the intensity vertex (or equivalently of the phase function) up to the second order [Eq. (102)] predicts that scattering is completely suppressed for such media [Eq. (107)]. Scattering may however occur due to the higher-order terms. Taking these into account leads to the definition of a criterion for optical transparency that reads (Leseur *et al.*, 2016)

$$\frac{L}{\ell_s^0} \ll k_r \ell_s^0, \quad (116)$$

derived here for point scatterers ($\ell_s = \ell_t$). This shows that stealth hyperuniformity does *not* completely suppress scattering. Optical transparency can be achieved in situations in which an uncorrelated disordered medium would be opaque ($L/\ell_s^0 \gg 1$) but only provided that the ratio ℓ_s^0/λ_r is sufficiently large.

3. Tunable light transport in photonic liquids

Spherical colloids are often considered as big atoms in soft matter physics (Poon, 2004). From this viewpoint, each colloidal particle takes the place of an atom that is interacting with its peers via specific colloidal interactions. For colloids in suspensions these interactions are often tunable both in strength and sign, such as the well-known double layer repulsion between charged microspheres suspended in salty water. Thus, depending on the volume fraction occupied by the particles and the interaction strength, different colloidal phases can be found such as correlated liquids, entropic glasses, jammed packings, or a crystal (Pusey and Van Meegen, 1986).

Early experiments of light scattering by charged particles, typically made of polystyrene or PMMA, were initiated in the mid 1970s, notably by Brown *et al.* (1975), who could measure the structure factor of colloidal suspensions of subwavelength particles beyond the first peak by conventional light scattering. The impact of structural correlations on light transport in the multiple-scattering regime was later studied by Fraden and Maret (1990) and Saulnier *et al.* (1990), who reported transmission and coherent backscattering measurements of the transport mean free path in optically thick materials composed of resonant (wavelength-scale) particles at various packing fractions, see also (Kaplan *et al.*, 1994; Yazhgur *et al.*, 2021). Both works observed an increase of the transport mean free path due to structural correlations. A further step forward was made by Rojas-Ochoa *et al.* (2004),

where it was shown that a fine control over structural correlations via Coulomb repulsion could induce a strong wavelength dependence of the optical properties of colloidal liquids and even negative values of the scattering anisotropy parameter, $g < 0$, i.e. $\ell_t < \ell_s$. In such “photonic liquids”, the strong spectral variations of transport parameters make that samples of intermediate optical thicknesses and/or partly absorbing become structurally colored in reflection. Note the overall excellent agreement between experiments and theoretical predictions based on direct measurements of $S(q)$ with small angle neutron scattering (SANS) (Rojas-Ochoa *et al.*, 2004).

Initial works (Fraden and Maret, 1990; Rojas-Ochoa *et al.*, 2004; Saulnier *et al.*, 1990) have not considered an effective index to correct the scattering wave number q . Fortunately, the outcome of doing so does not significantly impact the results due to the low index contrast.

4. Resonant effects in photonic glasses

Photonic glasses are solid materials composed of closed-packed dielectric spheres, with size comparable to the wavelength of light, arranged in a disordered way (García *et al.*, 2007). This is usually achieved by intentional colloidal flocculation and subsequent deposition. The mono-dispersity of the building blocks that compose them induces Mie resonances, which remain observable in the closely-packed systems (Aubry *et al.*, 2017). The resonances are all the stronger as a higher index contrast is achieved by evaporation of the host liquid. Besides, when the scattering material is solid, material stability is ensured by physical contacts between neighboring particles, thereby resulting in stronger short-range correlations compared to photonic liquids, and strong near-field interaction between particles. The latter impacts both the magnitude and frequency of the Mie resonance of the individual sphere (Sapienza *et al.*, 2007) and can transmit more light than expected from classical scattering theory (as developed in Sec. II) (Naraghi *et al.*, 2015).

The strong short-range correlation and near-field interactions makes the modelling of realistic photonic glasses very challenging. Recent works (Aubry *et al.*, 2017; Schertel *et al.*, 2019b) have argued that the effect of the near-field coupling on transport in photonic glasses could be captured by defining an effective wave number k_r with an index obtained from the energy-density coherent potential approximation (ECPA) (Busch and Soukoulis, 1995). This appears in contradiction with our rigorous derivation of Eqs. (107) and (108), which required neglecting near-field interaction between particles. Besides, it is surprising that an approach based on the evaluation of the energy density would correctly predict the average field phase velocity. The most advanced formalism to date to describe scattering and transport by dense,

particulate media possibly with high-index materials is the quasicrystalline approximation (QCA), exploited recently by Wang and Zhao (2018) to study the interplay between Mie resonances and structural correlations.

Alternatively, insight can be provided by numerical simulations. The complexity of the relation between structural correlations and light transport was evidenced in a recent work by Pattelli *et al.* (2018), where a graphics processing unit (GPU) implementation of the T-matrix method (Egel *et al.*, 2017) was used to investigate scattering by large assemblies of particles on a wide range of parameters. Simulations reveal that, given the wavelength and the particles size and refractive index, the shortest transport mean free path is obtained at intermediate degrees of correlations and particle densities.

Although much remains to be understood, photonic glasses and all resonant dense scattering media have demonstrated their great versatility and efficiency to harness light scattering and transport, with interesting applications in, e.g., structural colors and random lasing, as will be discussed in Sec. VI.

5. Modified diffusion in imperfect photonic crystals

An extreme case of correlated disordered media is that of a disordered photonic crystals, in which long range order is established by the almost-periodic structure and scattering can be induced by imperfections, defects or (intentional) contamination with additional scattering elements. In a crystal, light propagation is dictated by the photonic band diagram which maps the frequency-wavevector relation of propagating Bloch modes (Joannopoulos *et al.*, 2011). Perfectly periodic structures are typically characterized by strong variations of the group velocity and the formation of partial (or even complete) photonic gaps corresponding to a lack of propagating states. The scattering cross-section of a defect typically increases with the reduction of the group velocity and light will scatter only where propagating states exist, therefore very anisotropically.

Light multiple scattering and transport is expected to be strongly affected, while a more quantitative prediction requires a precise modelling of the kind of scattering and the crystal topology. Pioneering experiments on coherent backscattering (Huang *et al.*, 2001; Koenderink *et al.*, 2000) and diffuse light transport (Astratov *et al.*, 1995; Vlasov *et al.*, 1999) in photonic crystals searched for signatures of Bloch-mode mediated scattering but have merely shown standard light diffusion (Aeby *et al.*, 2020; Koenderink *et al.*, 2005; Rengarajan *et al.*, 2005). Single light scattering in a disordered photonic crystal have been measured, with clear modification of the scattering mean free path around the bandgap (García *et al.*, 2009), reflection studies have shown anisotropic scattering (Haines *et al.*, 2012), while dynamical studies have shown ex-

ceptionally reduced diffusion constants (Toninelli *et al.*, 2008).

Instead of relying on natural imperfections in otherwise ordered photonic crystal, correlated disordered media can be made by creating lattice vacancies in photonic crystals (García *et al.*, 2011). In these structures transport and scattering mean free path and the diffusion constant have been measured to present strong dispersion (García *et al.*, 2011). The transition from order to disorder in the structure and its impact on the transport parameters is still an active field of research (Schöps *et al.*, 2018), which has also motivated the development of hyperuniform materials, where such a transition can be driven by a single parameter, as will be discussed in Sec. V.

B. Anomalous transport in media with large-scale heterogeneity

We have been concerned so far with systems for which the distribution p_N for the number of scatterers in a window of volume $V \gg 1/\rho$ has a small variance, thereby making the system appear quite homogeneous on the scale of tens or hundreds of scatterers. Here, we will be concerned with disordered systems exhibiting large-scale heterogeneities leading to a large variance, also known as positively-correlated systems, as described in Sec. III. Such systems are ubiquitous in nature, a well-known example being cloudy atmospheres. The density of droplets in suspension in clouds can indeed fluctuate over orders of magnitude. As illustrated in the right panel of Fig. 4, one may find very sparse as well as denser regions, implying a strongly fluctuating scattering efficiency. Numerous developments and outcomes have been achieved to describe transport in such systems, mostly motivated by applications in radiative transfer through the atmosphere (Marshak and Davis, 2005) and neutron transport in pebble bed reactors (Behrens, 1949). As we shall now see, despite the absence of coherent interference effects between neighboring scatterers, such long-range correlations have a dramatic impact on transport.

1. Radiative transfer with non-exponential extinction

The first element to describe radiative transfer is extinction. Equations (11) and (12) in Sec. II impose that the coherent intensity $|\langle \mathbf{E} \rangle|^2$ should decay exponentially on an average distance given by the extinction mean free path ℓ_e . In strongly heterogeneous media, however, one may anticipate that the decay will be slower than exponential. An intuitive explanation is that spatially-extended non-scattering or weakly scattering regions promote trajectories much longer than the average decay length (i.e., the extinction mean free path). Discussions on non-exponential extinction date back to Davis and

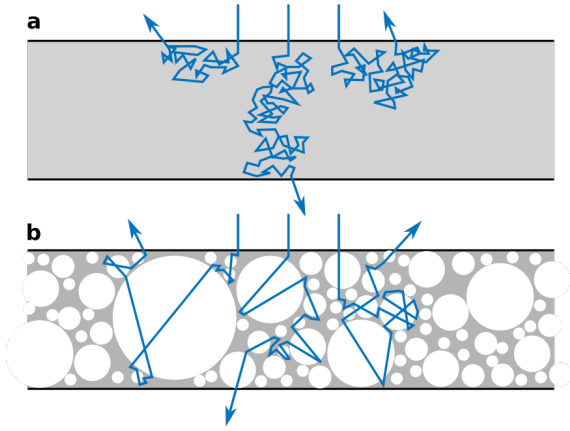


FIG. 8 Impact of large-scale heterogeneity on transport in multiple-scattering media. (a) Sketch of a transport process in a statistically homogeneous medium (gray shaded area). Within radiative transfer, transport can be described as a random walk process with exponentially-decaying step length distribution. For thick media, transport is well described by the diffusion equation. (b) Sketch of transport in a scattering medium containing large non-scattering regions (white disks). Transport is driven by long steps, making the step length distribution no longer exponential. For certain systems with fractal heterogeneity, such as Lévy glasses (Bertolotti *et al.*, 2010a), transport can experience a transient superdiffusive behavior.

Marshak (1997), who suggested that the extinction in clouds could decay as a power-law.

The most common approach to describe the non-exponential decay of the coherent intensity, proposed by several authors about two decades ago (Borovoi, 2002; Kostinski, 2001, 2002; Marshak *et al.*, 1998), consists in describing the heterogeneous medium as local “patches” or clusters of particles exhibiting a varying average extinction rate (or equivalently average particle densities). To describe this heuristic model, let us define a position-dependent particle density $\rho(\mathbf{r}) = \langle N(\mathbf{r}) \rangle / V$, with $\langle N \rangle$ the average number of scatterers in volume V . We consider a system that is dilute at all points of space ($\rho(\mathbf{r})\lambda^3 \gg 1$) such that radiative transfer applies. The key point of the approach is to assume that the distribution of number N of particles in the volume V , and consequently the distribution of number of extinction events, follows a Poisson distribution, $p_{N|N(\mathbf{r})} = \langle N \rangle^N \exp[-\langle N \rangle] / N!$. The patchiness leads to variations of $\langle N(\mathbf{r}) \rangle$ via a distribution $p_{\langle N \rangle}$. The distribution of extinction counts in a volume V should then be

$$\begin{aligned} p_N &= \int_0^\infty p_{N|N(\mathbf{r})} p_{\langle N \rangle} d\langle N \rangle \\ &= \int_0^\infty \frac{\langle N \rangle^N \exp[-\langle N \rangle]}{N!} p_{\langle N \rangle} d\langle N \rangle, \end{aligned} \quad (117)$$

The relation with the classical extinction (Beer-Lambert) law is established by noting that the probability to cross

the volume with no extinction event over a depth z is given by p_0 , and invoking the law of large numbers with $\langle N \rangle = z/\ell_e$. Taking $p_{\langle N \rangle} = \delta(\langle N \rangle - \beta)$ and the ballistic transmission $T_b = |\langle \mathbf{E} \rangle / E_0|^2$ of a planewave along the z -direction through a medium leads to

$$T_b(z) \equiv p_0(z) = \exp[-\langle \rho \rangle \sigma_e z], \quad (118)$$

where we have set $\beta = \langle \rho \rangle \sigma_e z$ and σ_e is the extinction cross-section. By contrast, the use of Γ or fractional Poisson distributions lead to asymptotic power-law decays with varying exponents m (Casasanta and Garra, 2018; Kostinski, 2001)

$$T_b(z) \sim (1 + \beta)^{-m}. \quad (119)$$

One key aspect of course is the determination of an actual function in realistic systems. Important efforts have notably been dedicated to the determination of particle density distribution in clouds (Kostinski and Jameson, 2000). Slower-than-exponential decays of the coherent intensity have also been observed in photosynthetic cultures (Knyazikhin *et al.*, 1998).

Very importantly, the radiative transfer equation [Eq. (36)] has been generalized to account for arbitrary non-exponential extinction. Defining a probability density function f_s of the random step length s as $f_s(s) \equiv T_b(s) / \int_0^\infty T_b(s) ds$, one reaches a generalized (scalar) radiative transfer equation (Larsen and Vasques, 2011)

$$\begin{aligned} &\left[\frac{\partial}{\partial s} + \mathbf{u} \cdot \nabla_{\mathbf{r}} + \Sigma_e(s) \right] I(\mathbf{r}, \mathbf{u}, s) \\ &= \delta(s) \gamma \int p(\mathbf{u}, \mathbf{u}') \Sigma_e(s') I(\mathbf{r}, \mathbf{u}', s') ds' d\mathbf{u}', \end{aligned} \quad (120)$$

where $\gamma = \ell_e/\ell_s$ is the single-scattering albedo (the probability to be scattered upon an extinction event) and $I(\mathbf{r}, \mathbf{u}, s)$ now depends on the step length s via

$$\Sigma_e(s) = \frac{f_s(s)}{1 - \int_0^s f_s(s') ds'}. \quad (121)$$

Equation (36) is recovered by taking $f_s(s) = \exp[-s/\ell_e]/\ell_e$. First, let us note that the distribution $f_s(s)$ should have a finite mean as to allow the definition of a mean free path ℓ_e . Second, one of the key features of transport with non-exponential step length distributions is the fact that it is a non-Markovian process, i.e. implying memory in the construction of individual steps, contrary to the classical Beer-Lambert law which is a Markovian (memoryless) process ($\exp[x + y] = \exp[x] \exp[y]$). Finally, – and this aspect has not been significantly emphasized previously – the formalism assumes an “annealed” disorder, meaning that the medium is randomized after each scattering event. As we will see below, correlations between successive scattering events due to a “quenched” disordered potential can have a significant

impact on transport.

Along similar lines, radiation transport can be efficiently modelled numerically in arbitrary geometries via random-walk (Monte Carlo) simulations with arbitrary step length distributions, including those with diverging second moment (Nolan, 2003). Such random walks are known as Lévy walks (Zaburdaev *et al.*, 2015) and have been proposed as a tool to describe radiation transport in clouds (Davis and Marshak, 1997), leading to enhanced ballistic transmission and transmitted intensity fluctuations.

2. From normal to super-diffusion

In classical radiative transfer, the average (incoherent) intensity is expected to follow the laws of diffusion after many scattering events, see Sec. II. Physically, diffusion is related to the Brownian motion of many independent moving elements (i.e. random walkers). As long as the second moment of the step length distribution $f_s(s)$ is finite, the central limit theorem shows that the average step length converges towards a normal distribution, eventually leading to a diffusive process, characterized by a mean square displacement $\langle r^2(t) \rangle \sim 2dDt$. Under these circumstances, the presence of large heterogeneities does not prevent the diffusion limit but leads to a modified diffusion constant. From a simple isotropic random walk consideration (Ben-Avraham and Havlin, 2000), it is possible to show that the diffusion constant for a step length distribution $f_s(s)$ is given by (Svensson *et al.*, 2013)

$$D = \frac{v}{2d} \frac{E[s^2]}{E[s]}, \quad (122)$$

with $E[X]$ is the expectation value of the random variable X . This expression is apparently not well known and yet very interesting. It shows that the fluctuations in the step length are as important as the mean step length. In practice, any correlated system exhibiting slower-than-exponential decay will experience an increased diffusion constant. The known expression $D = \frac{v\ell_t}{d}$ is only recovered for an exponentially-decaying function of $f_s(s)$ and using the similarity relation $\ell_t = \ell_s/(1 - g)$.

A fundamentally different behavior is observed when heterogeneities are so strong that they make the second moment of $f_s(s)$ diverge. This is the case for power-law decays $f_s(s) \sim s^{-(\alpha+1)}$ with $\alpha < 2$, defining the so-called Lévy walks. By virtue of the generalized central limit theorem (Gnedenko and Kolmogorov, 1954), one shows that the average step length should follow an α -stable Lévy distribution, which is identically heavy-tailed. Lévy walks lead to superdiffusive transport, characterized by a mean-square displacement growing faster than linear

with time (Zaburdaev *et al.*, 2015)

$$\langle r^2(t) \rangle \sim t^\gamma, \text{ with } 1 < \gamma \leq 2. \quad (123)$$

Lévy statistics and anomalous diffusion are widespread in science, from the random displacement of molecules in flows (Solomon *et al.*, 1993) to the foraging strategy of animals (Bartumeus *et al.*, 2005). While early studies had already evidenced modified path length distributions of light in fractal aggregates of particles (Dogariu *et al.*, 1992, 1996; Ishii *et al.*, 1998), the first experiments aiming to control the anomalous diffusion of light in disordered systems have been initiated by Barthelemy *et al.* (2008). So-called Lévy glasses are fabricated by incorporating in a disordered medium containing small scattering particles, a set of transparent, non-scattering spheres with sizes ranging over orders of magnitude acting as spacers (see the last panel in Fig. 5). By controlling the distribution of sphere diameters and assuming single scattering in the interstices between the spheres and annealed disorder, one can control the step length distribution $p(s)$ in the medium (Bertolotti *et al.*, 2010a). Latest time-resolved experiments on Lévy glasses showed indeed a (transient) superdiffusive light transport (Savo *et al.*, 2014). Lévy statistics in light transport has also been observed in hot atomic clouds (Araújo *et al.*, 2021; Baudouin *et al.*, 2014; Mercadier *et al.*, 2009), as a result from Doppler broadening (Baudouin *et al.*, 2014; Pereira *et al.*, 2004), not from structural correlations.

An important aspect of transport in Lévy glasses is the fact that the disorder is frozen or quenched. Classical transport models assume annealed disorder, in the sense that there is no correlation between successive scattering events – a photon “sees” a new structure after each scattering event. In real samples, successive steps are however not independent. There exists correlations due to the large empty regions. As shown by theory and experiments on scattering powders containing large monodisperse voids (Svensson *et al.*, 2014), quenched disorder leads to an effective reduction of the diffusion constant compared to annealed disorder. The impact of quenched disorder in Lévy-like systems has been subject to several numerical and theoretical investigations (Barthelemy *et al.*, 2010; Beenakker *et al.*, 2009; Buonsante *et al.*, 2011; Burioni *et al.*, 2010, 2012, 2014; Groth *et al.*, 2012), eventually showing that the actual observation of superdiffusive transport in finite-size system (hence with truncated step-length distribution) requires a proper finite-size scaling analysis and packing strategy (Burioni *et al.*, 2014).

V. MESOSCOPIC AND NEAR-FIELD EFFECTS

The interplay of order and disorder in photonic structures not only impacts light transport but also promotes

strong coherent effects, resulting in the emergence of sometimes unexpected phenomena for disordered systems. This section is devoted to the main mesoscopic and near-field phenomena that have attracted attention in the past decades, namely the opening of photonic gaps in disordered systems [Sec. V.A], transitions between various mesoscopic transport regimes [Sec. V.B], non-universal speckle correlations [Sec. V.C] and large local density of states fluctuations [Sec. V.D]. We attempt to provide a clear picture of the current understanding in the field.

A. Photonic gaps in disordered media

Photonic gaps are one of the most striking manifestations of structural parameters on optical transport. Similarly to electronic gaps in semiconductors, a photonic gap corresponds to a spectral range in which no propagating modes exist. The concept of photonic gap is known in optics since the early works on (one-dimensional) thin-film optical stacks (Yeh *et al.*, 1988), emerging as a consequence of the periodic modulation of the refractive index on the wavelength scale. The idea was generalized in the late 1980s to two and three-dimensional periodic structures (John, 1987; Yablonovitch, 1987) and has been at the heart of research in optics and photonics for about two decades. The interest in photonic gaps largely comes from the possibility to engineer defects states with high-quality factors and wavelength-scale confinement, opening unprecedented opportunities to control spontaneous light emission and light propagation for applications in all-optical integrated circuits (Joannopoulos *et al.*, 2011).

Probably because of the convenience of Bloch's theorem and the development of numerical methods exploiting periodicity to solve Maxwell's equations, it is widely believed in the optics and photonics community that the opening of photonic gaps requires the refractive index variation to be periodic in space, i.e. the structure to exhibit long-range periodic correlations. Early works investigating the impact of structural imperfections on optical properties however realized, by drawing a parallel with semiconductor physics were similar questions have been tackled (Phillips, 1971; Thorpe, 1973; Weaire, 1971), that certain gaps could persist even in absence of periodicity (Chan *et al.*, 1998; Jin *et al.*, 2001), thanks to local (Mie or short-range correlated) resonances (Lidrikis *et al.*, 2000). Later reports on photonic gaps in 3D disordered structures exhibiting short-range correlations (Edagawa *et al.*, 2008; Imagawa *et al.*, 2010; Liew *et al.*, 2011) and the proposition that hyperuniformity was a requirement for photonic gaps (Florescu *et al.*, 2009) greatly stimulated the community to unveil the relation between local morphology and structure, and the opening of spectrally wide gaps (Froufe-Pérez *et al.*, 2016; Klatt *et al.*, 2019; Ricouvier *et al.*, 2019; Sellers *et al.*, 2017).

1. Definition and identification of photonic gaps in disordered media

The notion of photonic gap is intimately linked with that of density of states (DOS). Formally, the DOS describes the spectral density of eigenmodes in the medium – i.e., the solutions of the source-free Maxwell's equations – around frequency ω . For instance, the DOS of a closed and non-absorbing system with volume V is simply

$$\rho(\omega) = \frac{1}{V} \sum_m \delta(\omega - \omega_m), \quad (124)$$

where ω_m is the frequency, that is the eigenvalue, associated to resonant mode m . For non-dissipative systems, this frequency is real. In this framework, a photonic gap thus corresponds to a spectral region wherein $\rho(\omega) = 0$, and can therefore easily be found from an eigenmode analysis. In the case of disordered media, a classical strategy, illustrated in Fig. 9a in the case of parallel dielectric cylinders in TM polarization, is to employ the planewave expansion method (Ho *et al.*, 1990; Johnson and Joannopoulos, 2001) on a periodic supercell that is sufficiently large to be representative of the statistics of the medium morphology. The system being conservative, a photonic gap is easily recognized as a spectral region containing no propagating modes [Fig. 9b]. This approach can only be numerical as the DOS is not directly accessible experimentally and real systems are always of finite size and open. The latter makes that the DOS can in fact never be strictly equal to zero.

A second approach, which may now be performed experimentally (Aubry *et al.*, 2020; Leistikow *et al.*, 2011; Lodahl *et al.*, 2004; Sapienza *et al.*, 2011), consists in performing a finite-size scaling analysis of the emitted power (or spontaneous emission rate) of a quantum emitter embedded in a finite-size systems, see Fig. 9c for an illustration. The power P_{em} emitted by a dipole source with moment $\mathbf{p} = p\mathbf{u}$, rigorously derived from Maxwell's equations (Carminati *et al.*, 2015; Novotny and Hecht, 2012), reads

$$P_{\text{em}} = \frac{\pi\omega^2}{4\epsilon_0} |\mathbf{p}|^2 \rho_e(\mathbf{r}, \mathbf{u}, \omega), \quad (125)$$

where ρ_e is the projected local density of states (LDOS) (in units of s.m^{-3}) defined as

$$\rho_e(\mathbf{r}, \mathbf{u}, \omega) = \frac{2\omega}{\pi c^2} \text{Im} [\mathbf{u} \cdot \mathbf{G}(\mathbf{r}, \mathbf{r}, \omega) \mathbf{u}]. \quad (126)$$

$\mathbf{G}(\mathbf{r}, \mathbf{r}', \omega)$ is the total Green tensor in the structured environment. Decomposing it as a sum of the Green tensor in the homogeneous background and the Green tensor due to the fluctuating permittivity, one readily understands that the suppression (resp., enhancement) of the LDOS results from destructive (resp., constructive) inter-

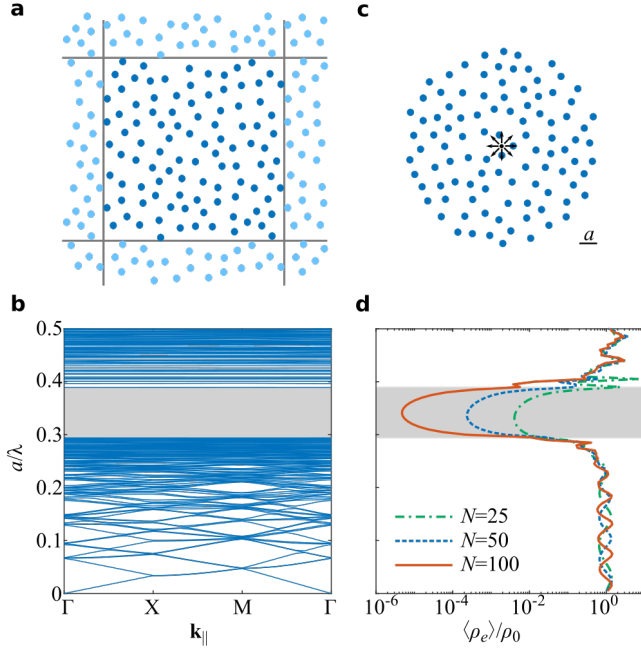


FIG. 9 Signatures of photonic gaps in short-range correlated ensembles of dielectric rods in TM polarization. The rods have a permittivity $\epsilon = 11.6$, a radius $r = 0.189a$, are placed in air and are packed by RSA at a surface filling fraction $f = 11.2\%$ (number density $n = a^{-2}$). (a) A disordered ensemble of rods is generated in a square region with periodic boundary conditions. (b) Photonic band structure with a gap that correspond to an absence of eigenmodes in a finite spectral range a/λ . Numerically, the eigenmodes can be computed using the plane-wave expansion method with the supercell approach. The band structure was calculated here for a supercell containing $N = 100$ rods. (c) A photonic gap can be identified by monitoring the spontaneous emission rate of a dipole source in the center of the system for varying system sizes. The emitter here is always placed in air. (d) Finite-size scaling of the spontaneous emission rate (or LDOS) for systems containing 25, 50 and 100 rods. $\langle \rho_e \rangle$ is the projected LDOS averaged over disorder configurations and ρ_0 is the projected LDOS in air. A gap leads to a strong damping of spontaneous emission with system size.

ference at the dipole position between the field radiated in the homogeneous background and the field scattered by the heterogeneities.

Equation (126) is general, yet it does not explicitly depend on the actual states of the system. To gain some physical insight, it is possible to express \mathbf{G} in terms of the eigenmodes of the system, see Appendix D for more details. The eigenmodes of open (non-Hermitian) systems, also known as quasinormal modes (QNMs) (Ching *et al.*, 1998; Lalanne *et al.*, 2018), are described by complex frequencies $\tilde{\omega}_m = \omega_m - i\gamma_m/2$ and normalized fields $\mathbf{E}_m(\mathbf{r})$, where the non-zero imaginary part stems from leakage. Physically, the existence of a photonic gap translates into the absence of resonant modes in the volume of the medium: the resonant modes may only be confined

to the boundaries of the medium, i.e. on a length scale of the order of the extinction (scattering) mean free path. Thus, their excitation by a source deep inside the system, the LDOS and the resulting emitted power are all expected to tend towards zero with increasing size in the photonic gap, while it should remain quite unchanged in presence of propagating modes [Fig. 9d].

Despite the conceptual simplicity of this second strategy, care should be taken with the interpretation of emitted power (or spontaneous emission decay rate) spectra measurements. Indeed, as we will see in Section V.D, LDOS fluctuations can be enormous in complex media, depending considerably on the local environment around the emitter position. Thus, only average quantities acquired over a large set of disorder realizations are statistically relevant. This raises a second difficulty related to the fact that quantum emitters like quantum dots have a finite size, thereby inducing a local spatial correlation, and they are usually not distributed uniformly in all materials composing the complex medium (e.g., a semiconductor and air). Thus, the configurational average of the LDOS for a real emitter will often not be strictly equal to the average LDOS, as may be computed numerically for instance. Although it seems reasonable to assume that the average LDOS should converge towards the DOS in the limit of infinite system size, it appears that the link between photon emission statistics and the existence of photonic gaps has only been established phenomenologically to date.

2. Competing viewpoints on the origin of photonic gaps

Discussions on the origin of the photonic gaps in disordered media started to emerge in the late 1990s, inspired by earlier works on electronic gaps in (periodic and amorphous) semiconductors. Two main mechanisms have been identified.

The first, generally accepted, mechanism is that photonic gaps build up from interference between counter-propagating waves on a periodic lattice, thereby placing long-range structural correlations at the core of the picture. It is the photonic analog of the nearly free electron model in solid-state physics (Kittel, 1976). Formally, the Bloch modes – the eigenmodes of periodic systems – result from a coupling between forward and backward propagating planewaves on the periodic lattice (Yeh *et al.*, 1988). In spectral gaps, they form stationary patterns that do not carry energy (in the lossless case) due to a backscattering phenomenon with precise phase-matching condition. Their propagation constant is complex, leading to a damping of an incident wave in the specular direction, without scattering. Photonic (band) gaps in 1D media, or in one particular direction in a 2D or 3D photonic crystal (Spry and Kosan, 1986), can exist even for vanishingly small refractive index contrasts. Om-

nidirectional gaps in higher dimensions requires higher contrasts and a finely-optimized structure and morphology (Joannopoulos *et al.*, 2011). Because such spectral gaps are created by long-range periodicity, they are expected to be very sensitive to lattice deformations.

The second proposed mechanism is that photonic gaps are formed by coupled resonances between short-range correlated neighboring scatterers. It is the photonic analog of the tight-binding model in solid-state physics, developed in particular to explain the origin of the electronic density of states of amorphous semiconductors (Weaire, 1971). Intuitively, similarly to the level repulsion observed in a pair of coupled resonances, interaction between nearest neighbors in ensembles of identical resonators may “push” the states of the coupled system away from the resonant frequency, provided that the coupling energy is sufficiently high. In this picture, the interaction between distant resonators, and thus long-range structural correlations, are irrelevant. As a consequence, one expects photonic gaps to exist in both periodic and disordered systems, provided that the resonances of the individual scatterers and the coupling constant between scatterers remain nearly the same throughout the entire structure.

A different, complementary viewpoint on this second mechanism is provided by considering the effective material parameters of assemblies of resonant objects (Lagendijk and Van Tiggelen, 1996). In particular, the effective permittivity ϵ_{eff} is predicted to exhibit a polaritonic response that possibly becomes negative in its real part for sufficiently strong resonances and high density. Having $\text{Re}[\epsilon_{\text{eff}}] < 0$ implies that $\text{Im}[n_{\text{eff}}] > \text{Re}[n_{\text{eff}}]$, corresponding to a coherent field propagating in the effective medium that is overdamped, as in a metal. As shown in Sec. II, stealthy hyperuniform structures (be they ordered or disordered) suppress scattering in the long-wavelength regime (up to the second order in the expansion of the intensity vertex). This implies that $\text{Im}[\epsilon_{\text{eff}}] \simeq 0$. Thus, one arrives to a situation where propagation is damped by coupled resonances and scattering is suppressed by structural correlations. This describes a system behaving as a homogeneous medium with no propagating states, that is a system exhibiting a photonic gap.

3. Reports of photonic gaps in the literature

The formation of photonic gaps very much depends on the dimensionality of the system and on the light polarization, for both periodic and disordered media. For instance, early works using numerical simulations with scalar waves have suggested that 3D face-centered cubic lattices of dielectric spheres could exhibit an omnidirectional gap, but vector wave calculations disproved this prediction (Ho *et al.*, 1990). Figure 10 shows various ex-

amples of disordered photonic structures exhibiting photonic gaps.

It was suggested and demonstrated numerically already about two decades ago that photonic gaps in 2D ensembles of dielectric (e.g. silicon) rods in TM polarization (electric field normal to the propagation plane) are created by the strong electric dipole resonance of individual rods (Jin *et al.*, 2001). Those gaps were actually observed previously in an experiment on light localization (Dalichaouch *et al.*, 1991) and interpreted as “vestiges” of the photonic band diagram of the periodic system. The structures do not need to be hyperuniform to exhibit gaps, but require a reasonable amount of short-range correlations. It is interesting to note that both the first and second gaps (in periodic arrays) are actually due to the same electric dipole resonance, while the intermediate conduction band is associated to the magnetic dipole resonance (Vynck *et al.*, 2009). In TE polarization (electric field in the propagation plane), a similar resonant behavior leading to a gap was pointed out by (O’Brien and Pendry, 2002) for very high index materials, but the gap closes for dielectric materials in the optical regime.

2D inverted structures made of circular air holes in dielectric exhibit photonic gaps that, by comparison, are much more sensitive to lattice deformations (Yang *et al.*, 2010b), suggesting that periodicity, at least on a few periods, is required. It was shown however that connected networks made of thin dielectric walls on a stealthy hyperuniform pattern are favorable to exhibit a photonic gap in TE polarization (Florescu *et al.*, 2009). First reports in non-periodic arrays were made on quasiperiodic structures (Chan *et al.*, 1998). This result is more unexpected than for the direct structures since one cannot define a unique scattering element in this case. Nevertheless, short-range correlations tend to homogenize locally the size distribution and shape of air pores, which, surrounded by dielectric walls in TE polarization, could be seen as nearly identical resonant scatterers. A recent study further revealed that stealth hyperuniformity was actually not necessary, short-range structural correlations being sufficient for the purpose (Froufe-Pérez *et al.*, 2016).

A greater challenge is to form photonic gaps in 3D disordered media. Studies nowadays tend to agree that the best solution for the purpose are 3D connected networks, basically consisting of air pores of nearly identical size surrounded by an array of dielectric rods (Edagawa *et al.*, 2008; Imagawa *et al.*, 2010; Liew *et al.*, 2011; Yin *et al.*, 2012). Recently, Sellers *et al.* (2017) put forward the idea of “local self-uniformity” to explain the formation of wide gaps. Such structures strongly resemble foams (Klatt *et al.*, 2019; Ricouvier *et al.*, 2019), which suggests the possibility to fabricate them with bottom-up techniques. Important efforts are underway to demonstrate experimentally 3D photonic gaps in the optical regime. First

results on samples realized by direct laser writing and double inversion to increase the refractive index contrast indicate a depletion of transmission (Muller *et al.*, 2017).

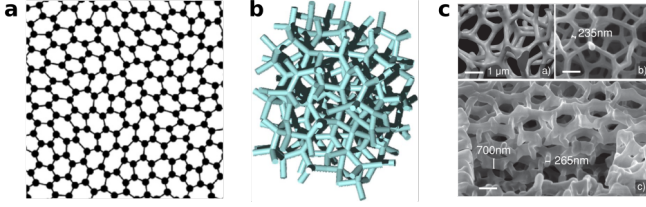


FIG. 10 . Photonic structures lacking long-range order that were shown to exhibit large photonic gaps. (a) 2D stealthy hyperuniform structure exhibiting a gap for both TM and TE polarizations. The TM gap is due to the resonances of the dielectric rods and the TE gap to the air pores surrounded by dielectric holes. Adapted with permission from (Florescu *et al.*, 2013). (b) 3D amorphous diamond structure exhibiting an omnidirectional photonic gap. The structure consists in a network of dielectric rods forming air pores of comparable sizes. Adapted with permission from (Edagawa *et al.*, 2008). (c) First experimental realizations of 3D disordered structures potentially exhibiting a photonic gap at optical frequencies. The silicon photonic medium was realized by direct laser writing followed by a double inversion process. Adapted with permission from (Muller *et al.*, 2013).

B. Mesoscopic transport and light localization

Mesoscopic transport in disordered systems refers to a regime wherein interferences between multiply-scattered waves lead to significant transport parameter deviations compared to classical approaches such as radiative transfer. Coherent effects, at the mesoscopic length scales, often lead to statistical distributions that are much broader and more complex than those expected from thermodynamic considerations. Signatures of mesoscopic effects, such as large sample-to-sample transmittance fluctuations, non-self-averaging transport parameters or long-range speckle intensity correlations, may still be visible on macroscopic scales provided that the signal has a sufficiently long coherence length compared to the characteristic lengths of the system. If many concepts in mesoscopic physics have been developed in the context of electronic transport (Akkermans and Montambaux, 2007; Altshuler *et al.*, 2012; Mello *et al.*, 2004; Sheng, 2006), research on classical waves brought a great deal of new ideas and challenges to the topic (Rotter and Gigan, 2017), stimulated by the unique possibility to engineer the scattering materials at the subwavelength scale.

One of the most fascinating phenomena in mesoscopic physics of classical waves is the Anderson localization (Anderson, 1958), see (Lagendijk *et al.*, 2009) for an historical overview of the topic and (Abrahams, 2010) for more technical details. The phenomenon takes its roots in the so-called weak localization effect,

which describes a small reduction of the diffusion constant (compared to that predicted from radiative transfer) due to interference between counter-propagating waves. This effect requires reciprocity to hold (van Tiggelen and Maynard, 1998), which is generally the case in non-magnetic optical materials. Strong (Anderson) localization is obtained by a progressive renormalization of the diffusion constant that eventually leads to a complete halt of transport, as described by the self-consistent diagrammatic theory due to Vollhardt and Wölfel (1982, 1980). In open finite-size systems, the localized regime is characterized by exponentially-decaying transmittance (Van Tiggelen *et al.*, 2000), anomalous time-dependent response (Skipetrov and Van Tiggelen, 2006), large transmitted speckle intensity fluctuations (Chabanov *et al.*, 2000) and multifractality of the field (Mirlin *et al.*, 2006).

A transition between extended and localized regimes is expected in three-dimensional (3D) systems when the scattering mean free path becomes comparable with the effective wavelength in the medium, $k_r \ell_s \approx 1$, also known as the Ioffe-Regel criterion (Ioffe and Regel, 1960). Experiments on high-index semiconductor powders and photonic glasses, which offer amongst the smallest ℓ_s in optics, have failed to provide evidence of light localization (Scheffold *et al.*, 1999; Scheffold and Wiersma, 2013; Skipetrov and Page, 2016; Sperling *et al.*, 2013; Wiersma *et al.*, 1997), contrary to studies on ultrasounds in elastic networks (Hu *et al.*, 2008) and matter waves in optical potentials (Jendrzejewski *et al.*, 2012; Kondov *et al.*, 2011). It turned out that the key role of polarization for electromagnetic waves and near-field effects had been largely underestimated (Bellando *et al.*, 2014; Skipetrov and Sokolov, 2014), thereby placing a finer engineering of the local morphology – and of structural correlations – at the heart of the problem.

In the literature, the challenge of reaching a localized regime in 3D in optics appears closely related to that of creating a photonic gap. In a founding work, John (1987) proposed that a slight disorder in a periodic medium exhibiting a photonic gap would promote Anderson localization near the gap edge, where some (but not all) propagation directions are inhibited. Anderson localization occurs in the band and differs in that sense from classical light confinement, where defect (cavity) modes – or bound states – are formed in the gap. This distinction has remained somewhat fuzzy in the literature in optics. Localized modes have been observed via numerical simulations in randomly-perturbed periodic inverse opals (Conti and Fratalocchi, 2008), where it was found that the strongest light localization was obtained at an optimal degree of disorder [Fig. 1(d)], as well as in amorphous diamond structures (Imagawa *et al.*, 2010) [Fig. 1(e)], but their precise nature is unclear. The transition between extended and Anderson-localized regimes (outside the photonic gap) has been

evidenced only recently in a numerical study on disordered hyperuniform structures thanks to a statistical analysis based on the self-consistent theory of localization (Haberko *et al.*, 2020). Although the effect of the kind of structural correlation on mesoscopic transport remains to be clarified, disorder engineering has clearly given a new hope for the experimental observation of 3D Anderson localization of light.

Light localization in two-dimensional (2D) disordered systems has experienced much less difficulties in comparison. Theoretical arguments developed for electronic transport (Abrahams *et al.*, 1979) let us expect that all waves be localized on some length scale ξ in two dimensions independently of the scattering strength of the medium. Despite the absence of a “true” transition, 2D systems have been very appealing because they can be fabricated, characterized (structurally and optically) and modelled much more easily than their 3D counterpart. The first report of localization of classical waves date back to Dalichaouch *et al.* (1991) with a study of microwave propagation in high-index dielectric cylinders in TM polarization, where a link with photonic gaps was already made. The first experimental demonstration of Anderson localization in the optical regime was obtained by Schwartz *et al.* (2007) in photonic lattices consisting of evanescently coupled parallel waveguides wherein localization occurs in the transverse direction (De Raedt *et al.*, 1989). In this configuration, the electromagnetic problem is mapped onto the time-dependent Schrödinger equation where the propagation direction plays the role of time, enabling the exploration of many interesting problems in condensed matter physics (Rechtsman *et al.*, 2013; Segev *et al.*, 2013; Weimann *et al.*, 2017). 2D Anderson localization has later been reported for in-plane propagation of near-infrared light in suspended high-index dielectric membranes perforated by disordered patterns of holes (Riboli *et al.*, 2011). Quantum dots incorporated in the membrane are excited locally by a near-field probe and their photoluminescence is collected by the same probe at the same position. A post-treatment allows recovering spatial and spectral information on the resonant modes of the system (Riboli *et al.*, 2014).

Structural correlations have not been considered specifically in these works, probably because they were not necessary to observe localized modes in 2D. Nevertheless, they can impact mesoscopic transport in mainly two ways: First, by creating a photonic gap in the vicinity of which localized modes appear, as shown experimentally in photonic lattices with short-range correlations (Rechtsman *et al.*, 2011) and randomly-perturbed periodic hole arrays in dielectric membranes (Garcia *et al.*, 2012). The latter study shows that the stronger confinement in periodic systems is obtained with an optimal level of disorder, similarly to (Conti and Fratalocchi, 2008). Second, by modifying the scattering and transport parameters of disordered systems, which in turn

modify the localization length ξ , as shown by Conley *et al.* (2014). Remarkably in 2D, small changes of structural correlations may induce variations of ξ over orders of magnitude, since this quantity is expected to grow exponentially with the mean free path (Abrahams *et al.*, 1979; Sheng, 2006). This allows moving very easily from a quasi-extended regime to a localized regime in finite-size systems. Numerical simulations performed for TE-polarized waves in 2D disordered patterns of holes in dielectric validate this possibility, although the agreement with theoretical predictions is only qualitative. Note also that the study covers a short-range correlation up to the onset of polycrystallinity, which might affect localization.

The variety of mesoscopic transport regimes in 2D disordered media was investigated recently by Froufe-Pérez *et al.* (2017), who proposed a transport phase diagram, shown in Fig. 11, for 2D stealthy hyperuniform structures made of high-index cylinders in TM polarization. Uncorrelated media (small values of χ) experience the standard behavior with quasi-extended and localized regimes depending on the scattering strength of the cylinders and the system size. At the opposite, strongly correlated media (high values of χ) are very transparent at low frequencies due to the suppressed single scattering over a finite range of scattering wavenumbers and exhibit a photonic gap (i.e., zero DOS in infinite media) at intermediate frequencies near the resonant frequency of the cylinder. The gap is surrounded by a low-DOS region containing weakly-coupled resonant states (defect modes) and the Anderson-localized regime. The phase diagram has been validated numerically (Froufe-Pérez *et al.*, 2017) and experimentally in the microwave regime (Aubry *et al.*, 2020). This diagram is specific to the considered system (including system size) and polarization. Nevertheless, it is quite representative of the different transport regimes that may be observed in correlated disordered media.

C. Near-field speckles on correlated materials

Upon scattering by one specific realization of a disordered medium, a speckle pattern is formed (Goodman, 2007). Universal intensity statistics are found in far-field speckle patterns, that are independent on the microscopic features of disorder. When speckle patterns are observed in the near field, *i.e.* at a distance from the output surface smaller than the wavelength of the incident light, the statistical properties of the speckle become dependent on the statistical features of the medium itself. In particular, as we will see, near-field speckles may exhibit direct signatures of the presence of spatial correlations in the scattering medium (Carminati, 2010; Naraghi *et al.*, 2016; Parigi *et al.*, 2016).

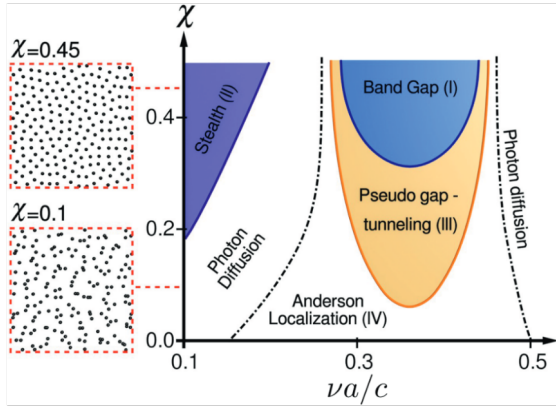


FIG. 11 Correlation-frequency ($\chi - \nu$) transport phase diagram for 2D disordered hyperuniform media. The system is stealthy hyperuniform array of high-index dielectric rods and the wave is TM-polarized. χ is the degree of stealthiness (Batten *et al.*, 2008), $\nu a/c \equiv a/\lambda$ is a reduced frequency with a the mean distance between scatterers (related to the cylinder density). Five transport regimes may be identified, as discussed in the main text. Note that the transition between photon diffusion (quasi-extended regime) and Anderson localization depends on system size. Adapted with permission from (Froufe-Pérez *et al.*, 2017).

1. Intensity and field correlations in bulk speckle patterns

A standard observable in the study of speckles is the correlation function of the intensity fluctuations δI at two different points \mathbf{r} and \mathbf{r}' , defined as

$$\langle \delta I(\mathbf{r}) \delta I(\mathbf{r}') \rangle = \langle I(\mathbf{r}) I(\mathbf{r}') \rangle - \langle I(\mathbf{r}) \rangle \langle I(\mathbf{r}') \rangle, \quad (127)$$

with the intensity $I(\mathbf{r}) = |\mathbf{E}(\mathbf{r})|^2$. As a measure of the degree of correlation of the intensity, one uses the normalized correlation function

$$C^I(\mathbf{r}, \mathbf{r}') = \frac{\langle \delta I(\mathbf{r}) \delta I(\mathbf{r}') \rangle}{\langle I(\mathbf{r}) \rangle \langle I(\mathbf{r}') \rangle} \quad (128)$$

which, in terms of the field amplitude, is a fourth-order correlation function. In the weak-scattering regime $k_r \ell_s \gg 1$, the field is a Gaussian random variable. Indeed, the field at any point in the speckle results from the summation of a large number of independent scattering sequences, leading to Gaussian statistics by virtue of the central-limit theorem (Goodman, 2015). Moreover, in a statistically homogeneous and isotropic medium, and far from sources, the speckle pattern can be considered to be unpolarized. In these conditions, the intensity correlation function factorizes in the form (Carminati and Schotland, 2021)

$$C^I(\mathbf{r}, \mathbf{r}') = \sum_i |C_{ii}^E(\mathbf{r}, \mathbf{r}')|^2, \quad (129)$$

where C_{ij}^E is the (i, j) component of the normalized correlation function between two vector components of the field, or normalized coherence tensor, defined as

$$\mathbf{C}^E(\mathbf{r}, \mathbf{r}') = \frac{\langle \mathbf{E}(\mathbf{r}) \otimes \mathbf{E}^*(\mathbf{r}') \rangle}{\sqrt{\langle I(\mathbf{r}) \rangle} \sqrt{\langle I(\mathbf{r}') \rangle}}. \quad (130)$$

Recall that the spatial correlation of the field in the numerator is described by the Bethe-Salpeter equation [Eq. (21)].

Let us first consider the simplest model of an infinite medium illuminated by a point source at position \mathbf{r}_0 . For large observation distances ($|\mathbf{r} - \mathbf{r}_0| \gg \ell_s$ and $|\mathbf{r}' - \mathbf{r}_0| \gg \ell_s$), one can derive the following general result (Carminati and Schotland, 2021; Dogariu and Carminati, 2015; Vynck *et al.*, 2014)

$$\mathbf{C}^E(\mathbf{r}, \mathbf{r}') = \frac{2\pi}{k_r} \text{Im} \langle \mathbf{G}(\mathbf{r}, \mathbf{r}') \rangle, \quad (131)$$

where $\langle \mathbf{G} \rangle$ is the averaged Green function in the medium. It is interesting to note that this form of the field correlation function is always found under general conditions of statistical homogeneity and isotropy of the field (Setälä *et al.*, 2003).

In order to characterize the field spatial correlation averaged over the polarization degrees of freedom, one often introduces the degree of spatial coherence

$$\gamma^E(\mathbf{r}, \mathbf{r}') = \text{Tr} [\mathbf{C}^E(\mathbf{r}, \mathbf{r}')] . \quad (132)$$

In an infinite medium, and for short-range correlation with $k_r \ell_c \ll 1$, with ℓ_c the correlation length of disorder, it is known that (Carminati *et al.*, 2015; Carminati and Schotland, 2021)

$$\gamma^E(\mathbf{r}, \mathbf{r}') = \text{sinc}(k_r R) \exp[-R/(2\ell_s)], \quad (133)$$

where $R = |\mathbf{r} - \mathbf{r}'|$. This expression takes the same form as that initially derived for scalar waves in (Shapiro, 1986). In an infinite medium, for a Gaussian and unpolarized speckle pattern, the field and intensity correlation functions have a range limited by the wavelength $\lambda_r = 2\pi/k_r$ and by the scattering mean free path ℓ_s .

The impact of structural correlations in the medium on speckle correlations (of the field or intensity) can occur on different levels. First, the value of ℓ_s is directly dependent on the degree of correlation of disorder. Second, the general shape of the field correlation function can also be substantially modified when near fields cannot be ignored in either the illumination process (*e.g.* under excitation by a localized source inside the medium, or close to its surface), or the detection process (*e.g.* detection at sub-wavelength distance from the surface). An example is discussed in the next subsection.

2. Near-field speckles on dielectrics

A speckle pattern observed at subwavelength distance from the surface of a disordered medium (near-field speckle) exhibits statistical properties that may strongly differ from the universal properties of far-field speckles. In the case of near-field speckles produced by rough surface scattering, it is known that in the single-scattering regime the spatial correlation function of the near-field intensity is linearly related to the spatial autocorrelation function of the surface profile (Greffet and Carminati, 1995). In the case of speckles produced by volume multiple scattering, the degree of spatial coherence can be evaluated in a plane at a distance z from the sample surface, in regimes ranging from the far field to the extreme near field (Carminati, 2010). For $z \gg \lambda$, we obtain

$$\gamma^E(\mathbf{r}, \mathbf{r}') = \text{sinc}(k_0 \rho), \quad (134)$$

where ρ is the distance separating the two observation points \mathbf{r} and \mathbf{r}' in a plane at a constant z (parallel to the sample surface). The width δ of the correlation function, that measures the average size of a speckle spot, is limited by diffraction and scales as $\delta \sim \lambda/2$. At subwavelength distance from the medium surface, near fields are dominated by quasi-static interactions. The scale of variation of the field is driven by geometrical length scales, and no more by the wavelength (Greffet and Carminati, 1997; Novotny and Hecht, 2012). Characterizing the structure by the correlation length ℓ_c , and assuming $\ell_c \ll \lambda$, we can distinguish two regimes. For $\ell_c \ll z \ll \lambda$, we have

$$\gamma^E(\mathbf{r}, \mathbf{r}') = \frac{1 - \rho^2/(8z^2)}{[1 + \rho^2/(4z^2)]^{5/2}}, \quad (135)$$

showing that $\delta \sim z$ due to quasi-static (evanescent) near fields. Finally, in the regime $\ell_c \simeq z \ll \lambda$ (extreme near field), we obtain

$$\gamma^E(\mathbf{r}, \mathbf{r}') = M\left(\frac{3}{2}, 1, \frac{-\rho^2}{\ell_c^2}\right) \quad (136)$$

where $M(a, b, x)$ is the confluent hypergeometric function, which here takes the form of a function decaying from 1 to 0 over a width $\delta \simeq \ell_c$. In summary, according to the theory in (Carminati, 2010), we expect the speckle spot size to decrease in the near field as the distance z to the surface, and to saturate at a size on the order of the correlation length of the medium.

The dependence of the speckle spot size at short distance can be probed experimentally using scanning near-field microscopy (SNOM). Studies have been reported in (Apostol and Dogariu, 2003, 2004; Emiliani *et al.*, 2003). The behavior described above has been confirmed recently (Parigi *et al.*, 2016), and the main result is summarized in Fig. 12. The measurement provides the intensity correlation function $C^I(\mathbf{r}, \mathbf{r}')$, the width of which,

according to Eq. (129), can be qualitatively compared to that of the degree of spatial coherence γ^E . By recording near-field speckle images at different distances z from the surface of sample with correlated disorder, the dependence of the speckle spot size δ on the distance to the surface can be extracted. The result is displayed in Fig. 12c. The decrease δ in the near field regime is clearly visible, as well as the non-universal dependence at very short distance (the two curves correspond to two samples with different structural correlations).

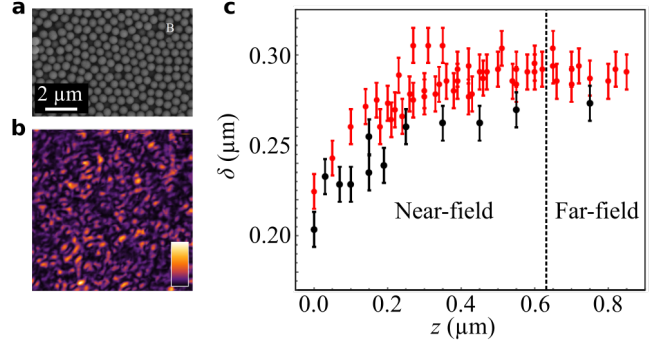


FIG. 12 Signatures of structural correlations on near-field speckles. (a) Scanning electron microscope image of the surface of a typical sample, consisting of several layers of silica spheres in a partially ordered arrangement. (b) Example of speckle image recorded with a scanning near-field optical microscope at a wavelength $\lambda = 633$ nm. (c) Measured correlation length δ in the speckle pattern versus the distance z to the sample surface, in the distance range for which the far-field to near-field transition is observed. The vertical dashed line corresponds to $z = \lambda$. The black and red curves correspond to two samples with an average diameter of the silica spheres $d = 276$ nm and $d = 430$ nm. The very short-distance behavior is expected to depend on the level of short-range order in the sample (size and local organization of the spheres in space). Adapted with permission from (Parigi *et al.*, 2016).

Retrieving information on structural correlations of disordered media from optical measurements is also possible via a stochastic polarimetry analysis of the scattered light (Haefner *et al.*, 2008). As shown by Haefner *et al.* (2010), the local anisotropic polarizabilities of a complex material generally depend on the volume of excitation (which may be controlled, for instance, via a near-field probe). It turns out that one can define a length scale corresponding to a maximum degree of local anisotropy, that is characteristic of the material morphology. This length scale has been evidenced in numerical simulations but not yet experimentally to our knowledge.

D. Local density of states fluctuations

The modification of the spontaneous emission rate from quantum emitters due to electromagnetic interaction with a structured environment is one of the ma-

major achievements in optics and photonics in the past decades (Pelton, 2015). As briefly discussed in Sec. V.A, this effect is formally described by the local density of states (LDOS) that is expressed as a function of the Green tensor $\mathbf{G}(\mathbf{r}, \mathbf{r})$ at the origin [Eq. (126)]. Expectedly, the LDOS should be highly sensitive to the local environment with which it interacts, especially in the near field.

The near-field interaction regime has been initially described using numerical simulations of LDOS distributions inside disordered media and a single-scattering theory (Froufe-Pérez *et al.*, 2007). The model system is a spherical domain with radius R , filled with subwavelength dipole scatterers. The LDOS is calculated at the center of the domain and surrounded by a spherical exclusion volume of radius R_0 . The length scale R_0 is a microscopic length scale that characterizes the local environment (R_0 can be understood as the minimum distance to the nearest scatterer). It was shown that the statistical distribution of the LDOS is strongly influenced by the proximity of scatterers in the near field, and by the local correlations in the disorder (Cazé *et al.*, 2010; Leseur *et al.*, 2017). As in the case of near-field speckle, this is a consequence of quasi-static near-field interactions that make the LDOS sensitive to the local geometry.

Statistical distributions of LDOS in strongly scattering dielectric samples have been measured experimentally at optical wavelength. The approach consists in dispersing fluorescent nanosources inside a scattering material (Birowosuto *et al.*, 2010; Sapienza *et al.*, 2011). Experiments mimicking the model systems studied theoretically use powders made of polydisperse spheres of high-index material (such a ZnO at wavelength $\lambda \sim 600 - 700$ nm). An example of measured LDOS distributions is shown in Fig. 13. The LDOS distribution (top panel), inferred from the distribution of the decay rate Γ of nanoscale fluorescent beads, exhibits a high asymmetric shape with a long tail that is a feature of near-field interactions. This experiment confirms the sensitivity of LDOS fluctuations to the local environment in a volume scattering material in the multiple scattering regime. Comparison with numerical simulations (bottom panel) demonstrates the substantial role of the microscopic length scale R_0 on the shape of the distributions.

Disordered metallic films made by deposition of noble metals (silver or gold) on an insulating substrate (glass) are also known to produce large near-field intensity fluctuations close to the percolation threshold. On the surface of such materials, the near field intensity localizes in subwavelength domains (hot spots) (Laverdant *et al.*, 2008; Seal *et al.*, 2005; Shalaev, 2007). The near-field LDOS exhibits enhanced spatial fluctuations in this regime, that reveal the existence of spatially localized modes (Carminati *et al.*, 2015; Cazé *et al.*, 2013; Krachmalnicoff *et al.*, 2010). Disordered metallic films close to percolation are an example of nanoscale disordered ma-

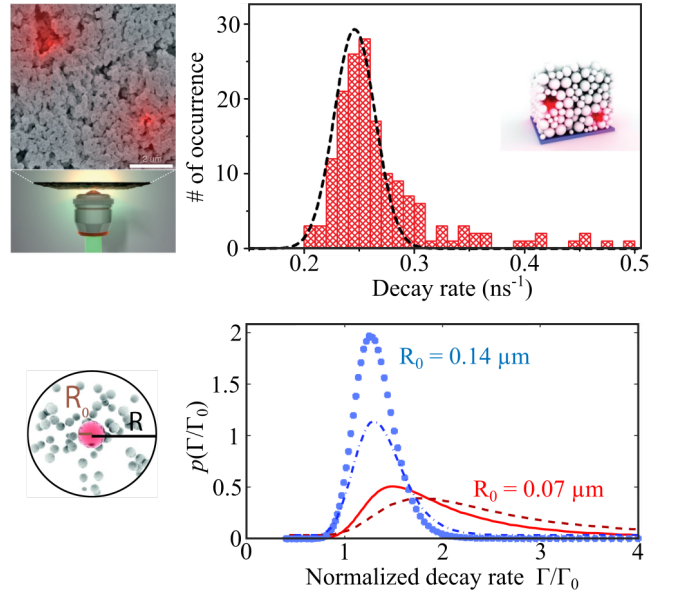


FIG. 13 Impact of structural correlations on LDOS fluctuations. Top: Measured statistical distributions of the spontaneous decay rate $\Gamma \propto \rho$ (LDOS) of fluorescent beads (nanosources with 20 nm diameter) in a ZnO powder with transport mean free path $\ell_t = 0.9 \mu\text{m}$. A scanning electron microscope image of the sample is shown on the left, together with a schematic view of the illumination/detection geometry. The asymmetric shape of the statistical distribution of LDOS and the long tail is a signature of near-field interactions occurring inside the sample. Bottom: Numerical simulations of the statistical distribution of the normalized decay rate $\Gamma/\Gamma_0 = \rho/\rho_0$ of a dipole emitter placed at the center of a disordered cluster mimicking the ZnO powder. The emitter is surrounded by an exclusion volume with radius R_0 . This length scale describes local correlations in the positions of the scatterers in the sample. Blue curves correspond to an exclusion radius $R_0 = 0.14 \mu\text{m}$ while red curves correspond to an exclusion radius $R_0 = 0.07 \mu\text{m}$ (the two curves in the same color correspond to two different densities of scatterers). The simulation demonstrates the substantial influence of R_0 (near-field interactions and local correlations in the disorder) on the shape of the distribution. Adapted with permission from (Sapienza *et al.*, 2011).

terials in which correlations in the disorder substantially influence the optical properties.

Being the LDOS very sensitive to small changes in the local environment of the emitter, the study of the statistics of LDOS, accessible through the decay rate Γ , can be related to the structural properties of a dynamical system of interacting, and hence correlated, scatterers. As an example, it has been numerically demonstrated that the statistical distributions of single emitter lifetimes in a scattering medium can evolve from a unimodal distribution to a different one when the system undergoes a phase transition. The regions of phase coexistence in small systems often turn out to be dynamical phase switching regions, where the entire systems switches between the

two phases (Berry *et al.*, 1984; Briant and Burton, 1975; Honeycutt and Andersen, 1987; Labastie and Whetten, 1990; Wales and Berry, 1994). The signature of the phase switching regime in the Γ statistics can be dramatic, since the distribution can be bimodal in the phase switching regime regions while unimodal in the pure phases. This striking behavior can be related to the statistics of neighboring scatterers surrounding the emitter and is not signaled by other light transport properties such as scattering cross section statistics for instance (de Sousa *et al.*, 2016). Bimodal distributions of LDOS have been also described for emitters embedded in single layers of disordered but correlated lattices (de Sousa *et al.*, 2014).

Figure 14 shows numerical predictions for a system of ~ 1000 resonant point dipoles interacting through a Lennard-Jones potential and tightly confined within a spherical volume (de Sousa *et al.*, 2016). The system is kept at a temperature corresponding to the liquid-gas transition. Due to strong finite size effects, the system is not in phase coexistence but rather switches randomly between the two phases. We see that the emitter decay rates are strongly correlated to the energetic state of the system, leading to two clearly-distinguishable modes. Thus, slight differences in structural correlations can clearly be identified by a statistical analysis of decay rate measurements.

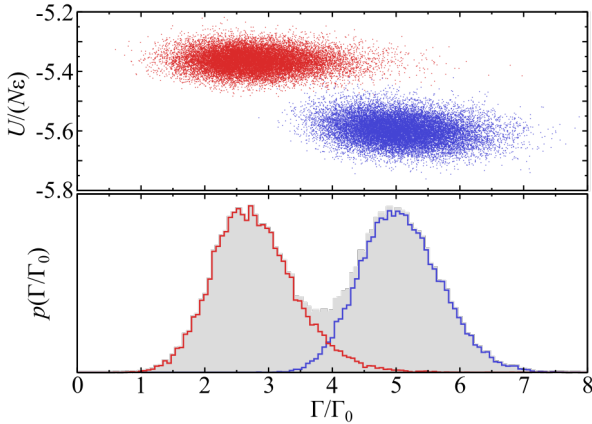


FIG. 14 Signature of structural phase transition in LDOS statistics. Monte Carlo sampling of energy per particle normalized to the energy minimum ε (top) and decay rate normalized to the vacuum one Γ_0 (bottom) for a single emitter placed at the center of a tightly confined system of resonant point scatterers interacting via Lennard-Jones potential. The temperature is such that the systems entirely switches between two phases randomly. On the bottom, the corresponding decay rates distributions are represented for the low energy branch (red), high energy branch (blue). The gray area shows the sum of both distributions. Adapted with permission from (de Sousa *et al.*, 2016).

Recent experiments have shown strongly inhibited spontaneous emission in systems undergoing an order-disorder phase transition (Schöps *et al.*, 2018). The

formation of clusters exhibiting short-range correlations leads to a strong suppression of emission that is apparently comparable to that of an ordered structure.

VI. PHOTONICS APPLICATIONS

The considerable advances in nanofabrication in the past decades have opened new opportunities in the engineering of disordered materials at the subwavelength scale. In this section, we describe the main applications of correlated disordered media in optics and photonics, namely in light management [Sec. VI.A], random lasing [Sec. VI.B] and visual appearance design [Sec. VI.C].

A. Light trapping in layered media

Enhancing the interaction of light with matter is of paramount importance for various applications, including photovoltaics, white light emission and gas spectroscopy. The enhanced light-matter interaction generally translates into a stronger light absorption, be it exploited for photocurrent generation, converted into emission by fluorescence, or simply monitored.

The most popular light trapping strategy for thick ($L \gg \lambda$) bulk materials rely on randomly textured surfaces, acting as Lambertian diffusers to efficiently spread light along all directions within the medium for an arbitrary incoming wave (Green, 2002; Yablonovitch, 1982). Structural correlations on random rough surfaces provide angular and spectral control over scattering (Martins *et al.*, 2013), described via the so-called Bidirectional Scattering Distribution Function (BSDF) (Stover, 1995). Volume scattering constitutes an interesting alternative to surface scattering, as multiple scattering tends to increase the interaction between light and matter (Benzaouia *et al.*, 2019; Mupparapu *et al.*, 2015; Muskens *et al.*, 2008; Rothenberger *et al.*, 1999). Quite counter-intuitively, one should note that the average path length for a Lambertian illumination in non-absorbing media is independent of the scattering strength of the material (Pierrat *et al.*, 2014) and equivalent to the surface scattering light trapping, as predicted from the equipartition theorem (Yablonovitch, 1982) and as verified experimentally recently (Savo *et al.*, 2017). The absorption efficiency therefore depends strongly on the ratio between scattering and absorption. The benefit of structural correlations on light absorption in disordered media has only been considered recently (Bigourdan *et al.*, 2019; Sheremet *et al.*, 2020) and remains largely to be explored.

Stimulated by technological development in next-generation photovoltaic panels, considerable efforts have been dedicated to light trapping in thin films ($L \approx \lambda$) in the past two decades, exploiting coherent phenomena as a new means for enhancing light-matter interac-

tion (Fahr *et al.*, 2008; Gomard *et al.*, 2013; Mokkaṭṭi and Catchpole, 2012). Fundamentally, coupling between an incident planewave and a resonant mode in the layered medium is enabled by fulfilling a matching condition between the projected wavevectors parallel to the interface \mathbf{k}_{\parallel} in the two media (Yu *et al.*, 2010). For periodic photonic crystals, this condition is found for leaky Bloch modes having wavevectors in the light cone $k_{B,\parallel} < k_0 n_{\text{str}}$, where n_{str} is the refractive index of the superstrate or substrate. In periodic structures, the absorption peaks are spectrally narrow and strongly depend on $k_{B,\parallel}$. A further improvement can be obtained by creating imperfections that broaden the spectral and angular response, leading to an overall improved optical efficiency (Oskooi *et al.*, 2012; Peretti *et al.*, 2013).

For disordered media, the quantity of interest is the so-called spectral function, defined as (Sheng, 2006),

$$\rho_s(\mathbf{k}, \omega) = \frac{2\omega}{\pi c^2} \text{Im} [\text{Tr} \langle \mathbf{G}(\mathbf{k}, \omega) \rangle], \quad (137)$$

which is the average density of states resolved in spatial frequencies and is obtained from the Fourier transform of the average Green tensor $\langle \mathbf{G}(\mathbf{r}, \mathbf{r}', \omega) \rangle$. At a given frequency, the spectral function typically exhibits a peak centered on the effective wavevector in the disordered medium, k_r , and a width that is inversely proportional to the extinction mean free path, see Fig. 15. As shown by Vynck *et al.* (2012), short-range correlations allow a fine tuning of the spectral function, including in the radiative zone, eventually leading to a spectrally and angularly optimal light absorption (Bozzola *et al.*, 2014; Pratesi *et al.*, 2013). Experiments on correlated disordered hole patterns (Trompoukis *et al.*, 2016), nanowire arrays exhibiting fractality on some scale (Fazio *et al.*, 2016) and complex nanostructured patterns (Lee *et al.*, 2017) have clearly demonstrated the benefit of disorder engineering for light trapping. A recent work shows that stealthy hyperuniform structures can lead to even higher overall absorption efficiency (integrated over a spectrum of interest) compared to short-range correlated and periodic media (Liu *et al.*, 2018).

Finally, let us point out that the coupling process between free space and thin-film layers is very relevant also in the optimization of light extraction from light-emitting devices like organic LEDs (Gomard *et al.*, 2016), where correlated disordered photonic structures could be realized on large scales, for instance, by inkjet-printing of polymer blends (Donie *et al.*, 2021).

B. Random lasing

Random lasers, where light is trapped in the gain medium by multiple scattering, offer new possibilities for efficient lasing architectures. The disordered matrix folds the optical paths inside the medium by multiple scatter-

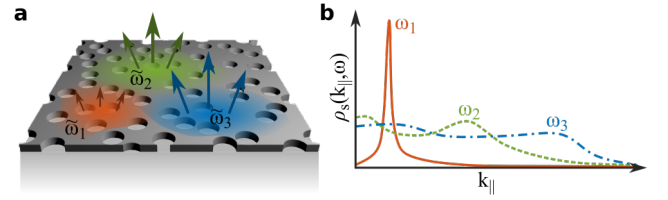


FIG. 15 Process of light coupling and decoupling between a thin dielectric membrane and free-space modes. (a) Sketch of a photonic structure with correlated disorder containing several leaky resonant modes (QNMs). The QNMs are described by different complex frequencies and are coupled to free-space modes. (b) Spectral functions of a short-range correlated disordered photonic structure at different frequencies. At low frequencies, the spectral function is a narrow peak. The value at $k_{\parallel} = 0$ provides information on the coupling efficiency at normal incidence. At higher frequencies, the peaks broaden as a result from stronger scattering and reach higher values for small wavevectors, indicating more efficient coupling.

ing, effectively increasing the probability of stimulated emission, which in turns provides optical gain and the amplification that triggers lasing (Cao, 2005; Wiersma, 2008), see Fig. 16.

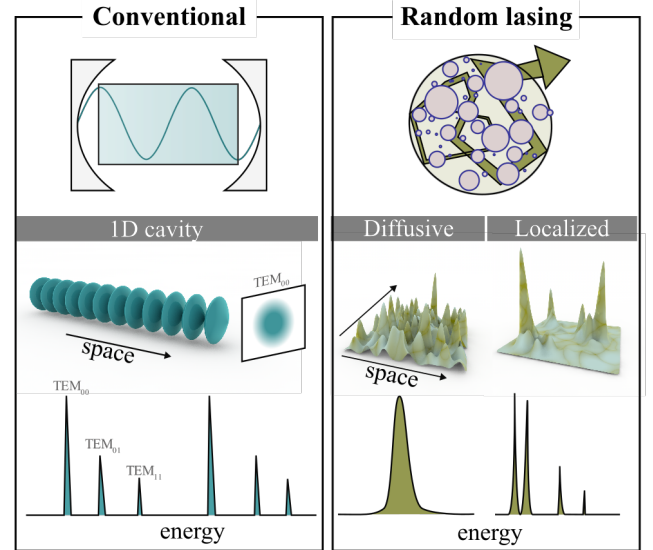


FIG. 16 Conventional vs Random lasing. While a conventional laser (left) is usually composed of a two-mirrors cavity which defines the optical modes, a random laser (right) exploits the confinement by multiple scattering to enhance the probability of stimulated emission. It lases on the “speckle” modes of the disordered medium, either delocalized (bottom left) or localised (bottom right). In both lasers lasing occurs when the gain is larger than the losses, above a certain pumping threshold energy, when stimulated emission becomes the dominant emission process. Lasing peaks can appear in both diffusive or localised regimes, but are easily washed out by temporal or spatial averaging in diffusive media. Adapted with permission from (Sapienza, 2019).

Its functioning principle is the same as in conventional

lasing but without the need for carefully aligned optical elements. The emission of a random laser is also surprisingly coherent, with photon statistics close to that of normal laser emission (Florescu and John, 2004), with strong mode coupling (Türeci *et al.*, 2008) non-trivial modes organization (symmetry replica breaking) (Ghofraniha *et al.*, 2015) and unbounded (Lévy distributed) intensity fluctuations (Uppu and Mujumdar, 2015). Due to the volumetric and (on average) isotropic nature of its lasing patterns a random laser is expected to feature β -factors close to one, i.e. a threshold-less behaviour (van Soest and Lagendijk, 2002). The result (Fig. 16) is an opaque medium in which laser light is generated along random paths in all directions, and over a broad spectral range, with complex temporal profiles (Leonetti *et al.*, 2011).

In the multiple scattering regime, the random lasing threshold can be related to a critical volume or size, such that lasing action can only be achieved for sample sizes larger than this critical dimension. Similar to the critical volume in a neutron bomb, the critical size ensures that the photons sustain net amplification and therefore that the light emerging from the sample is mostly due to spontaneous emission. For a three-dimensional scattering medium, with isotropic scattering and no correlation, embedded in a slab geometry, the critical thickness L_{cr} has been calculated by using the radiative transfer equation (Pierrat and Carminati, 2007) and is solution of

$$\frac{1}{\ell_s} - \frac{1}{\ell_g} = \frac{\pi}{(L_{cr} + 2z_0) \tan(\pi\ell_s/(L_{cr} + 2z_0))} \quad (138)$$

where $z_0 = 0.7104\ell_s$ is the extrapolation length and ℓ_g the net-gain length. Eq. (138) reduces to $L_{cr} = \pi\sqrt{\ell_s\ell_g/3}$ in the diffusive limit with $z_0 = 0$. For anisotropic scattering, we get $L_{cr} = \pi\sqrt{\ell_t\ell_g/3}$. In typical samples, the critical length is of the order of 1 to 100 μm , e.g. $L_{cr} \sim \ell_t$ with $\ell_t \sim 4\mu\text{m}$ in (Caixeiro *et al.*, 2016) and $L_{cr} \sim 300\ell_s$ in (Froufe-Pérez *et al.*, 2009).

The initial scattering architectures for lasing have been 3D disordered semiconductors powders or randomly fluctuating colloids in solution, which can be well thought of and described as a random cloud of dipoles, i.e. without any correlation. Pure randomness is the assumption which simplifies the complexity of the problem to make it treatable with theoretical models. Despite the many successes of this type of uncorrelated disorder, a new generation of disordered lasing architectures, with more robust and collective light-trapping schemes (Gottardo *et al.*, 2008), and new topologies (Gaio *et al.*, 2019).

In particular, spatial correlations between scatterers is a very effective approach for tuning the spectral properties, the number of lasing modes and their threshold by designing photonic band-edge states at the position of the gain. For example, localised modes near the edge of a (2D) photonic gap have been exploited for random lasing (Liu *et al.*, 2014) and single-mode oper-

ation has been achieved in compositionally disordered photonic crystals (Lee *et al.*, 2019). The role of the gap edge has been highlighted in semiconductor membranes with pseudo-random patterning (Yang *et al.*, 2010a), randomly mixed photonic crystals (Kim *et al.*, 2010) and amorphous network structures (Wan *et al.*, 2011), while in photonic amorphous structures, the short-range order improves optical confinement and enhances the quality factor of lasing modes (Yang *et al.*, 2011).

Modelling lasing action in correlated disordered media is often a challenge. In particular lasing occurs for the modes with highest net gain, often escaping the transport models which instead deal with the average intensity. While a full-wave solution of the Maxwell's equations, coupled to the dynamics of the gain, as for example Maxwell-Bloch models (Conti and Fratalocchi, 2008) would contain all the relevant phenomena, it is very hard to implement in realistic samples due to its computational requirements. Advanced *ab-initio* theoretical models have been developed. Let us mention the self-consistent laser theory (Ge *et al.*, 2010; Türeci *et al.*, 2008), which relies on a decomposition of the lasing field on a basis of resonant modes, and the Euclidean matrix theory by Goetschy and Skipetrov (2011), which relies on analytical predictions for the random Green's matrix of a system. Alternatively, more simplified models that neglect the coherence of the modes and describes transport with the radiative transfer equation (or within the diffusion approximation) can be used. The diffusion approximation stems from the initial proposal by Letokhov (1968) and simplifies the calculations significantly (Gaio *et al.*, 2015; Wiersma and Lagendijk, 1996). These models can be extended to include scattering correlations, to modify the scattering and gain parameters, following the theory described in Sec. II.

C. Visual appearance

1. Photonic structures in nature

Living organisms produce a vast variety of photonic mechanisms to modulate their color appearance by exploiting a wide range of biopolymers and architectures. colors produced by these organisms are referred to as structural colors as they are mainly influenced by the nanostructural features of the materials, rather than pigments. However, it is not necessarily straightforward to categorise photonic structures found in nature due both to the lack of consistent methods and tools of analysis and to the incredibly large number of species showing different architectures. Every species uses different materials, structures and strategies for as many biological functions (to attract mates, hide from predators or act as a defence mechanism) (Seago *et al.*, 2008; Vignolini *et al.*, 2012; Whitney *et al.*, 2009; Wilts *et al.*, 2014). Another

degree of difficulty arises from the fact that such natural architectures are often hierarchical, and their visual appearance depends on several factors, including geometrical features, the addition of absorbing pigments and finally, the visual system for which such structures are build (different animals and insects have different perceptions).

Therefore, in the following paragraphs, only a limited selection of explanative examples will be discussed and analysed in this review, keeping in mind that the examples reported here are only a minimal fraction of the efforts that have been done in this field to characterise and categorise such natural photonic structures systematically.

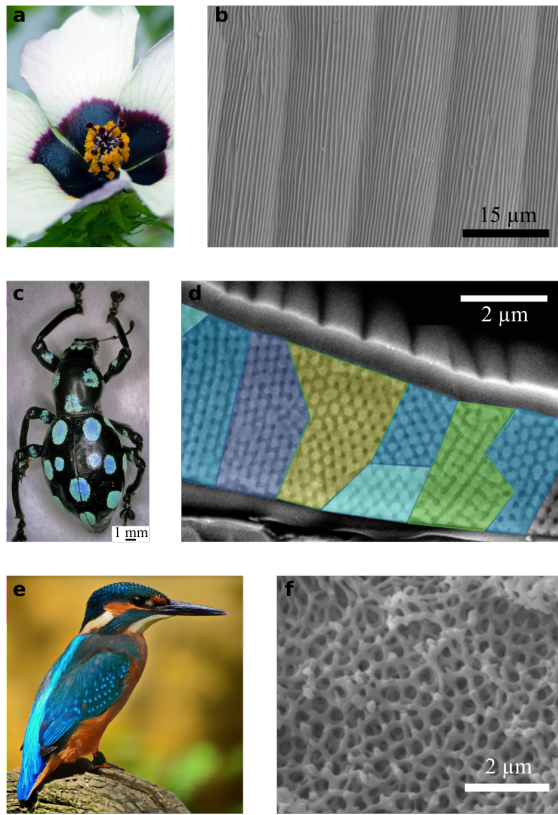


FIG. 17 (a) Flower of Hibiscus Trionum, the blue coloration at the petal base is due to a correlated 1D structure that can be observed in the SEM image in (b). Adapted with permission from (Moyroud *et al.*, 2017). (c) Pachyrhynchus sarcitis Weevils, the blue colored spot in the weevil exoskeleton are the results of a polydomain diamond photonic structures, shown in the SEM image on (d). Adapted with permission from (Chang *et al.*, 2020). (e) Kingfisher, the angular independent blue coloration of the bird feather is the result of a correlated 3D structure, which is shown in the SEM image in (f). Image courtesy of PIXABAY and B. Wilts, respectively. More info in (Stavenga *et al.*, 2011)

In nature, it is possible to find examples within all the distinct classes of correlated disordered media defined in

Sec. III. Many one-dimensional multi-layered structures found in exoskeleton of beetles (Del Rio *et al.*, 2016; Hunt *et al.*, 2007) can be well approximated to the case of imperfect disorder (Onelli *et al.*, 2017), as with Fig. 5. These structures are usually built by the polymerisation of melanin during the ecdysis and the change in the layer spacing during the skeletisation of the cuticle (Onelli *et al.*, 2017). This process is not uniform within the entire cuticle and results in an imperfect ordered structure, as shown by their structure factor (Johansen *et al.*, 2017). The presence of such disorder is not dominant in the visual appearance of these beetles which appear very metallic and iridescent (color-changes in function of illumination condition). Similar imperfect ordered (multi-layered) structures have been found in leaves (Vignolini *et al.*, 2016) and algae (Chandler *et al.*, 2017) but also in this case the disorder does not seem to play any specific evolutionary function, if not to broaden the reflection peaks. Such multilayer structures however can also show fractal geometry to achieve broadband reflectivity, as in the golden chrysalis of the butterfly *Euploea core* (Bossard *et al.*, 2016), which might be considered as an example of fractal disorder.

Another one-dimensional case of imperfect ordered structures are diffraction gratings-like ones. Such imperfect periodic surface striations give rise to strong angle-dependent responses which are very common in several beetles from the order *Coleoptera* (Seago *et al.*, 2008). However, in the case of beetles, not much attention has been given to understanding the role of disorder as their function in biological terms have not been proved yet (they might be present only to reduce friction (Seago *et al.*, 2008)). In contrast, imperfect ordered structures in surfaces striations have been proved a functional tool for flowers to enhance signalling to pollinators (Moyroud *et al.*, 2017). As an example, bees prefer color contrast to iridescent signals, so flowers disordered structure, promoting a not-angular dependent coloration, can pay a major biological advantage.

Disordered structures with short-range correlations capable of producing angular independent colorations such as the one described in the introduction are found in bacteria (Schertel *et al.*, 2020), butterflies (Prum *et al.*, 2006) but also in animals. Most famous examples are the feathers of the eastern bluebird *Cotinga maynana* (Prum *et al.*, 1998) Kingfisher (Stavenga *et al.*, 2011) which present short range correlation of keratin fibrillary network but also several other one such as the *I. puella* as (Noh *et al.*, 2010). Similar short-range correlations between the position of scattering sphere made of collagen are found a convergent strategy to produce blue angular independent coloration in avian skin (Prum and Torres, 2003). The same strategy with same material (collagen) is also exploited in mammalian skin (primates) (Prum and Torres, 2003). Interestingly, these types of structures are always producing blue and green colorations in

nature (Hwang *et al.*, 2021; Jacucci *et al.*, 2020b; Magkiriadou *et al.*, 2014).

Many examples of polycrystalline structures are exploited for coloration in insect wings using three-dimensional photonic crystal structures such as diamond and gyroids. In these cases, polydomains provide a more angular independent response which might again be functional for signalling and camouflaging (Michielsen and Stavenga, 2007). Examples are the diamond-like structures observed inside the scales of the weevils *Lamprocyphus augustus* (Galusha *et al.*, 2008) and *Entimus imperialis* (Wilts *et al.*, 2012) and *Pachyrhynchus weevils* (Chang *et al.*, 2020). Similarly, gyroid structures are found in many lycaenid and papilionid butterflies by (Michielsen and Stavenga, 2007) and in various species such as *C. rubi* (Michielsen *et al.*, 2009; Schröder-Turk *et al.*, 2011), *C. remus*, *P. sesostris* (Wilts *et al.*, 2011), and *T. opisena* (Wilts *et al.*, 2017).

In absence of strong correlation but in case of anisotropy, whiteness can be actually optimised, several natural examples have been recently reviewed by Jacucci *et al.* (2020a). A notable example of optimised whiteness is found on the scales of the beetle genus *Cyphochilus* show a brilliant white coloration whilst only being 5-7 μm thick (Burg *et al.*, 2019; Buresi *et al.*, 2014; Luke *et al.*, 2010; Vukusic *et al.*, 2007; Wilts *et al.*, 2018b). Optical and anatomical studies confirm that anisotropy of the random polymeric network structure in such beetles scales are crucial for scattering optimisation at low refractive indices (Cortese *et al.*, 2015; Jacucci *et al.*, 2019; Lee *et al.*, 2020; Utel *et al.*, 2019).

For larger structures, light cannot be considered coherent across the structure, but little is known on how this affects natural photonic structures and coloration. (Bell *et al.*, 2014) suggested that the locally ordered multilayers in a globally disordered arrangement makes the structural color of the pyjama squid (*Sepioloidea lineolata*) unaffected by changes in light coherence properties, thus making it suitable for having a consistent appearance in an underwater light environment. Light coherence is also important to predict correctly angle-resolved spectra from simulations, which would otherwise be dominated by speckle patterns. Saito *et al.* (2011) investigated this effect for a 2D natural photonic system, however the work has not been expanded since. It is therefore an area that deserves more attention as it may be an important factor for determining reflection and correlation properties in disordered natural photonic structures.

2. Synthetic structural colors

The ability to control visual appearance with correlated photonic structures, both in terms of color and scattering response, is critical in photonic pigments to achieve more angular independent colors. With the im-

provements in the fabrication techniques, it is now possible to assemble such photonic materials cheaply and on a large scale and therefore, their use to replace traditional pigments is becoming a reality (Goerlitzer *et al.*, 2018; Lan *et al.*, 2018). Of particular interest are correlated structures (Shi *et al.*, 2013b). The simplest way to achieve such materials in film consisted in a rapid drying of colloidal suspensions to form photonic glasses (Forster *et al.*, 2010; García *et al.*, 2007; Schertel *et al.*, 2019a). However, this approach has so far only been capable of providing faint blue and green colors. In order to expand the visible palette toward red hues, core-shell photonic glass (Kim *et al.*, 2017; Shang *et al.*, 2018) and inverse photonic structures have been exploited (Zhao *et al.*, 2020) — however their color purity and the reflected intensity remains a problem (Jacucci *et al.*, 2020b). Therefore, short-range crystalline systems with carefully tuned domain orientations or the geometry of the system might allow to overcome these issue (Song *et al.*, 2019).

The design of structural colors with artificial materials also raises questions about their predictability with theoretical models or numerical methods, and the inverse design of artificial materials.

The starting point to predict a color is the computation of the reflectance or transmittance spectra of the disordered material. These spectra are then weighted by the spectral power distribution of the illuminant and by color matching functions for the chromatic response of the observer, to be finally projected onto a specific color space (Ohta and Robertson, 2006), such as CIE 1931 XYZ. The computation of the reflectance and transmittance spectra is evidently the most tedious step. Most studies have relied on finite-difference time-domain (FDTD) simulations (Taflöv and Hagness, 2005), for instance for 3D particulate media (Dong *et al.*, 2010) and porous dielectric networks (Galinski *et al.*, 2017), yet at the cost of heavy computational loads (although this is mitigated by efficient parallelization). Analytical expressions based on diffusion theory have also been used (Schertel *et al.*, 2019a), but care should be taken on the validity of diffusion approximation ($L/\ell_t \gg 1$). A good alternative is to rely on Monte Carlo light transport simulations (Alerstam *et al.*, 2008; Wang and Jacques, 1992) — the numerical counterpart of radiative transfer — wherein positional correlations can be taken into account analytically via Eqs. (107) and (108) and assuming that an effective index can be defined. This allows for a more efficient exploration of the parameter space, as done recently (Hwang *et al.*, 2021).

The inverse design of structural colors is, by comparison, still in its infancy. Powerful topology optimization techniques (Jensen and Sigmund, 2011), also known as adjoint methods, have been used recently to design complex dielectric network materials creating targeted colors in reflection (Andkjær *et al.*, 2014; Auzinger *et al.*, 2018). Although the role of structural correlations on coloration

is implicit, a subsequent structural analysis of the optimal designs could lead to the definition of recipes for materials creating vivid colors.

VII. SUMMARY AND PERSPECTIVES

Research on disorder engineering in optics and photonics has considerably grown in the past decade stimulated by the advent of new concepts and applications. In this last section, we attempt to identify some of the most promising developments for future research along with the theoretical and experimental challenges that will need to be tackled.

A. Near-field-mediated mesoscopic transport in 3D high-index correlated media

Multiple light scattering in disordered media has been treated for many years as a process wherein the vector nature of light could be simplified either by keeping its transverse component only, as we have done in Sec. II, or by treating light just as a scalar wave (Akkermans and Montambaux, 2007). Whereas these approximations may be well justified in dilute media (for both) and far from any polarized source in an opaque medium (for the latter), it recently turned out that the importance of the longitudinal component, which appears in the near-field regime, on mesoscopic transport in dense systems has been largely underestimated so far (Escalante and Skipetrov, 2017; Naraghi *et al.*, 2015; Naraghi and Dogariu, 2016; Skipetrov and Sokolov, 2014). We believe that this aspect deserves full attention from the community. A first attempt to incorporate the longitudinal component in the theory has been proposed very recently by van Tiggelen and Skipetrov (2020) for random ensembles of resonant point scatterers, giving physical ground to the existence of near-field channels in light transport. Near-field interaction processes are dramatically impacted by subwavelength-scale structural correlations, as we have seen in Sec. V.C, and developing a theoretical framework to describe radiative transfer in arbitrary correlated media including the near-field contribution would certainly be an important step forward.

Related to this are the determination of effective material parameters for dense, resonant disordered media and their use to describe light scattering and transport, which are still matter of investigation (Aubry *et al.*, 2017; Yazhgur *et al.*, 2021), as quantitative agreement with experiments and numerics has remained difficult to reach with classical models. On this aspect, let us point out the recent works by Gower *et al.* (2019a,b), demonstrating that multiple coherent waves with different wavenumbers (at fixed frequency) should actually contribute to the average field. This may have important consequences for

scattering by finite-size systems (Gower and Kristensson, 2021) and raises the question of whether these multiple waves are affected in a similar way by structural correlations.

The prominent role played by the precise morphology of 3D disordered media on the emergence of photonic gap and Anderson-localized regimes also deserves clarification. 3D high-index connected (foam-like) structures appear as the best candidates for this purpose according to numerical simulations (Haberkorn *et al.*, 2020; Imagawa *et al.*, 2010; Klatt *et al.*, 2019; Liew *et al.*, 2011; Sellers *et al.*, 2017) but the underlying physical mechanisms have remained difficult to grasp, thereby calling for further theoretical advances. In addition to near-field effects, future works may need to consider high-order n -point correlation functions (with $n > 2$) in the description of structural characteristics (Torquato, 2013; Torquato and Kim, 2021) as well as high-order diagrams in the multiple-scattering expansion (Vollhardt and Wölfle, 1980), which can contribute significantly in strongly correlated media as shown recently (Leseur *et al.*, 2016). Numerical investigations will continue in parallel, and we believe that progress would greatly benefit from the development of numerical methods to solve electromagnetic problems on large systems more efficiently. A possibility could be to generalize the recent concept of global polarizability matrix (GPM) (Bertrand *et al.*, 2020), inspired by earlier methods based on fictitious sources (Wriedt, 1999), to treat systems with connected topologies at lower computational loads.

Experimental demonstrations of photonic gaps and 3D Anderson localization of light in the optical regime have remained out of reach until now and would be great scientific milestones. The main challenge to overcome at this stage is the fabrication of 3D connected structures with finely-tuned correlated morphologies with sufficiently high refractive indices (ideally offering an index contrast above 3) and sufficiently large thicknesses ($L \gg \ell_t$). The steady progress on bottom-up approaches such as bio-templating (Galusha *et al.*, 2010), DNA-origami (Zhang and Yan, 2017) and microfluidic-based foam processing (Maimouni *et al.*, 2020) gives hope for first successful realizations in the next few years. As a longer-term objective, the design and fabrication of 3D *stealthy* hyperuniform media would be an outstanding result. Ultimately, the availability of such high-index nanostructured materials will unlock the possibility to explore experimentally the physics of mesoscopic phase transitions (Evers and Mirlin, 2008) for (polarized) electromagnetic waves.

B. Mesoscopic optics in fractal and long-range correlated media

Light propagation in positively-correlated media is characterized by a non-exponential decay of the coherent intensity. As discussed in Sec. IV.B, materials exhibiting fractal heterogeneities in the form of non-scattering regions of varying sizes can lead in certain conditions to a superdiffusive behavior (Burioni *et al.*, 2014; Savo *et al.*, 2014). Anomalous transport processes (Klages *et al.*, 2008) and dynamics on fractal networks (Nakayama *et al.*, 1994) have a long history, but optical studies on fractal media have so far been mostly concerned with structure factor measurements in the single scattering regime (Lin *et al.*, 1989) (note that the optical properties of semicontinuous metal films near percolation, on which there exists a vast literature (Shalaev, 2007), strongly rely on near-field plasmonic effects and not on light transport). Coherent optical phenomena in “Lévy-like” media have been sparsely addressed until now (Burrelli *et al.*, 2012). Multiple scattering formalisms have been extended to media described by fractal dimensions (Akkermans *et al.*, 1988; Wang and Lu, 1994) or exhibiting superdiffusion (Bertolotti *et al.*, 2010b), disregarding however several difficulties related to the definition of the self-energy and the effective index (Tarasov, 2015), and perhaps more importantly to the quenched nature of disorder (Barthelemy *et al.*, 2010; Burioni *et al.*, 2014). All in all, the development of a rigorous *ab-initio* theory for multiple light scattering in strongly-heterogeneous materials would be a formidable achievement.

Numerical and experimental studies on 1D and quasi-1D Lévy-like systems have revealed anomalous conductance fluctuations and scaling (Ardakani and Nezhad-haghighi, 2015; Fernández-Marín *et al.*, 2014; Lima *et al.*, 2019). Higher-dimensional systems are likely to exhibit a similarly rich physics, which fully remains to be explored. One example is the critical dimension of 2 above which the Anderson transition exists (Abrahams *et al.*, 1979) that may be lowered, depending on the fractality or lacunarity of the system. Optical experiments and numerical simulations could be performed in this regard on high-index planar photonic structures similarly to (Riboli *et al.*, 2014), giving access to LDOS statistics, or to (Yamilov *et al.*, 2014) for transmittance and internal light intensity measurements.

An alternative route for the experimental study of mesoscopic phenomena in long-range correlated systems could rely on disordered photonic network (Gaio *et al.*, 2019) – an optical implementation of random graphs (Janson *et al.*, 2011) –, wherein light propagates through 1D waveguides and is scattered at the waveguide vertices. The waveguide lengths and vertices connectivity thus take the role of structural correlations. The network is a low-dimensional medium embedded in three-dimensional space, and allow to de-

sign light transport and the optical modes. Complex networks with finely-controlled parameters can be fabricated by self-assembly (Gaio *et al.*, 2019), by standard lithography techniques or implemented on macroscopic systems (Lepri *et al.*, 2017).

C. Towards novel applications

The sensitivity of the LDOS to the local environment discussed in Sec. V.D makes quantum emitters interesting optical probes of nanostructured materials (Pelton, 2015). Many studies have reported the dramatic impact of the local morphology of a complex medium on the spontaneous emission statistics from neighboring fluorescent molecules or quantum dots (Birowosuto *et al.*, 2010; Krachmalnicoff *et al.*, 2010; Riboli *et al.*, 2017; Sapienza *et al.*, 2011; de Sousa *et al.*, 2016). A key question to address will be whether optical measurements mediated by near-field probes could reveal statistical information on an unknown morphology, which could be extremely interesting for the remote monitoring of structural phases deep inside a 3D volume (de Sousa *et al.*, 2016). This would require a deep understanding on the relation between subwavelength-scale correlations and near-field phenomena. In addition to LDOS measurements, measuring the cross spectral density of states (CDOS) (Cazé *et al.*, 2013), which describes mode connectivity in structured media and could be obtained from coherence measurements on the light emitted from two classical or quantum dipole sources (Canaguier-Durand *et al.*, 2019), may bring precious additional information. First CDOS measurements have recently been realized in the microwave regime (Rustomji *et al.*, 2021).

The coherent control of light waves in disordered media is an important branch of research in multiple light scattering that has been powered in recent years by wavefront shaping techniques (Rotter and Gigan, 2017). We have seen in Sec. V that structural correlations can result into strong spectral variations of scattering, transport and localization, suggesting that correlated disorder could yield higher degrees of spectral and spatial control, with applications in optical imaging. Disordered media are also being exploited as an unconventional platform for quantum walks and quantum state engineering (Defienne *et al.*, 2016; Leedumrongwatthanakun *et al.*, 2020). These are very delicate experiments that require lossless materials, so far attempted in multimode fibers, but which could benefit in the future from correlated disordered media for multiplexing and spectral resolution.

The design of visual appearance is another aspect of research on correlated disorder that has considerably grown in importance in recent years. As beautifully illustrated by many diverse examples in the living world, the interplay of order and disorder has a direct impact on appearance at macroscopic scales, yielding increased trans-

parency or whiteness, iridescent or non-iridescent colors [Sec. VI.C]. The numerical modelling of *realistic* correlated materials, considering for instance local imperfections (Chung *et al.*, 2012) and large-scale random variations (Chan *et al.*, 2019) in certain ordered systems, will be an essential development of the field in the near future. Our perception of objects indeed relies on many attributes of visual appearance (Hunter and Harold, 1987) – not only color, but also gloss, haze, translucency, texture, etc. –, which are affected by multiple scattering and are rarely considered in full. Understanding how optical properties created by structural correlations at the microscopic scale translate into visual effects at the macroscopic scale is a great and exciting challenge for the coming years. Beyond appearance, correlated disordered media will play an important role in thermal management, for example for radiative cooling (Wang and Zhao, 2020), where broadband light control is needed from inexpensive self-assembled media. Correlated disordered materials could be used to realize multifunctional materials, where optical (visual) properties could be combined with desired thermal, electrical, mechanical or tribological functionalities. Last but not least, efforts should be amplified to develop and promote low-carbon footprint, ecologically-responsible material synthesis, which can be best achieved in disordered assemblies as those discussed in this review.

ACKNOWLEDGMENTS

We are very grateful to Aristide Dogariu (CREOL, University of Central Florida, USA) and Akhlesh Lakhtakia (Penn State University, USA) for fruitful discussions. KV acknowledges funding from the french National Agency for Research (ANR) via the projects “NanoMiX” (ANR-16-CE30-0008) and “Nano-Appearance” (ANR-19-CE09-0014-01). RP and RC acknowledge funding from LABEX WIFI (Laboratory of Excellence within the French Program “Investments for the Future”) under references ANR-10-LABX-24 and ANR-10-IDEX-0001-02 PSL*. This research was supported by the Swiss National Science Foundation through project numbers 169074, 188494 (FS) and 197146 (LSFP). RS and SV acknowledge funding by the Engineering and Physical Sciences Research Council (EPSRC). SV acknowledges the European Research Council (ERC-2014-STG H2020 639088).

Appendix A: Green functions in Fourier space

1. Dyadic Green tensor

We consider a statistically homogeneous and translationally-invariant medium. The dyadic Green tensor in a uniform background medium with auxiliary

permittivity ϵ_b is given by Eq. (14) and related to its Fourier transform as

$$\mathbf{G}_b(\mathbf{r} - \mathbf{r}') = \frac{1}{(2\pi)^3} \int \mathbf{G}_b(\mathbf{k}) e^{i\mathbf{k} \cdot (\mathbf{r} - \mathbf{r}')} d\mathbf{k}. \quad (\text{A1})$$

The Green tensor in Fourier space is given by

$$\begin{aligned} \mathbf{G}_b(\mathbf{k}) &= [k_b^2 \mathbf{1} - \mathbf{k} \otimes \mathbf{k} - k_b^2 \mathbf{1}]^{-1} \quad (\text{A2}) \\ &= \left[-k_b^2 \frac{\mathbf{k} \otimes \mathbf{k}}{k^2} + (k^2 - k_b^2) \left(\mathbf{1} - \frac{\mathbf{k} \otimes \mathbf{k}}{k^2} \right) \right]^{-1} \quad (\text{A3}) \\ &= \frac{1}{k_b^2} \left[-\frac{\mathbf{k} \otimes \mathbf{k}}{k^2} + \frac{k_b^2}{k^2 - (k_b + i0)^2} \left(\mathbf{1} - \frac{\mathbf{k} \otimes \mathbf{k}}{k^2} \right) \right]. \quad (\text{A4}) \end{aligned}$$

The small imaginary part $i0$ introduced here is relevant in integrals involving $\mathbf{G}_b(\mathbf{k})$. Using Eq. (31), the Green tensor can finally be rewritten as

$$\begin{aligned} \mathbf{G}_b(\mathbf{k}) &= \frac{1}{k_b^2} \left[-\frac{\mathbf{k} \otimes \mathbf{k}}{k^2} + \text{PV} \left\{ \frac{k_b^2}{k^2 - k_b^2} \right\} \left(\mathbf{1} - \frac{\mathbf{k} \otimes \mathbf{k}}{k^2} \right) \right] \\ &\quad + i\pi \delta(k^2 - k_b^2) \left(\mathbf{1} - \frac{\mathbf{k} \otimes \mathbf{k}}{k^2} \right). \quad (\text{A5}) \end{aligned}$$

2. Dressed Green tensor

Following Eq. (55), the Green tensor can be decomposed into local and non-local terms, the latter being also known as the Lorentz propagator. In Fourier space, we thus have

$$\mathbf{g}_b(\mathbf{k}) = -\frac{1}{3k_b^2} + \int_{r < a} \mathbf{G}_b(\mathbf{r}) e^{-i\mathbf{k} \cdot \mathbf{r}} d\mathbf{r}, \quad (\text{A6})$$

$$\tilde{\mathbf{G}}_b(\mathbf{k}) \equiv \mathbf{G}_b(\mathbf{k}) - \mathbf{g}_b(\mathbf{k}). \quad (\text{A7})$$

Specific expressions for arbitrary values of the radius a are provided by Bedeaux and Mazur (1973). For $k_b a \ll 1$, we have

$$\mathbf{g}_b(\mathbf{r}) = -\frac{1}{3k_b^2} \delta(\mathbf{r} - \mathbf{r}') \mathbf{1}, \quad (\text{A8})$$

which simply leads to

$$\tilde{\mathbf{G}}_b(\mathbf{k}) \equiv \mathbf{G}_b(\mathbf{k}) + \frac{1}{3k_b^2}. \quad (\text{A9})$$

Let us now consider a medium composed of small volume elements within the Maxwell-Garnett approximation. Setting the auxiliary permittivity to that of the host medium, $\epsilon_b = \epsilon_h$, the average transition operator describing scattering by a single volume element is then given by

$$\langle \tilde{\mathbf{T}}(\mathbf{k}) \rangle = k_h^2 \rho \alpha_0 \mathbf{1}, \quad (\text{A10})$$

with α_0 the polarizability. The Fourier transform of the

propagator $\hat{\mathbf{G}}_b$ defined in Eq. (67) then reads

$$\hat{\mathbf{G}}_h(\mathbf{k}) = \left[\mathbf{1} - k_h^2 \rho \alpha_0 \tilde{\mathbf{G}}_h(\mathbf{k}) \right]^{-1} \tilde{\mathbf{G}}_h(\mathbf{k}) \quad (\text{A11})$$

$$= \left[\mathbf{1} - \frac{\rho \alpha_0}{3} \mathbf{1} - \rho \alpha_0 k_h^2 \mathbf{G}_h(\mathbf{k}) \right]^{-1} \left(\mathbf{G}_h(\mathbf{k}) + \frac{\mathbf{1}}{3k_h^2} \right). \quad (\text{A12})$$

Taking into account the definition of the Maxwell-Garnett permittivity ϵ_{MG} in Eq. (75), the dressed propagator can eventually be written as

$$\hat{\mathbf{G}}_h(\mathbf{k}) = \left(\frac{\epsilon_{\text{MG}} + 2\epsilon_h}{3\epsilon_h} \right)^2 \left(\mathbf{G}_{\text{MG}}(\mathbf{k}) + \frac{\epsilon_{\text{MG}}}{\epsilon_{\text{MG}} + 2\epsilon_h} \frac{\mathbf{1}}{k_{\text{MG}}^2} \right), \quad (\text{A13})$$

where $\mathbf{G}_{\text{MG}}(\mathbf{k})$ is the Green tensor with k_h replaced by the Maxwell-Garnett wave number $k_{\text{MG}} = k_0 \sqrt{\epsilon_{\text{MG}}}$.

In absence of absorption, the imaginary part of $\hat{\mathbf{G}}_h$ is given by

$$\text{Im} \hat{\mathbf{G}}_h(\mathbf{k}) = \pi \left(\frac{\epsilon_{\text{MG}} + 2\epsilon_h}{3\epsilon_h} \right)^2 \delta(k^2 - k_{\text{MG}}^2) \left(\mathbf{1} - \frac{\mathbf{k} \otimes \mathbf{k}}{k^2} \right), \quad (\text{A14})$$

leading to Eq. (76).

Appendix B: Derivation of Eq. (26)

In the Fourier domain and by making use of the average Green function

$$\langle \mathbf{G}(\mathbf{k}, \omega) \rangle = \left[k^2 \mathbf{P}(\hat{\mathbf{k}}) - k_b^2 \mathbf{1} - \Sigma(\mathbf{k}) \right]^{-1}, \quad (\text{B1})$$

we obtain

$$\begin{aligned} & \left\{ \mathbf{1} \otimes \left[k'^2 \mathbf{P}(\hat{\mathbf{k}}') - \Sigma^*(\mathbf{k}') \right] - \left[k^2 \mathbf{P}(\hat{\mathbf{k}}) - \Sigma(\mathbf{k}) \right] \otimes \mathbf{1} \right\} \\ & \cdot \mathbf{C}(\mathbf{k}, \mathbf{k}') = \left[\langle \mathbf{G}(\mathbf{k}) \rangle \otimes \mathbf{1} - \mathbf{1} \otimes \langle \mathbf{G}^*(\mathbf{k}') \rangle \right] \\ & \cdot \int \Gamma(\mathbf{k}, \boldsymbol{\kappa}, \mathbf{k}', \boldsymbol{\kappa}') \cdot \mathbf{C}(\boldsymbol{\kappa}, \boldsymbol{\kappa}') \frac{d\boldsymbol{\kappa}}{8\pi^3} \frac{d\boldsymbol{\kappa}'}{8\pi^3} \quad (\text{B2}) \end{aligned}$$

where we have neglected the source term $\langle \mathbf{E} \rangle \otimes \langle \mathbf{E}^* \rangle$ and used the tensorial relation

$$(\mathbf{1} \otimes \mathbf{B} - \mathbf{A} \otimes \mathbf{1})^{-1} \cdot (\mathbf{A}^{-1} \otimes \mathbf{1} - \mathbf{1} \otimes \mathbf{B}^{-1}) = \mathbf{A}^{-1} \otimes \mathbf{B}^{-1}. \quad (\text{B3})$$

$\mathbf{1}$ is the identity tensor. Since we are dealing with dilute media and since the longitudinal part of the Green tensor is irrelevant regarding light transport, we now consider the transverse approximation which consists in taking the transverse part of all operators involved in Eq. (B2) (Barabanenkov *et al.*, 1995; Cherroret *et al.*,

2016). Using the definitions

$$\begin{aligned} \Gamma_{\perp}(\mathbf{k}, \boldsymbol{\kappa}, \mathbf{k}', \boldsymbol{\kappa}') &= \mathbf{P}(\mathbf{u}) \otimes \mathbf{P}(\mathbf{u}') \cdot \Gamma(\mathbf{k}, \boldsymbol{\kappa}, \mathbf{k}', \boldsymbol{\kappa}'), \\ \mathbf{C}_{\perp}(\mathbf{k}, \mathbf{k}') &= \mathbf{P}(\mathbf{u}) \otimes \mathbf{P}(\mathbf{u}') \cdot \mathbf{C}(\mathbf{k}, \mathbf{k}'), \end{aligned}$$

we obtain

$$\begin{aligned} & [k'^2 - k^2 - \Sigma_{\perp}^*(\mathbf{k}') + \Sigma_{\perp}(\mathbf{k})] \mathbf{C}_{\perp}(\mathbf{k}, \mathbf{k}') \\ &= [\langle G_{\perp}(\mathbf{k}) \rangle - \langle G_{\perp}^*(\mathbf{k}') \rangle] \\ & \times \int \Gamma_{\perp}(\mathbf{k}, \boldsymbol{\kappa}, \mathbf{k}', \boldsymbol{\kappa}') \cdot \mathbf{C}_{\perp}(\boldsymbol{\kappa}, \boldsymbol{\kappa}') \frac{d\boldsymbol{\kappa}}{8\pi^3} \frac{d\boldsymbol{\kappa}'}{8\pi^3}. \quad (\text{B4}) \end{aligned}$$

Still considering that we have statistical homogeneity for the disordered medium, we have $\Gamma(\mathbf{r}', \mathbf{r}'', \boldsymbol{\rho}', \boldsymbol{\rho}'') = \Gamma(\mathbf{r}' + \Delta\mathbf{r}, \mathbf{r}'' + \Delta\mathbf{r}, \boldsymbol{\rho}' + \Delta\mathbf{r}, \boldsymbol{\rho}'' + \Delta\mathbf{r})$ which leads to

$$\begin{aligned} \Gamma_{\perp}(\mathbf{k}, \boldsymbol{\kappa}, \mathbf{k}', \boldsymbol{\kappa}') &= 8\pi^3 \delta(\mathbf{k} - \mathbf{k}' - \boldsymbol{\kappa} + \boldsymbol{\kappa}') \\ & \times \bar{\Gamma}_{\perp}(\mathbf{k}, \boldsymbol{\kappa}, \mathbf{k}', \boldsymbol{\kappa}') \quad (\text{B5}) \end{aligned}$$

in the Fourier space. By a change of variable, we also now define the correlation

$$\mathbf{L}_{\perp}(\mathbf{q}, \mathbf{k}) \equiv \mathbf{C}_{\perp} \left(\mathbf{k} + \frac{\mathbf{q}}{2}, \mathbf{k} - \frac{\mathbf{q}}{2} \right) \quad (\text{B6})$$

which leads to this new form of the Bethe-Salpeter equation in the Fourier domain

$$\begin{aligned} & \left[\left(\mathbf{k} - \frac{\mathbf{q}}{2} \right)^2 - \left(\mathbf{k} + \frac{\mathbf{q}}{2} \right)^2 - \Sigma_{\perp}^* \left(\mathbf{k} - \frac{\mathbf{q}}{2} \right) + \Sigma_{\perp} \left(\mathbf{k} + \frac{\mathbf{q}}{2} \right) \right] \\ & \times \mathbf{L}_{\perp}(\mathbf{q}, \mathbf{k}) = \left[\langle G_{\perp} \left(\mathbf{k} + \frac{\mathbf{q}}{2} \right) \rangle - \langle G_{\perp}^* \left(\mathbf{k} - \frac{\mathbf{q}}{2} \right) \rangle \right] \\ & \times \int \bar{\Gamma}_{\perp} \left(\mathbf{k} + \frac{\mathbf{q}}{2}, \mathbf{k}' + \frac{\mathbf{q}}{2}, \mathbf{k} - \frac{\mathbf{q}}{2}, \mathbf{k}' - \frac{\mathbf{q}}{2} \right) \cdot \mathbf{L}_{\perp}(\mathbf{k}', \mathbf{q}) \frac{d\mathbf{k}'}{(2\pi)^3} \quad (\text{B7}) \end{aligned}$$

which is Eq. (26).

Appendix C: Configurational average for statistically homogeneous systems

1. Particle correlation functions

We consider a random ensemble of N particles circumscribed in a volume V and centered at positions $\mathbf{R} = [\mathbf{R}_1, \mathbf{R}_2, \dots, \mathbf{R}_N]$. A specific configuration is described by a normalized probability distribution $P^{(N)}$ such that

$$P^{(N)}(\mathbf{R}_1, \dots, \mathbf{R}_N) d\mathbf{R}_1 \dots d\mathbf{R}_N \quad (\text{C1})$$

is the probability of finding a configuration in which particle j is centered between \mathbf{R}_j and $\mathbf{R}_j + d\mathbf{R}_j$.

Assuming that the particles are spherically symmetric (otherwise, the distribution would also include orientational variables, Ω_j) and identical, the distribution is symmetric in the labels $1, \dots, N$ and we can define the

M -particle density $\rho^{(M)}(\mathbf{R}_1, \dots, \mathbf{R}_M)$ as the probability of finding a configuration of M particles whatever the configuration of the remaining $N - M$ particles

$$\rho^{(M)}(\mathbf{R}_1, \dots, \mathbf{R}_M) = \frac{N!}{(N - M)!} \times \int P^{(N)}(\mathbf{R}_1, \dots, \mathbf{R}_N) d\mathbf{R}_{M+1} \dots d\mathbf{R}_N \quad (\text{C2})$$

The instantaneous particle number density $\rho(\mathbf{r})$ for a given configuration of particles, $\mathbf{R} = [\mathbf{R}_1, \dots, \mathbf{R}_N]$, is defined as

$$\rho(\mathbf{r}) \equiv \sum_{j=1}^N \delta(\mathbf{r} - \mathbf{R}_j), \quad (\text{C3})$$

and its configurational average $\langle \rho(\mathbf{r}) \rangle$ is given by

$$\begin{aligned} \langle \rho(\mathbf{r}) \rangle &= \left\langle \sum_j \delta(\mathbf{r} - \mathbf{R}_j) \right\rangle \\ &= N \int \dots \int P^{(N)}(\mathbf{r}, \mathbf{R}_2, \dots, \mathbf{R}_N) d\mathbf{R}_2 \dots d\mathbf{R}_N. \end{aligned} \quad (\text{C4})$$

$$(\text{C5})$$

In the limit of infinite system size and assuming a statistically homogeneous and isotropic medium (i.e. all properties are statistically invariant by translation and rotation), both the number of particles and the volume of the material tend to infinity (i.e. $\{N, V\} \rightarrow \infty$), and one can define an average particle number density, $\rho \equiv \langle \rho(\mathbf{r}) \rangle = N/V$, that is constant.

One can then define the n -particle probably density functions $\rho_n(\mathbf{r}_1, \mathbf{r}_2, \dots, \mathbf{r}_n)$ as

$$\rho_n(\mathbf{r}_1, \dots, \mathbf{r}_n) \equiv \left\langle \sum_{\substack{j_1, \dots, j_n=1 \\ j_1 \neq j_2 \neq \dots \neq j_n}}^N \delta(\mathbf{r}_1 - \mathbf{R}_{j_1}) \dots \delta(\mathbf{r}_n - \mathbf{R}_{j_n}) \right\rangle, \quad (\text{C6})$$

as well as the n -particle correlation function

$$g_n(\mathbf{r}_1, \mathbf{r}_2, \dots, \mathbf{r}_n) \equiv \frac{\rho_n(\mathbf{r}_1, \mathbf{r}_2, \dots, \mathbf{r}_n)}{\rho^n}. \quad (\text{C7})$$

The important quantity in most systems is the pair correlation function $g_2(\mathbf{r}_1, \mathbf{r}_2)$, that describes the conditional probability of finding a particle at \mathbf{r}_2 given at particle fixed at \mathbf{r}_1 . For isotropic media, g_2 only depends on the radial distance $r_{12} = |\mathbf{r}_1 - \mathbf{r}_2|$. The total correlation function $h_2(\mathbf{r})$ defined as

$$h_2(\mathbf{r}) \equiv g_2(\mathbf{r}) - 1, \quad (\text{C8})$$

has the benefit of converging to zero at separation distances larger than a correlation length ℓ_c .

2. Fluctuations of the number of particles in a volume

The fluctuations of the number of particles N in a given volume v can be defined as

$$\delta_N \equiv \frac{1}{\rho v} \left(\langle N^2 \rangle - \langle N \rangle^2 \right) = \frac{1}{v} \int_v \frac{\langle \Delta \rho(\mathbf{r}) \Delta \rho(\mathbf{r}') \rangle}{\rho} d\mathbf{r} d\mathbf{r}'$$

with

$$\begin{aligned} \frac{\langle \Delta \rho(\mathbf{r}_1) \Delta \rho(\mathbf{r}_2) \rangle}{\rho} &= \frac{\langle \rho(\mathbf{r}_1) \rho(\mathbf{r}_2) \rangle - \rho^2}{\rho} \\ &= \frac{1}{\rho} \left[\left\langle \sum_{a=1}^N \delta(\mathbf{r}_1 - \mathbf{R}_a) \delta(\mathbf{r}_2 - \mathbf{R}_a) \right\rangle \right. \\ &\quad \left. + \left\langle \sum_a \sum_{b \neq a} \delta(\mathbf{r}_1 - \mathbf{R}_a) \delta(\mathbf{r}_2 - \mathbf{R}_b) \right\rangle - \rho^2 \right] \\ &= \delta(\mathbf{r}_1 - \mathbf{r}_2) + \rho \left(\frac{\rho_2(\mathbf{r}_1 - \mathbf{r}_2)}{\rho^2} - 1 \right) \\ &\equiv \delta(\mathbf{r}_1 - \mathbf{r}_2) + \rho h_2(\mathbf{r}_1 - \mathbf{r}_2). \end{aligned} \quad (\text{C10})$$

If v is a sphere of radius R_s , one gets (Torquato and Stillinger, 2003; Van Kranendonk and Sipe, 1977)

$$\begin{aligned} \delta_N &= 1 \\ &+ \rho \int h_2(r_{12}) \left[1 - \frac{3}{4} \frac{r}{R_s} + \frac{1}{16} \left(\frac{r}{R_s} \right)^3 \right] 4\pi r^2 dr_{12} \\ &\sim 1 + \rho \int h_2(r_{12}) 4\pi r^2 dr_{12}, \end{aligned} \quad (\text{C11})$$

where, in the last step, we assumed that R_s is larger than the correlation length ℓ_c of $h_2(r)$. Expressions exist also for two-dimensional systems and non-spherical excluded volumes (Torquato and Stillinger, 2003).

The static structure factor $S(\mathbf{k})$ is related to the Fourier transform of $h_2(\mathbf{r})$ via the expression

$$S(\mathbf{k}) \equiv 1 + \rho h_2(\mathbf{k}), \quad (\text{C12})$$

with $h_2(\mathbf{k}) = \int h_2(\mathbf{r}) e^{-i\mathbf{k} \cdot \mathbf{r}} d\mathbf{r}$.

Appendix D: Local density of states and quasinormal modes

The local density of states (LDOS) is defined from the projected LDOS, Eq. (126), as

$$\rho_e(\mathbf{r}, \omega) = \frac{2\omega}{\pi c^2} \text{Im} [\text{Tr} \mathbf{G}(\mathbf{r}, \mathbf{r}, \omega)]. \quad (\text{D1})$$

We will now express this quantity in terms of the eigenmodes of the system.

The eigenmodes of non-conservative (non-Hermitian) systems, also known as quasinormal modes (QNMs), are described by complex frequencies $\tilde{\omega}_m = \omega_m - i\gamma_m/2$ and normalized fields $\tilde{\mathbf{E}}_m(\mathbf{r})$, the non-zero imaginary part stemming from leakage. QNMs have a long history (Baum,

1976; Ching *et al.*, 1998) and are receiving considerable attention from the photonics community since a few years (Lalanne *et al.*, 2018). Following a recent QNM formalism (Sauvan *et al.*, 2014, 2013; Yan *et al.*, 2018), we can write the field \mathbf{E} generated by a dipole emitter in terms of QNMs as

$$\mathbf{E}(\mathbf{r}, \omega) = \sum_m \alpha_m(\omega) \tilde{\mathbf{E}}_m(\mathbf{r}), \quad (\text{D2})$$

with α_m the excitation coefficients, defined as

$$\alpha_m(\omega) = -\frac{\omega}{2\epsilon_0(\omega - \tilde{\omega}_m)} \mathbf{p} \cdot \tilde{\mathbf{E}}_m(\mathbf{r}). \quad (\text{D3})$$

Quite expectedly, the efficiency of excitation of a mode depends on the amplitude of the QNM field at the dipole position and the spectral distance with the resonance frequency. Having further that $\mathbf{E}(\mathbf{r}, \omega) = \mu_0 \omega^2 \mathbf{G}(\mathbf{r}, \mathbf{r}', \omega) \mathbf{p}$, one arrives to a modal decomposition of the dyadic Green function

$$\mathbf{G}(\mathbf{r}, \mathbf{r}', \omega) = -\frac{c^2}{2\omega} \sum_m \frac{\tilde{\mathbf{E}}_m(\mathbf{r}) \otimes \tilde{\mathbf{E}}_m(\mathbf{r}')}{\omega - \tilde{\omega}_m}. \quad (\text{D4})$$

Note that Eq. (D4) can also be obtained from the Mittag-Leffler theorem which introduces the residues of the Green tensor at the QNM complex frequencies (Muljarov and Langbein, 2016). Inserting Eq. (D4) in Eq. (D1) finally leads to

$$\rho_e(\mathbf{r}, \omega) = -\frac{1}{\pi} \text{Im} \left[\sum_m \frac{\text{Tr} [\tilde{\mathbf{E}}_m(\mathbf{r}) \otimes \tilde{\mathbf{E}}_m(\mathbf{r})]}{\omega - \tilde{\omega}_m} \right]. \quad (\text{D5})$$

The LDOS is now explicitly expressed as a sum over resonant modes. To further convince ourselves, we can take the limit of vanishing leakage, in which case both \mathbf{E}_m and $\tilde{\omega}_m$ tend to become real. Using $\lim_{\eta \rightarrow 0^+} \frac{1}{x + i\eta} = \text{PV} \left[\frac{1}{x} \right] - i\pi \delta(x)$, we arrive to the well-known expression of the LDOS for conservative systems (Carminati *et al.*, 2015; Novotny and Hecht, 2012)

$$\rho_e(\mathbf{r}, \omega) = \sum_m |\tilde{\mathbf{E}}_m(\mathbf{r})|^2 \delta(\omega - \omega_m). \quad (\text{D6})$$

REFERENCES

- Abrahams, Elihu (2010), *50 years of Anderson Localization*, Vol. 24 (world scientific).
- Abrahams, Elihu, PW Anderson, DC Licciardello, and TV Ramakrishnan (1979), “Scaling theory of localization: Absence of quantum diffusion in two dimensions,” *Physical Review Letters* **42** (10), 673.
- Acquista, Charles (1976), “Light scattering by tenuous particles: a generalization of the rayleigh-gans-rocand approach,” *Applied Optics* **15** (11), 2932–2936.
- Aeby, Stefan, Geoffroy J Aubry, Nicolas Muller, and Frank Scheffold (2020), “Scattering from controlled defects in woodpile photonic crystals,” *Advanced Optical Materials*, 2001699.
- Akkermans, E, PE Wolf, R Maynard, and G Maret (1988), “Theoretical study of the coherent backscattering of light by disordered media,” *Journal de Physique* **49** (1), 77–98.
- Akkermans, Eric, and Gilles Montambaux (2007), *Mesoscopic physics of electrons and photons* (Cambridge university press).
- Akkermans, Eric, PE Wolf, and R Maynard (1986), “Coherent backscattering of light by disordered media: Analysis of the peak line shape,” *Physical Review Letters* **56** (14), 1471.
- van Albada, Meint P, Bart A van Tiggelen, Ad Lagendijk, and Adriaan Tip (1991), “Speed of propagation of classical waves in strongly scattering media,” *Physical Review Letters* **66** (24), 3132.
- Alerstam, Erik, Tomas Svensson, and Stefan Andersson-Engels (2008), “Parallel computing with graphics processing units for high-speed monte carlo simulation of photon migration,” *Journal of Biomedical Optics* **13** (6), 060504.
- Allain, Cloitre, and M Cloitre (1991), “Characterizing the lacunarity of random and deterministic fractal sets,” *Physical Review A* **44** (6), 3552.
- Altissimo, Matteo (2010), “E-beam lithography for micro-/nanofabrication,” *Biomicrofluidics* **4** (2), 026503.
- Altshuler, Boris L’vovich, Patrick A Lee, and W Richard Webb (2012), *Mesoscopic phenomena in solids* (Elsevier).
- Anderson, Joshua A, Chris D. Lorenz, and A. Travesset (2008), “General purpose molecular dynamics simulations fully implemented on graphics processing units,” *Journal of Computational Physics* **227** (10), 5342 – 5359.
- Anderson, Philip W (1958), “Absence of diffusion in certain random lattices,” *Physical Review* **109** (5), 1492.
- Anderson, Philip W (1985), “The question of classical localization a theory of white paint?” *Philosophical Magazine B* **52** (3), 505–509.
- Andkjær, Jacob, Villads Egede Johansen, Kasper Storgaard Friis, and Ole Sigmund (2014), “Inverse design of nanostructured surfaces for color effects,” *JOSA B* **31** (1), 164–174.
- Apostol, A, and A Dogariu (2003), “Spatial correlations in the near field of random media,” *Physical Review Letters* **91** (9), 093901.
- Apostol, Adela, and Aristide Dogariu (2004), “First-and second-order statistics of optical near fields,” *Optics Letters* **29** (3), 235–237.
- Apresyan, L A, and Y. A. Kravtsov (1996), *Radiation Transfer: Statistical and Wave Aspects* (Gordon and Breach Publishers, Amsterdam).
- Araújo, Michelle O, Thierry Passerat de Silans, and Robin Kaiser (2021), “Lévy flights of photons with infinite mean free path,” *Physical Review E* **103** (1), L010101.
- Ardakani, Abbas Ghasempour, and Mohsen Ghasemi Nezhadhighi (2015), “Controlling anderson localization in disordered heterostructures with Lévy-type distribution,” *Journal of Optics* **17** (10), 105601.
- Asatryan, AA, PA Robinson, LC Botten, RC McPhedran, NA Nicorovici, and C Martijn de Sterke (1999), “Effects of disorder on wave propagation in two-dimensional photonic crystals,” *Physical Review E* **60** (5), 6118.
- Astratov, VN, AM Adawi, S Fricker, MS Skolnick, DM Whitaker, and PN Pusey (2002), “Interplay of order and disorder in the optical properties of opal photonic crystals,”

- Physical Review B **66** (16), 165215.
- Astratov, VN, VN Bogomolov, AA Kaplyanskii, AV Prokofiev, LA Samoilovich, SM Samoilovich, and Yu A Vlasov (1995), “Optical spectroscopy of opal matrices with cds embedded in its pores: Quantum confinement and photonic band gap effects,” *Il Nuovo Cimento D* **17** (11-12), 1349–1354.
- Aubry, Geoffroy J, Luis S Froufe-Pérez, Ulrich Kuhl, Olivier Legrand, Frank Scheffold, and Fabrice Mortessagne (2020), “Experimental tuning of transport regimes in hyperuniform disordered photonic materials,” *Physical Review Letters* **125** (12), 127402.
- Aubry, Geoffroy J, Lukas Schertel, Mengdi Chen, Henrik Weyer, Christof M Aegerter, Sebastian Polarz, Helmut Cölfen, and Georg Maret (2017), “Resonant transport and near-field effects in photonic glasses,” *Physical Review A* **96** (4), 043871.
- Auzinger, Thomas, Wolfgang Heidrich, and Bernd Bickel (2018), “Computational design of nanostructural color for additive manufacturing,” *ACM Transactions on Graphics (TOG)* **37** (4), 1–16.
- Bahadur, Jitendra, Andrzej P Radlinski, Yuri B Melnichenko, Maria Mastalerz, and Arndt Schimmelmann (2015), “Small-angle and ultras-small-angle neutron scattering (sans/usans) study of new albany shale: a treatise on microporosity,” *Energy & Fuels* **29** (2), 567–576.
- Barabanenkov, Y N, and V. M. Finkel’berg (1968), “Radiation transport equation for correlated scatterers,” *Sov. Phys. JETP* **26**, 587–591.
- Barabanenkov, Y N, L. Zurk, and M. Y. Barabanenkov (1995), “Poynting’s theorem and electromagnetic wave multiple scattering in dense media near resonance: modified radiative transfer equation,” *Journal of Electromagnetic Waves and Applications* **9** (11-12), 1393–1420.
- Barkema, Gerard T, and Normand Mousseau (2000), “High-quality continuous random networks,” *Physical Review B* **62** (8), 4985.
- Barthelemy, Pierre, Jacopo Bertolotti, Kevin Vynck, Stefano Lepri, and Diederik S Wiersma (2010), “Role of quenching on superdiffusive transport in two-dimensional random media,” *Physical Review E* **82** (1), 011101.
- Barthelemy, Pierre, Jacopo Bertolotti, and Diederik S Wiersma (2008), “A lévy flight for light,” *Nature* **453** (7194), 495.
- Bartumeus, Frederic, M G E da Luz, Gandhimohan M Viswanathan, and Jordi Catalan (2005), “Animal search strategies: a quantitative random-walk analysis,” *Ecology* **86** (11), 3078–3087.
- Batten, Robert D, Frank H Stillinger, and Salvatore Torquato (2008), “Classical disordered ground states: Super-ideal gases and stealth and equi-luminous materials,” *Journal of Applied Physics* **104** (3), 033504.
- Baudouin, Q, R Pierrat, A Eloy, EJ Nunes-Pereira, P-A Cuniasse, N Mercadier, and R Kaiser (2014), “Signatures of lévy flights with annealed disorder,” *Physical Review E* **90** (5), 052114.
- Baum, Carl E (1976), “The singularity expansion method,” in *Transient electromagnetic fields* (Springer) pp. 129–179.
- Baus, Marc, and Jean-Louis Colot (1987), “Thermodynamics and structure of a fluid of hard rods, disks, spheres, or hyperspheres from rescaled virial expansions,” *Physical Review A* **36** (8), 3912.
- Bedeaux, D, and P Mazur (1973), “On the critical behaviour of the dielectric constant for a nonpolar fluid,” *Physica* **67** (1), 23–54.
- Bedeaux, D, MM Wind, and MA van Dijk (1987), “The effective dielectric constant of a dispersion of clustering spheres,” *Zeitschrift für Physik B Condensed Matter* **68** (2-3), 343–354.
- Beenakker, CWJ, CW Groth, and AR Akhmerov (2009), “Nonalgebraic length dependence of transmission through a chain of barriers with a Lévy spacing distribution,” *Physical Review B* **79** (2), 024204.
- Behrens, DJ (1949), “The effect of holes in a reacting material on the passage of neutrons,” *Proceedings of the Physical Society. Section A* **62** (10), 607.
- Bell, George RR, Lydia M Mähgler, Meng Gao, Stephen L Senft, Alan M Kuzirian, George W Kattawar, and Roger T Hanlon (2014), “Diffuse white structural coloration from multilayer reflectors in a squid,” *Advanced Materials* **26** (25), 4352–4356.
- Bellando, L, A Gero, E Akkermans, and R Kaiser (2014), “Cooperative effects and disorder: A scaling analysis of the spectrum of the effective atomic hamiltonian,” *Physical Review A* **90** (6), 063822.
- Ben-Avraham, Daniel, and Shlomo Havlin (2000), *Diffusion and reactions in fractals and disordered systems* (Cambridge university press).
- Benedek, GB (1971), “Theory of transparency of the eye,” *Applied Optics* **10** (3), 459–473.
- Benzaouia, Mohammed, Grgur Tokić, Owen D Miller, Dick KP Yue, and Steven G Johnson (2019), “From solar cells to ocean buoys: Wide-bandwidth limits to absorption by metaparticle arrays,” *Physical Review Applied* **11** (3), 034033.
- Berry, R Stephen, Julius Jellinek, and Grigory Natanson (1984), “Melting of clusters and melting,” *Physical Review A* **30** (2), 919.
- Bertolotti, Jacopo, Kevin Vynck, Lorenzo Pattelli, Pierre Barthelemy, Stefano Lepri, and Diederik S Wiersma (2010a), “Engineering disorder in superdiffusive levý glasses,” *Advanced Functional Materials* **20** (6), 965–968.
- Bertolotti, Jacopo, Kevin Vynck, and Diederik S Wiersma (2010b), “Multiple scattering of light in superdiffusive media,” *Physical Review Letters* **105** (16), 163902.
- Bertrand, Maxime, Alexis Devilez, Jean-Paul Hugonin, Philippe Lalanne, and Kevin Vynck (2020), “Global polarizability matrix method for efficient modeling of light scattering by dense ensembles of non-spherical particles in stratified media,” *JOSA A* **37** (1), 70–83.
- Bibette, J, TG Mason, Hu Gang, DA Weitz, and P Poulin (1993), “Structure of adhesive emulsions,” *Langmuir* **9** (12), 3352–3356.
- Bicout, Dominique, and Christian Brosseau (1992), “Multiply scattered waves through a spatially random medium: entropy production and depolarization,” *Journal de Physique I* **2** (11), 2047–2063.
- Bigourdan, Florian, Romain Pierrat, and Rémi Carminati (2019), “Enhanced absorption of waves in stealth hyperuniform disordered media,” *Optics Express* **27** (6), 8666–8682.
- Birowosuto, MD, SE Skipetrov, Willem L Vos, and AP Mosk (2010), “Observation of spatial fluctuations of the local density of states in random photonic media,” *Physical Review Letters* **105** (1), 013904.
- de Boer, Jan (1949), “Molecular distribution and equation of state of gases,” *Reports on Progress in Physics* **12** (1), 305.
- Bohren, Craig F, and Donald R Huffman (2008), *Absorption and scattering of light by small particles* (John Wiley &

- Sons).
- Borovoi, Anatoli (2002), “On the extinction of radiation by a homogeneous but spatially correlated random medium: comment,” *JOSA A* **19** (12), 2517–2520.
- Bossard, Jeremy A, Lan Lin, and Douglas H Werner (2016), “Evolving random fractal cantor superlattices for the infrared using a genetic algorithm,” *Journal of the Royal Society Interface* **13** (114), 20150975.
- Böttcher, Carl Johan Friedrich, Oenes Christoffel van Belle, Paul Bordewijk, and Arie Rip (1978), *Theory of electric polarization*, Vol. 2 (Elsevier Science Ltd).
- Bozzola, Angelo, Marco Liscidini, and Lucio Claudio Andreani (2014), “Broadband light trapping with disordered photonic structures in thin-film silicon solar cells,” *Prog. Photovoltaics Res. Appl.* **22** (12), 1237–1245.
- Briant, CL, and JJ Burton (1975), “Molecular dynamics study of the structure and thermodynamic properties of argon microclusters,” *The Journal of Chemical Physics* **63** (5), 2045–2058.
- Brooks, Bernard R, Charles L Brooks III, Alexander D Mackerell Jr, Lennart Nilsson, Robert J Petrella, Benoît Roux, Youngdo Won, Georgios Archontis, Christian Bartels, Stefan Boresch, *et al.* (2009), “CHARMM: the biomolecular simulation program,” *Journal of Computational Chemistry* **30** (10), 1545–1614.
- Brown, Judith C, PN Pusey, JW Goodwin, and RH Ottewill (1975), “Light scattering study of dynamic and time-averaged correlations in dispersions of charged particles,” *Journal of Physics A: Mathematical and General* **8** (5), 664.
- Bruggeman, Von DAG (1935), “Berechnung verschiedener physikalischer konstanten von heterogenen substanzen. i. dielektrizitätskonstanten und leitfähigkeiten der mischkörper aus isotropen substanzen,” *Annalen der Physik* **416** (7), 636–664.
- Buonsante, P, R Burioni, and A Vezzani (2011), “Transport and scaling in quenched two-and three-dimensional lévy quasicrystals,” *Physical Review E* **84** (2), 021105.
- Burg, S L, A. Washington, D. M. Coles, A. Bianco, D. McLoughlin, O. O. Mykhaylyk, J. Villanova, A. J. C. Dennison, C. J. Hill, P. Vukusic, S. Doak, S. J. Martin, M. Hutchings, S. R. Parnell, C. Vasilev, N. Clarke, A. J. Ryan, W. Furnass, M. Croucher, R. M. Dalgliesh, S. Prevost, R. Dattani, A. Parker, R. A. L. Jones, J. P. A. Fairclough, and A. J. Parnell (2019), “Liquid–liquid phase separation morphologies in ultra-white beetle scales and a synthetic equivalent,” *Commun Chem* **2**, 100.
- Burioni, Raffaella, Luca Caniparoli, and Alessandro Vezzani (2010), “Lévy walks and scaling in quenched disordered media,” *Physical Review E* **81** (6), 060101.
- Burioni, Raffaella, Serena di Santo, Stefano Lepri, and Alessandro Vezzani (2012), “Scattering lengths and universality in superdiffusive Lévy materials,” *Physical Review E* **86** (3), 031125.
- Burioni, Raffaella, Enrico Ubaldi, and Alessandro Vezzani (2014), “Superdiffusion and transport in two-dimensional systems with lévy-like quenched disorder,” *Physical Review E* **89** (2), 022135.
- Burresi, Matteo, Lorenzo Cortese, Lorenzo Pattelli, Mathias Kolle, Peter Vukusic, Diederik S Wiersma, Ullrich Steiner, and Silvia Vignolini (2014), “Bright-white beetle scales optimise multiple scattering of light,” *Scientific Reports* **4**, 6075.
- Burresi, Matteo, Vivekananthan Radhalakshmi, Romolo Savo, Jacopo Bertolotti, Kevin Vynck, and Diederik S Wiersma (2012), “Weak localization of light in superdiffusive random systems,” *Physical Review Letters* **108** (11), 110604.
- Busch, K, and CM Soukoulis (1995), “Transport properties of random media: A new effective medium theory,” *Physical Review Letters* **75** (19), 3442.
- Caixeiro, Soraya, Michele Gaio, Benedetto Marelli, Fiorenzo G. Omenetto, and Riccardo Sapienza (2016), “Silk-Based Biocompatible Random Lasing,” *Advanced Optical Materials* **4** (7), 998–1003.
- Canaguier-Durand, Antoine, Romain Pierrat, and Rémi Carminati (2019), “Cross density of states and mode connectivity: Probing wave localization in complex media,” *Physical Review A* **99** (1), 013835.
- Cao, Hui (2005), “Review on latest developments in random lasers with coherent feedback,” *Journal of Physics A: Mathematical and General* **38** (49), 10497.
- Carminati, R (2010), “Subwavelength spatial correlations in near-field speckle patterns,” *Physical Review A* **81** (5), 053804.
- Carminati, Rémi, Alexandre Cazé, Da Cao, F Peragut, V Krachmalnicoff, Romain Pierrat, and Yannick De Wilde (2015), “Electromagnetic density of states in complex plasmonic systems,” *Surface Science Reports* **70** (1), 1–41.
- Carminati, Rémi, and John C. Schotland (2021), *Principles of Scattering and Transport of Light* (Cambridge University Press).
- Casasanta, Giampietro, and Roberto Garra (2018), “Towards a generalized beer-lambert law,” *Fractal and Fractional* **2** (1), 8.
- Cazé, A, R Pierrat, and R Carminati (2013), “Spatial coherence in complex photonic and plasmonic systems,” *Physical Review Letters* **110** (6), 063903.
- Cazé, Alexandre, Romain Pierrat, and Rémi Carminati (2010), “Near-field interactions and nonuniversality in speckle patterns produced by a point source in a disordered medium,” *Physical Review A* **82** (4), 043823.
- Chabanov, AA, M Stoytchev, and AZ Genack (2000), “Statistical signatures of photon localization,” *Nature* **404** (6780), 850–853.
- Chan, Chun Lam Clement, Mélanie M Bay, Gianni Jacucci, Roberto Vadrucchi, Cyan A Williams, Gea T van de Kerkhof, Richard M Parker, Kevin Vynck, Bruno Frka-Petesic, and Silvia Vignolini (2019), “Visual appearance of chiral nematic cellulose-based photonic films: Angular and polarization independent color response with a twist,” *Advanced Materials* **31** (52), 1905151.
- Chan, YS, Che Ting Chan, and ZY Liu (1998), “Photonic band gaps in two dimensional photonic quasicrystals,” *Physical Review Letters* **80** (5), 956.
- Chandler, Chris J, Bodo D Wilts, Juliet Brodie, and Silvia Vignolini (2017), “Structural color in marine algae,” *Adv. Opt. Mater.* **5** (5).
- Chandrasekhar, Subrahmanyan (1960), *Radiative transfer* (Dover Publications).
- Chang, Yin, Yu Ogawa, Gianni Jacucci, Olimpia D Onelli, Hui-Yun Tseng, and Silvia Vignolini (2020), “Hereditary character of photonics structure in pachyrhynchus sarcitis weevils: Color changes via one generation hybridization,” *Advanced Optical Materials* **8** (15), 2000432.
- Cherret, Nicolas, Dominique Delande, and Bart A van Tiggelen (2016), “Induced dipole-dipole interactions in light diffusion from point dipoles,” *Physical Review A* **94** (1), 012702.

- Ching, ESC, PT Leung, A Maassen van den Brink, WM Suen, SS Tong, and K Young (1998), “Quasinormal-mode expansion for waves in open systems,” *Reviews of Modern Physics* **70** (4), 1545.
- Chung, Kyungjae, Sunkyu Yu, Chul-Joon Heo, Jae Won Shim, Seung-Man Yang, Moon Gyu Han, Hong-Seok Lee, Yongwan Jin, Sang Yoon Lee, Namkyoo Park, *et al.* (2012), “Flexible, angle-independent, structural color reflectors inspired by morpho butterfly wings,” *Advanced Materials* **24** (18), 2375–2379.
- Conley, Gaurasundar M, Matteo Burrelli, Filippo Pratesi, Kevin Vynck, and Diederik S Wiersma (2014), “Light transport and localization in two-dimensional correlated disorder,” *Physical Review Letters* **112** (14), 143901.
- Conti, C, and A Fratalocchi (2008), “Dynamic light diffusion, three-dimensional anderson localization and lasing in inverted opals,” *Nature Physics* **4** (10), 794.
- Contini, Daniele, Fabrizio Martelli, and Giovanni Zaccanti (1997), “Photon migration through a turbid slab described by a model based on diffusion approximation. i. theory,” *Applied Optics* **36** (19), 4587–4599.
- Cortese, Lorenzo, Lorenzo Pattelli, Francesco Utel, Silvia Vignolini, Matteo Burrelli, and Diederik S Wiersma (2015), “Anisotropic light transport in white beetle scales,” *Advanced Optical Materials* **3** (10), 1337–1341.
- Dalichaouch, Rachida, JP Armstrong, Sheldon Schultz, PM Platzman, and SL McCall (1991), “Microwave localization by two-dimensional random scattering,” *Nature* **354** (6348), 53–55.
- Davis, A, and A Marshak (1997), “Lévy kinetics in slab geometry: Scaling of transmission probability,” *Fractal Frontiers*, 63–72.
- Davis, Anthony B, and Mark Mineev (2008), *Radiation transport through random media represented as measurable functions: Positive versus negative spatial correlations*, Tech. Rep. (Los Alamos National Lab.(LANL), Los Alamos, NM (United States)).
- De Raedt, Hans, AD Lagendijk, and Pedro de Vries (1989), “Transverse localization of light,” *Physical Review Letters* **62** (1), 47.
- De Sousa, N, JJ Sáenz, Frank Scheffold, A García-Martín, and LS Froufe-Pérez (2016), “Self-diffusion and structural properties of confined fluids in dynamic coexistence,” *Journal of Physics: Condensed Matter* **28** (13), 135101.
- Defienne, Hugo, Marco Barbieri, Ian A Walmsley, Brian J Smith, and Sylvain Gigan (2016), “Two-photon quantum walk in a multimode fiber,” *Science Advances* **2** (1), e1501054.
- Del Rio, Lia Fernandez, Hans Arwin, and Kenneth Järrendahl (2016), “Polarizing properties and structure of the cuticle of scarab beetles from the chrysina genus,” *Phys. Rev. E* **94** (1), 012409.
- Denk, Winfried, James H Strickler, and Watt W Webb (1990), “Two-photon laser scanning fluorescence microscopy,” *Science* **248** (4951), 73–76.
- Deparis, Olivier, Nadia Khuzayim, Andrew Parker, and Jean Pol Vigneron (2009), “Assessment of the antireflection property of moth wings by three-dimensional transfer-matrix optical simulations,” *Physical Review E* **79** (4), 041910.
- Deubel, Markus, Georg Von Freymann, Martin Wegener, Suresh Pereira, Kurt Busch, and Costas M Soukoulis (2004), “Direct laser writing of three-dimensional photonic-crystal templates for telecommunications,” *Nature Materials* **3** (7), 444.
- Dintinger, José, Stefan Mühlig, Carsten Rockstuhl, and Toralf Scharf (2012), “A bottom-up approach to fabricate optical metamaterials by self-assembled metallic nanoparticles,” *Optical Materials Express* **2** (3), 269–278.
- Dogariu, A, J Uozumi, and T Asakura (1992), “Enhancement of the backscattered intensity from fractal aggregates,” *Waves in Random Media* **2**, 259–263.
- Dogariu, Aristide, and Remi Carminati (2015), “Electromagnetic field correlations in three-dimensional speckles,” *Physics Reports* **559**, 1–29.
- Dogariu, Aristide, Jun Uozumi, and Toshimitsu Asakura (1996), “Enhancement factor in the light backscattered by fractal aggregated media,” *Optical Review* **3** (2), 71–82.
- Dong, BQ, XH Liu, TR Zhan, LP Jiang, HW Yin, F Liu, and J Zi (2010), “Structural coloration and photonic pseudogap in natural random close-packing photonic structures,” *Optics Express* **18** (14), 14430–14438.
- Donie, Yidenekachew J, Stefan Schliske, Radwanul H Siddique, Adrian Mertens, Vinayak Narasimhan, Fabian Schackmar, Manuel Pietsch, Ihteaz M Hossain, Gerardo Hernandez-Sosa, Uli Lemmer, *et al.* (2021), “Phase-separated nanophotonic structures by inkjet printing,” *ACS Nano*.
- Doty, Paul, and Robert F Steiner (1952), “Macro-ions. i. light scattering theory and experiments with bovine serum albumin,” *The Journal of Chemical Physics* **20** (1), 85–94.
- Doyle, William T (1989), “Optical properties of a suspension of metal spheres,” *Physical Review B* **39** (14), 9852.
- Draine, Bruce T, and Piotr J Flatau (1994), “Discrete-dipole approximation for scattering calculations,” *JOSA A* **11** (4), 1491–1499.
- Dufresne, Eric R, Heeso Noh, Vinodkumar Saranathan, Simon GJ Mochrie, Hui Cao, and Richard O Prum (2009), “Self-assembly of amorphous biophotonic nanostructures by phase separation,” *Soft Matter* **5** (9), 1792–1795.
- Dyson, Freeman J (1949a), “The radiation theories of tomonaga, schwinger, and feynman,” *Phys. Rev.* **75** (3), 486.
- Dyson, Freeman J (1949b), “The s matrix in quantum electrodynamics,” *Phys. Rev.* **75** (11), 1736.
- Edagawa, Keiichi (2014), “Photonic crystals, amorphous materials, and quasicrystals,” *Science and Technology of Advanced Materials* **15** (3), 034805.
- Edagawa, Keiichi, Satoshi Kanoko, and Masaya Notomi (2008), “Photonic amorphous diamond structure with a 3d photonic band gap,” *Physical Review Letters* **100** (1), 013901.
- Egel, Amos, Lorenzo Pattelli, Giacomo Mazzamuto, Diederik S Wiersma, and Uli Lemmer (2017), “Celes: Cuda-accelerated simulation of electromagnetic scattering by large ensembles of spheres,” *Journal of Quantitative Spectroscopy and Radiative Transfer* **199**, 103–110.
- Einstein, Albert (1910), “Theorie der opaleszenz von homogenen flüssigkeiten und flüssigkeitsgemischen in der nähe des kritischen zustandes,” *Ann. Phys.* **338** (16), 1275–1298.
- Emiliani, V, F Intonti, M Cazayous, DS Wiersma, M Colocci, F Aliev, and A Lagendijk (2003), “Near-field short range correlation in optical waves transmitted through random media,” *Physical Review Letters* **90** (25), 250801.
- Escalante, Jose M, and Sergey E Skipetrov (2017), “Longitudinal optical fields in light scattering from dielectric spheres and anderson localization of light,” *Annalen der Physik* **529** (8), 1700039.
- Evers, Ferdinand, and Alexander D Mirlin (2008), “Anderson

- transitions,” *Reviews of Modern Physics* **80** (4), 1355.
- Fahr, Stephan, Carsten Rockstuhl, and Falk Lederer (2008), “Engineering the randomness for enhanced absorption in solar cells,” *Applied Physics Letters* **92** (17), 171114.
- Fayard, N, A Caze, R Pierrat, and Rémi Carminati (2015), “Intensity correlations between reflected and transmitted speckle patterns,” *Physical Review A* **92** (3), 033827.
- Fazio, Barbara, Pietro Artoni, Maria Antonia Iatì, Cristiano D’andrea, Maria Josè Lo Faro, Salvatore Del Sorbo, Stefano Pirotta, Pietro Giuseppe Gucciardi, Paolo Musumeci, Cirino Salvatore Vasi, *et al.* (2016), “Strongly enhanced light trapping in a two-dimensional silicon nanowire random fractal array,” *Light: Science & Applications* **5** (4), e16062–e16062.
- Felderhof, BU (1974), “On the propagation and scattering of light in fluids,” *Physica* **76** (3), 486–502.
- Felderhof, BU, GW Ford, and EGD Cohen (1982), “Cluster expansion for the dielectric constant of a polarizable suspension,” *Journal of Statistical Physics* **28** (1), 135–164.
- Fernandes, Susete N, Yong Geng, Silvia Vignolini, Beverley J. Glover, Ana C. Trindade, João P. Canejo, Pedro L. Almeida, Pedro Brogueira, and Maria H. Godinho (2013), “Structural color and iridescence in transparent sheared cellulosic films,” *Macromolecular Chemistry and Physics* **214** (1), 25–32.
- Fernández-Marín, Antonio Alejandro, JA Méndez-Bermúdez, J Carbonell, F Cervera, J Sánchez-Dehesa, and VA Gopar (2014), “Beyond anderson localization in 1d: anomalous localization of microwaves in random waveguides,” *Physical Review Letters* **113** (23), 233901.
- Fikioris, JG, and PC Waterman (1964), “Multiple scattering of waves. ii. “hole corrections” in the scalar case,” *Journal of Mathematical Physics* **5** (10), 1413–1420.
- Finkel’berg, VM (1964), “Mean field strength in an inhomogeneous medium,” *Sov. Phys. JETP* **19**, 494–498.
- Fischer, Joachim, and Martin Wegener (2011), “Three-dimensional direct laser writing inspired by stimulated-emission-depletion microscopy,” *Optical Materials Express* **1** (4), 614–624.
- Florescu, Lucia, and Sajeev John (2004), “Photon statistics and coherence in light emission from a random laser,” *Physical Review Letters* **93** (1), 013602.
- Florescu, Marian, Paul J Steinhardt, and Salvatore Torquato (2013), “Optical cavities and waveguides in hyperuniform disordered photonic solids,” *Phys. Rev. B* **87** (16), 165116.
- Florescu, Marian, Salvatore Torquato, and Paul J Steinhardt (2009), “Designer disordered materials with large, complete photonic band gaps,” *Proceedings of the National Academy of Sciences* **106** (49), 20658–20663.
- Florescu, Marian, Salvatore Torquato, and Paul J. Steinhardt (2010), “Effects of random link removal on the photonic band gaps of honeycomb networks,” *Applied Physics Letters* **97** (20), 201103.
- Foldy, Leslie L (1945), “The multiple scattering of waves. i. general theory of isotropic scattering by randomly distributed scatterers,” *Physical Review* **67** (3-4), 107.
- Forster, Jason D, Heeso Noh, Seng Fatt Liew, Vinodkumar Saranathan, Carl F Schreck, Lin Yang, Jin-Gyu Park, Richard O Prum, Simon GJ Mochrie, Corey S O’Hern, *et al.* (2010), “Biomimetic isotropic nanostructures for structural coloration,” *Advanced Materials* **22** (26-27), 2939–2944.
- Fraden, Seth, and Georg Maret (1990), “Multiple light scattering from concentrated, interacting suspensions,” *Physical Review Letters* **65** (4), 512.
- Frenkel, DJVR, RJ Vos, CG De Kruif, and A Vrij (1986), “Structure factors of polydisperse systems of hard spheres: A comparison of monte carlo simulations and percus–yevick theory,” *The Journal of Chemical Physics* **84** (8), 4625–4630.
- Froufe-Pérez, LS, R Carminati, and JJ Sáenz (2007), “Fluorescence decay rate statistics of a single molecule in a disordered cluster of nanoparticles,” *Physical Review A* **76** (1), 013835.
- Froufe-Pérez, Luis S, Michael Engel, Pablo F Damasceno, Nicolas Muller, Jakub Haberko, Sharon C Glotzer, and Frank Scheffold (2016), “Role of short-range order and hyperuniformity in the formation of band gaps in disordered photonic materials,” *Physical Review Letters* **117** (5), 053902.
- Froufe-Pérez, Luis S, Michael Engel, Juan José Sáenz, and Frank Scheffold (2017), “Band gap formation and anderson localization in disordered photonic materials with structural correlations,” *Proceedings of the National Academy of Sciences* **114** (36), 9570–9574.
- Froufe-Pérez, Luis S, William Guerin, Rémi Carminati, and Robin Kaiser (2009), “Threshold of a random laser with cold atoms,” *Physical Review Letters* **102** (17), 173903.
- Gaio, Michele, Matilda Peruzzo, and Riccardo Sapienza (2015), “Tuning random lasing in photonic glasses,” *Optics Letters* **40** (7), 1611–1614.
- Gaio, Michele, Dhruv Saxena, Jacopo Bertolotti, Dario Pisignano, Andrea Camposeo, and Riccardo Sapienza (2019), “A nanophotonic laser on a graph,” *Nature Communications* **10** (1), 1–7.
- Galinski, Henning, Gael Favraud, Hao Dong, Juan S Totero Gongora, Grégory Favaro, Max Döbeli, Ralph Spolenak, Andrea Fratalocchi, and Federico Capasso (2017), “Scalable, ultra-resistant structural colors based on network metamaterials,” *Light: Science & Applications* **6** (5), e16233–e16233.
- Galisteo-López, Juan F, Marta Ibisate, Riccardo Sapienza, Luis S Froufe-Pérez, Álvaro Blanco, and Cefe López (2011), “Self-assembled photonic structures,” *Advanced Materials* **23** (1), 30–69.
- Galusha, Jeremy W, Matthew R Jorgensen, and Michael H Bartl (2010), “Diamond-structured titania photonic-bandgap crystals from biological templates,” *Advanced Materials* **22** (1), 107–110.
- Galusha, Jeremy W, Lauren R Richey, John S Gardner, Jennifer N Cha, and Michael H Bartl (2008), “Discovery of a diamond-based photonic crystal structure in beetle scales,” *Physical Review E* **77** (5), 050904.
- Gansel, Justyna K, Michael Thiel, Michael S Rill, Manuel Decker, Klaus Bade, Volker Saile, Georg von Freymann, Stefan Linden, and Martin Wegener (2009), “Gold helix photonic metamaterial as broadband circular polarizer,” *Science* **325** (5947), 1513–1515.
- García, PD, R Sapienza, J Bertolotti, MD Martín, A Blanco, A Altube, L Vina, DS Wiersma, and C López (2008), “Resonant light transport through mie modes in photonic glasses,” *Physical Review A* **78** (2), 023823.
- García, PD, R Sapienza, LS Froufe-Pérez, and C López (2009), “Strong dispersive effects in the light-scattering mean free path in photonic gaps,” *Physical Review B* **79** (24), 241109.
- García, Pedro David, R Sapienza, C Toninelli, Cefe López, and Diederik S Wiersma (2011), “Photonic crystals with

- controlled disorder,” *Physical Review A* **84** (2), 023813.
- García, Pedro David, Riccardo Sapienza, Álvaro Blanco, and Cefe López (2007), “Photonic glass: a novel random material for light,” *Advanced Materials* **19** (18), 2597–2602.
- Garcia, Pedro David, Søren Stobbe, Immo Söllner, and Peter Lodahl (2012), “Nonuniversal intensity correlations in a two-dimensional anderson-localizing random medium,” *Physical Review Letters* **109** (25), 253902.
- Gast, Alice P, and William B Russel (1998), “Simple ordering in complex fluids,” *Physics Today* **51**, 24–31.
- Ge, Li, YD Chong, and A Douglas Stone (2010), “Steady-state ab initio laser theory: generalizations and analytic results,” *Physical Review A* **82** (6), 063824.
- Geigenmüller, U, and P Mazur (1986), “The effective dielectric constant of a dispersion of spheres,” *Physica A: Statistical Mechanics and its Applications* **136** (2-3), 316–369.
- Ghofraniha, N, I Viola, F Di Maria, G Barbarella, G Gigli, L Leuzzi, and C Conti (2015), “Experimental evidence of replica symmetry breaking in random lasers,” *Nature Communications* **6**, 6058.
- Gnedenko, BV, and AN Kolmogorov (1954), “Limit distributions for sums of independent,” *Am. J. Math* **105**.
- Goerlitz, Eric SA, Robin N Klupp Taylor, and Nicolas Vogel (2018), “Bioinspired photonic pigments from colloidal self-assembly,” *Advanced Materials* **30** (28), 1706654.
- Goetschy, A, and SE Skipetrov (2011), “Euclidean matrix theory of random lasing in a cloud of cold atoms,” *EPL (Europhysics Letters)* **96** (3), 34005.
- Gomard, Guillaume, Romain Peretti, Emmanuel Drouard, Xianqin Meng, and Christian Seassal (2013), “Photonic crystals and optical mode engineering for thin film photovoltaics,” *Opt. Express* **21** (103), A515–A527.
- Gomard, Guillaume, Jan B Preinfalk, Amos Egel, and Uli Lemmer (2016), “Photon management in solution-processed organic light-emitting diodes: a review of light outcoupling micro- and nanostructures,” *Journal of Photonics for Energy* **6** (3), 030901.
- Goodman, Joseph W (2007), *Speckle phenomena in optics: theory and applications* (Roberts and Company Publishers).
- Goodman, Joseph W (2015), *Statistical optics* (John Wiley & Sons).
- Gorodnichev, EE, AI Kuzovlev, and DB Rogozkin (2014), “Depolarization coefficients of light in multiply scattering media,” *Physical Review E* **90** (4), 043205.
- Gottardo, Stefano, Riccardo Sapienza, Pedro D García, Álvaro Blanco, Diederik S Wiersma, and Cefe López (2008), “Resonance-driven random lasing,” *Nature Photonics* **2** (7), 429.
- Gower, Artur L, I David Abrahams, and William J Parnell (2019a), “A proof that multiple waves propagate in ensemble-averaged particulate materials,” *Proceedings of the Royal Society A* **475** (2229), 20190344.
- Gower, Artur L, William J Parnell, and I David Abrahams (2019b), “Multiple waves propagate in random particulate materials,” *SIAM Journal on Applied Mathematics* **79** (6), 2569–2592.
- Gower, Artur L, Michael JA Smith, William J Parnell, and I David Abrahams (2018), “Reflection from a multi-species material and its transmitted effective wavenumber,” *Proceedings of the Royal Society A: Mathematical, Physical and Engineering Sciences* **474** (2212), 20170864.
- Gower, Artur Lewis, and Gerhard Kristensson (2021), “Effective waves for random three-dimensional particulate materials,” *New Journal of Physics*.
- Graves, Sara M, and Thomas G Mason (2008), “Transmission of visible and ultraviolet light through charge-stabilized nanoemulsions,” *The Journal of Physical Chemistry C* **112** (33), 12669–12676.
- Green, Martin A (2002), “Lambertian light trapping in textured solar cells and light-emitting diodes: analytical solutions,” *Progress in Photovoltaics: Research and Applications* **10** (4), 235–241.
- Greffet, Jean-Jacques, and Rémi Carminati (1995), “Relationship between the near-field speckle pattern and the statistical properties of a surface,” *Ultramicroscopy* **61** (1-4), 43–50.
- Greffet, Jean-Jacques, and Rémi Carminati (1997), “Image formation in near-field optics,” *Progress in Surface Science* **56** (3), 133–237.
- Grimes, Craig A, and Dale M Grimes (1991), “Permeability and permittivity spectra of granular materials,” *Physical Review B* **43** (13), 10780.
- Grishina, DA, CAM Hartevelde, A Pacureanu, D Devashish, A Lagendijk, P Cloetens, and WL Vos (2018), “X-ray imaging non-destructively identifies functional 3d photonic nanostructures,” *arXiv preprint arXiv:1808.01392*.
- Grishina, DA, Cornelis AM Hartevelde, LA Woldering, and Willem L Vos (2015), “Method for making a single-step etch mask for 3d monolithic nanostructures,” *Nanotechnology* **26** (50), 505302.
- Groth, CW, AR Akhmerov, and CWJ Beenakker (2012), “Transmission probability through a lévy glass and comparison with a lévy walk,” *Physical Review E* **85** (2), 021138.
- Haberko, Jakub, Luis S Froufe-Pérez, and Frank Scheffold (2020), “Transition from light diffusion to localization in three-dimensional amorphous dielectric networks near the band edge,” *Nature Communications* **11** (1), 1–9.
- Haberko, Jakub, Nicolas Muller, and Frank Scheffold (2013), “Direct laser writing of three-dimensional network structures as templates for disordered photonic materials,” *Physical Review A* **88** (4), 043822.
- Haberko, Jakub, and Frank Scheffold (2013), “Fabrication of mesoscale polymeric templates for three-dimensional disordered photonic materials,” *Optics Express* **21** (1), 1057–1065.
- Haefner, D, S Sukhov, and A Dogariu (2008), “Stochastic scattering polarimetry,” *Physical Review Letters* **100** (4), 043901.
- Haefner, David, Sergey Sukhov, and Aristide Dogariu (2010), “Scale-dependent anisotropic polarizability in mesoscopic structures,” *Physical Review E* **81** (1), 016609.
- Haines, Andrew I, Chris E Finlayson, David RE Snoswell, Peter Spahn, G Peter Hellmann, and Jeremy J Baumberg (2012), “Anisotropic resonant scattering from polymer photonic crystals,” *Advanced Materials* **24** (44), OP305–OP308.
- Hansen, Jean-Pierre, and Ian R McDonald (1990), *Theory of simple liquids* (Elsevier).
- Hart, Robert W, and Richard A Farrell (1969), “Light scattering in the cornea,” *JOSA* **59** (6), 766–774.
- He, Mingxin, Johnathon P Gales, Étienne Ducrot, Zhe Gong, Gi-Ra Yi, Stefano Sacanna, and David J Pine (2020), “Colloidal diamond,” *Nature* **585** (7826), 524–529.
- Henkel, C (1997), “Radiative Transfer and Atom Transport,” [arXiv:physics/0505023v1](https://arxiv.org/abs/physics/0505023v1).

- Ho, KM, Che Ting Chan, and Costas M Soukoulis (1990), "Existence of a photonic gap in periodic dielectric structures," *Physical Review Letters* **65** (25), 3152.
- Honeycutt, J Dana, and Hans C Andersen (1987), "Molecular dynamics study of melting and freezing of small lennard-jones clusters," *Journal of Physical Chemistry* **91** (19), 4950–4963.
- Hu, Hefei, A Strybulevych, JH Page, Sergey E Skipetrov, and Bart A van Tiggelen (2008), "Localization of ultrasound in a three-dimensional elastic network," *Nature Physics* **4** (12), 945.
- Huang, Jiandong, N Eradat, ME Raikh, ZV Vardeny, AA Zakhidov, and RH Baughman (2001), "Anomalous coherent backscattering of light from opal photonic crystals," *Physical Review Letters* **86** (21), 4815.
- Hunt, Toby, Johannes Bergsten, Zuzana Levkanicova, Anna Papadopoulou, Oliver St John, Ruth Wild, Peter M Hammond, Dirk Ahrens, Michael Balke, Michael S Caterino, *et al.* (2007), "A comprehensive phylogeny of beetles reveals the evolutionary origins of a superradiation," *Science* **318** (5858), 1913–1916.
- Hunter, Richard S, and Richard W Harold (1987), *The measurement of appearance* (John Wiley & Sons).
- Hwang, Victoria, Anna B Stephenson, Solomon Barkley, Soeren Brandt, Ming Xiao, Joanna Aizenberg, and Vinodhan N Manoharan (2021), "Designing angle-independent structural colors using monte carlo simulations of multiple scattering," *Proceedings of the National Academy of Sciences* **118** (4).
- Hynne, F, and Robert K Bullough (1987), "The scattering of light. ii. the complex refractive index of a molecular fluid," *Philosophical Transactions of the Royal Society of London. Series A, Mathematical and Physical Sciences* **321** (1559), 305–360.
- Imagawa, Shigeki, Keiichi Edagawa, Keisuke Morita, Toshiki Niino, Yutaka Kagawa, and Masaya Notomi (2010), "Photonic band-gap formation, light diffusion, and localization in photonic amorphous diamond structures," *Physical Review B* **82** (11), 115116.
- Ioffe, AF, and AR Regel (1960), "Non-crystalline, amorphous and liquid electronic semiconductors," *Prog. Semiconductor* **4** (89), 237–291.
- Ishii, Katsuhiro, Toshiaki Iwai, Jun Uozumi, and Toshimitsu Asakura (1998), "Optical free-path-length distribution in a fractal aggregate and its effect on enhanced backscattering," *Applied Optics* **37** (21), 5014–5018.
- Ishimaru, Akira (1978), *Wave propagation and scattering in random media*, Vol. 2 (Academic press New York).
- Izrailev, Felix M, Arkadii A Krokhn, and NM Makarov (2012), "Anomalous localization in low-dimensional systems with correlated disorder," *Physics Reports* **512** (3), 125–254.
- Jacucci, Gianni, Jacopo Bertolotti, and Silvia Vignolini (2019), "Role of anisotropy and refractive index in scattering and whiteness optimization," *Advanced Optical Materials* **7** (23), 1900980.
- Jacucci, Gianni, Lukas Schertel, Yating Zhang, Han Yang, and Silvia Vignolini (2020a), "Light management with natural materials: From whiteness to transparency," *Advanced Materials*, 2001215.
- Jacucci, Gianni, Silvia Vignolini, and Lukas Schertel (2020b), "The limitations of extending nature's color palette in correlated, disordered systems," *Proceedings of the National Academy of Sciences* **117** (38), 23345–23349.
- Janson, Svante, Tomasz Luczak, and Andrzej Rucinski (2011), *Random graphs*, Vol. 45 (John Wiley & Sons).
- Jendrzejewski, Fred, Alain Bernard, Killian Mueller, Patrick Cheinet, Vincent Josse, Marie Piraud, Luca Pezzé, Laurent Sanchez-Palencia, Alain Aspect, and Philippe Bouyer (2012), "Three-dimensional localization of ultracold atoms in an optical disordered potential," *Nature Physics* **8** (5), 398–403.
- Jensen, Jakob Søndergaard, and Ole Sigmund (2011), "Topology optimization for nano-photonics," *Laser & Photonics Reviews* **5** (2), 308–321.
- Jiao, Yang, and Salvatore Torquato (2011), "Maximally random jammed packings of platonic solids: Hyperuniform long-range correlations and isostaticity," *Physical Review E* **84** (4), 041309.
- Jin, Chongjun, Xiaodong Meng, Bingying Cheng, Zhaolin Li, and Daozhong Zhang (2001), "Photonic gap in amorphous photonic materials," *Physical Review B* **63** (19), 195107.
- Joannopoulos, John D, Steven G Johnson, Joshua N Winn, and Robert D Meade (2011), *Photonic crystals: molding the flow of light* (Princeton University Press).
- Johansen, Villads Egede, Olimpia Domitilla Onelli, Lisa Maria Steiner, and Silvia Vignolini (2017), "Photonics in nature: from order to disorder," in *Functional surfaces in biology III* (Springer) pp. 53–89.
- John, Sajeed (1984), "Electromagnetic absorption in a disordered medium near a photon mobility edge," *Physical Review Letters* **53** (22), 2169.
- John, Sajeed (1987), "Strong localization of photons in certain disordered dielectric superlattices," *Physical Review Letters* **58** (23), 2486.
- Johnson, Steven G, and John D Joannopoulos (2001), "Block-iterative frequency-domain methods for maxwell's equations in a planewave basis," *Optics Express* **8** (3), 173–190.
- Kaplan, PD, AD Dinsmore, AG Yodh, and DJ Pine (1994), "Diffuse-transmission spectroscopy: a structural probe of opaque colloidal mixtures," *Physical Review E* **50** (6), 4827.
- Keller, Joseph B (1964), "Stochastic equations and wave propagation in random media," *Stochastic processes in mathematical physics and engineering* **16**, 145.
- Kim, Jaekuk, Ge Zhang, Frank H Stillinger, and Salvatore Torquato (2018), "Inversion problems for fourier transforms of particle distributions," *Journal of Statistical Mechanics: Theory and Experiment* **2018** (11), 113302.
- Kim, Seung-Hyun, Sofia Magkiriadou, Do Kyung Rhee, Doo Sung Lee, Pil J Yoo, Vinodhan N Manoharan, and Gi-Ra Yi (2017), "Inverse photonic glasses by packing bidisperse hollow microspheres with uniform cores," *ACS Applied Materials & Interfaces* **9** (28), 24155–24160.
- Kim, Sunghwan, Sungjoon Yoon, Hyojun Seok, Jeongkug Lee, and Heonsu Jeon (2010), "Band-edge lasers based on randomly mixed photonic crystals," *Optics Express* **18** (8), 7685–7692.
- Kinoshita, Shuichi, and Shinya Yoshioka (2005), "Structural colors in nature: the role of regularity and irregularity in the structure," *ChemPhysChem* **6** (8), 1442–1459.
- Kirkwood, John G (1936), "On the theory of dielectric polarization," *The Journal of Chemical Physics* **4** (9), 592–601.
- Kittel, Charles (1976), *Introduction to solid state physics*, Vol. 8 (Wiley New York).
- Klages, Rainer, Günter Radons, and Igor M Sokolov (2008), *Anomalous transport: foundations and applications* (John Wiley & Sons).

- Klar, Thomas A, Richard Wollhofen, and Jaroslaw Jacak (2014), “Sub-abbe resolution: from sted microscopy to sted lithography,” *Physica Scripta* **2014** (T162), 014049.
- Klatt, Michael A, Paul J Steinhardt, and Salvatore Torquato (2019), “Phoamtonic designs yield sizeable 3d photonic band gaps,” *Proceedings of the National Academy of Sciences* **116** (47), 23480–23486.
- Knyazikhin, Yuri, Jörn Kranigk, Ranga B Myneni, Oleg Panforyov, and Gode Gravenhorst (1998), “Influence of small-scale structure on radiative transfer and photosynthesis in vegetation canopies,” *Journal of Geophysical Research: Atmospheres* **103** (D6), 6133–6144.
- Koenderink, A Femius, Ad Lagendijk, and Willem L Vos (2005), “Optical extinction due to intrinsic structural variations of photonic crystals,” *Physical Review B* **72** (15), 153102.
- Koenderink, A Femius, Mischa Megens, Gijs van Soest, Willem L Vos, and Ad Lagendijk (2000), “Enhanced backscattering from photonic crystals,” *Physics Letters A* **268** (1-2), 104–111.
- Kondov, SS, WR McGehee, JJ Zirbel, and B DeMarco (2011), “Three-dimensional anderson localization of ultracold matter,” *Science* **334** (6052), 66–68.
- Kostinski, AB, and AR Jameson (2000), “On the spatial distribution of cloud particles,” *Journal of the Atmospheric Sciences* **57** (7), 901–915.
- Kostinski, Alexander B (2001), “On the extinction of radiation by a homogeneous but spatially correlated random medium,” *JOSA A* **18** (8), 1929–1933.
- Kostinski, Alexander B (2002), “On the extinction of radiation by a homogeneous but spatially correlated random medium: reply to comment,” *JOSA A* **19** (12), 2521–2525.
- Krachmalnicoff, V, E Castanié, Y De Wilde, and R Carminati (2010), “Fluctuations of the local density of states probe localized surface plasmons on disordered metal films,” *Physical Review Letters* **105** (18), 183901.
- Krauss, Thomas F, M Richard, and Stuart Brand (1996), “Two-dimensional photonic-bandgap structures operating at near-infrared wavelengths,” *Nature* **383** (6602), 699.
- Kristensson, Gerhard (2015), “Coherent scattering by a collection of randomly located obstacles—an alternative integral equation formulation,” *Journal of Quantitative Spectroscopy and Radiative Transfer* **164**, 97–108.
- Labastie, Pierre, and Robert L Whetten (1990), “Statistical thermodynamics of the cluster solid-liquid transition,” *Physical Review Letters* **65** (13), 1567.
- Lagendijk, Aart, Bart Van Tiggelen, and Diederik S Wiersma (2009), “Fifty years of anderson localization,” *Phys. Today* **62** (8), 24–29.
- Lagendijk, Ad, and Bart A Van Tiggelen (1996), “Resonant multiple scattering of light,” *Physics Reports* **270** (3), 143–215.
- Lakhtakia, Akhlesh (1992), “General theory of the purcell-pennypacker scattering approach and its extension to bianisotropic scatterers,” *The Astrophysical Journal* **394**, 494–499.
- Lalanne, Philippe, Wei Yan, Kevin Vynck, Christophe Sauvan, and Jean-Paul Hugonin (2018), “Light interaction with photonic and plasmonic resonances,” *Laser & Photonics Reviews* **12** (5), 1700113.
- LAMMPS, (2019), “LAMMPS Molecular Dynamics Simulator,” <https://lammps.sandia.gov/>.
- Lan, Yang, Alessio Caciagli, Giulia Guidetti, Ziyi Yu, Ji Liu, Villads E Johansen, Marlous Kamp, Chris Abell, Silvia Vignolini, Oren A Scherman, *et al.* (2018), “Unexpected stability of aqueous dispersions of raspberry-like colloids,” *Nature Communications* **9** (1), 3614.
- Landau, LD, and EM Lifshitz (1980), “Statistical physics,” *Course of Theoretical Physics* **5**, 396–400.
- Landau, Lev Davidovich, EM Lifshitz, and JB Sykes (2013), *Electrodynamics of continuous media*, Vol. 8 (elsevier).
- Larsen, Edward W, and Richard Vasques (2011), “A generalized linear boltzmann equation for non-classical particle transport,” *Journal of Quantitative Spectroscopy and Radiative Transfer* **112** (4), 619–631.
- Laverdant, Julien, Stéphanie Buil, Bruno Bérini, and Xavier Quélin (2008), “Polarization dependent near-field speckle of random gold films,” *Physical Review B* **77** (16), 165406.
- Lax, Melvin (1951), “Multiple scattering of waves,” *Reviews of Modern Physics* **23** (4), 287.
- Lax, Melvin (1952), “Multiple scattering of waves. ii. the effective field in dense systems,” *Physical Review* **85** (4), 621.
- Lebowitz, JL, and JK Percus (1963), “Integral equations and inequalities in the theory of fluids,” *Journal of Mathematical Physics* **4** (12), 1495–1506.
- Ledermann, Alexandra, Ludovico Cademartiri, Martin Hermatschweiler, Costanza Toninelli, Geoffrey A Ozin, Diederik S Wiersma, Martin Wegener, and Georg Von Freymann (2006), “Three-dimensional silicon inverse photonic quasicrystals for infrared wavelengths,” *Nature Materials* **5** (12), 942.
- Lee, Cheuk-Yu, Zbigniew H Stachurski, and T Richard Welberry (2010), “The geometry, topology and structure of amorphous solids,” *Acta Materialia* **58** (2), 615–625.
- Lee, Myungjae, Ségolène Callard, Christian Seassal, and Heonsu Jeon (2019), “Taming of random lasers,” *Nature Photonics*, 1.
- Lee, Seung Ho, Sang M. Han, and Sang Eon Han (2020), “Anisotropic diffusion in cyphochilus white beetle scales,” *APL Photonics* **5** (5), 056103.
- Lee, Won-Kyu, Shuangcheng Yu, Clifford J Engel, Thaddeus Reese, Dongjoon Rhee, Wei Chen, and Teri W Odom (2017), “Concurrent design of quasi-random photonic nanostructures,” *Proceedings of the National Academy of Sciences* **114** (33), 8734–8739.
- Leedumrongwatthanakun, Saroch, Luca Innocenti, Hugo Diefenne, Thomas Juffmann, Alessandro Ferraro, Mauro Paternostro, and Sylvain Gigan (2020), “Programmable linear quantum networks with a multimode fibre,” *Nature Photonics* **14** (3), 139–142.
- Leistikow, MD, AP Mosk, E Yeganegi, SR Huisman, Aart Lagendijk, and Willem L Vos (2011), “Inhibited spontaneous emission of quantum dots observed in a 3d photonic band gap,” *Physical Review Letters* **107** (19), 193903.
- Leonetti, Marco, Claudio Conti, and Cefe Lopez (2011), “The mode-locking transition of random lasers,” *Nature Photonics* **5** (10), 615.
- Lepri, Stefano, Cosimo Trono, and Giovanni Giacomelli (2017), “Complex active optical networks as a new laser concept,” *Physical Review Letters* **118** (12), 123901.
- Leseur, Olivier, Romain Pierrat, and Rémi Carminati (2016), “High-density hyperuniform materials can be transparent,” *Optica* **3** (7), 763–767.
- Leseur, Olivier, Romain Pierrat, and Rémi Carminati (2017), “Spatial correlations of the spontaneous decay rate as a probe of dense and correlated disordered materials,” *The European Physical Journal Special Topics* **226** (7), 1423–1432.

- Letokhov, VS (1968), “Generation of light by a scattering medium with negative resonance absorption,” *Soviet Journal of Experimental and Theoretical Physics* **26**, 835.
- Lidorikis, E, MM Sigalas, Eleftherios N Economou, and CM Soukoulis (2000), “Gap deformation and classical wave localization in disordered two-dimensional photonic-band-gap materials,” *Physical Review B* **61** (20), 13458.
- Liew, Seng Fatt, Jin-Kyu Yang, Heeso Noh, Carl F Schreck, Eric R Dufresne, Corey S O’Hern, and Hui Cao (2011), “Photonic band gaps in three-dimensional network structures with short-range order,” *Physical Review A* **84** (6), 063818.
- Lima, Jonas RF, Luiz Felipe C Pereira, and Anderson LR Barbosa (2019), “Dirac wave transmission in Lévy-disordered systems,” *Physical Review E* **99** (3), 032118.
- Lin, MY, HM Lindsay, DA Weitz, RC Ball, R Klein, and P Meakin (1989), “Universality of fractal aggregates as probed by light scattering,” in *Proc. R. Soc. Lond. A*, Vol. 423 (The Royal Society Publishing) pp. 71–87.
- Lin, Shawn-yu, JG Fleming, DL Hetherington, BK Smith, R Biswas, KM Ho, MM Sigalas, W Zubrzycki, SR Kurtz, and Jim Bur (1998), “A three-dimensional photonic crystal operating at infrared wavelengths,” *Nature* **394** (6690), 251.
- Liu, Jin, PD Garcia, Sara Ek, Niels Gregersen, T Suhr, Martin Schubert, Jesper Mørk, Søren Stobbe, and Peter Lodahl (2014), “Random nanolasing in the anderson localized regime,” *Nature Nanotechnology* **9** (4), 285.
- Liu, MQ, CY Zhao, BX Wang, and Xing Fang (2018), “Role of short-range order in manipulating light absorption in disordered media,” *JOSA B* **35** (3), 504–513.
- Lodahl, Peter, A Floris Van Driel, Ivan S Nikolaev, Arie Iman, Karin Overgaag, Daniël Vanmaekelbergh, and Willem L Vos (2004), “Controlling the dynamics of spontaneous emission from quantum dots by photonic crystals,” *Nature* **430** (7000), 654.
- López, Cefe (2003), “Materials aspects of photonic crystals,” *Advanced Materials* **15** (20), 1679–1704.
- Lorentz, Hendrik Antoon (1880), “Ueber die beziehung zwischen der fortpflanzungsgeschwindigkeit des liches und der körperdichte,” *Annalen der Physik* **245** (4), 641–665.
- Lorenz, Ludvig (1880), “Ueber die refractionsconstante,” *Annalen der Physik* **247** (9), 70–103.
- Lubachevsky, Boris D, and Frank H. Stillinger (1990), “Geometric properties of random disk packings,” *Journal of Statistical Physics* **60** (5), 561–583.
- Luke, Stephen M, Benny T Hallam, and Peter Vukusic (2010), “Structural optimization for broadband scattering in several ultra-thin white beetle scales,” *Applied Optics* **49** (22), 4246–4254.
- Mackay, Tom G, and Akhlesh Lakhtakia (2015), *Modern analytical electromagnetic homogenization* (Morgan & Claypool Publishers).
- Magerle, Robert (2000), “Nanotomography,” *Physical Review Letters* **85** (13), 2749.
- Magkiriadou, Sofia, Jin-Gyu Park, Young-Seok Kim, and Vinodhan N Manoharan (2012), “Disordered packings of core-shell particles with angle-independent structural colors,” *Optical Materials Express* **2** (10), 1343–1352.
- Magkiriadou, Sofia, Jin-Gyu Park, Young-Seok Kim, and Vinodhan N. Manoharan (2014), “Absence of red structural color in photonic glasses, bird feathers, and certain beetles,” *Commun Chem* **90**, 062302.
- Maimouni, Ilham, Maryam Morvaridi, Maria Russo, Gianluca Lui, Konstantin Morozov, Janine Cossy, Marian Florescu, Matthieu Labousse, and Patrick Tabeling (2020), “Micrometric monodisperse solid foams as complete photonic bandgap materials,” *ACS Applied Materials & Interfaces* **12** (28), 32061–32068.
- Man, Weining, Marian Florescu, Eric Paul Williamson, Yingquan He, Seyed Reza Hashemizad, Brian YC Leung, Devin Robert Liner, Salvatore Torquato, Paul M Chaikin, and Paul J Steinhardt (2013), “Isotropic band gaps and freeform waveguides observed in hyperuniform disordered photonic solids,” *Proceedings of the National Academy of Sciences* **110** (40), 15886–15891.
- Mandel, Leonard, and Emil Wolf (1995), *Optical coherence and quantum optics* (Cambridge University Press).
- Mandelbrot, Benoit (1967), “How long is the coast of britain? statistical self-similarity and fractional dimension,” *Science* **156** (3775), 636–638.
- Manoharan, Vinodhan N, Mark T Elssesser, and David J Pine (2003), “Dense packing and symmetry in small clusters of microspheres,” *Science* **301** (5632), 483–487.
- Marichy, Catherine, Nicolas Muller, Luis S Froufe-Pérez, and Frank Scheffold (2016), “High-quality photonic crystals with a nearly complete band gap obtained by direct inversion of woodpile templates with titanium dioxide,” *Scientific Reports* **6**, 21818.
- Markel, Vadim A (2016), “Introduction to the maxwell garnett approximation: tutorial,” *JOSA A* **33** (7), 1244–1256.
- Marshak, Alexander, and Anthony Davis (2005), *3D radiative transfer in cloudy atmospheres* (Springer Science & Business Media).
- Marshak, Alexander, Anthony Davis, Warren Wiscombe, and Robert Cahalan (1998), “Radiative effects of sub-mean free path liquid water variability observed in stratiform clouds,” *Journal of Geophysical Research: Atmospheres* **103** (D16), 19557–19567.
- Martin, Ph A, and T Yalcin (1980), “The charge fluctuations in classical coulomb systems,” *Journal of Statistical Physics* **22** (4), 435–463.
- Martins, Emiliano R, Juntao Li, YiKun Liu, Valérie Depauw, Zhanxu Chen, Jianying Zhou, and Thomas F Krauss (2013), “Deterministic quasi-random nanostructures for photon control,” *Nature Communications* **4** (1), 1–7.
- Maurice, David M (1957), “The structure and transparency of the cornea,” *The Journal of Physiology* **136** (2), 263–286.
- Maxwell Garnett, JC (1904), “Xii. colours in metal glasses and in metallic films,” *Philosophical Transactions of the Royal Society of London. Series A, Containing Papers of a Mathematical or Physical Character* **203** (359-371), 385–420.
- Meakin, Paul (1987), “Fractal aggregates,” *Advances in Colloid and Interface science* **28**, 249–331.
- Meakin, Paul, and Remi Jullien (1992), “Random sequential adsorption of spheres of different sizes,” *Physica A: Statistical Mechanics and its Applications* **187** (3-4), 475–488.
- Mello, Pier A, Pier A Mello, Narendra Kumar, and Dr Narendra Kumar (2004), *Quantum transport in mesoscopic systems: complexity and statistical fluctuations, a maximum-entropy viewpoint*, Vol. 4 (Oxford University Press on Demand).
- Mercadier, Nicolas, William Guerin, Martine Chevrollier, and Robin Kaiser (2009), “Lévy flights of photons in hot atomic vapours,” *Nature Physics* **5** (8), 602–605.
- Meseguer, F, A Blanco, H Miguez, F Garcia-Santamaria, M Ibisate, and C Lopez (2002), “Synthesis of inverse

- opals,” *Colloids and Surfaces A: Physicochemical and Engineering Aspects* **202** (2-3), 281–290.
- Messiah, A (1999), *Quantum Mechanics* (Dover, New York).
- Michel, Bernhard, and Akhlesh Lakhtakia (1995), “Strong-property-fluctuation theory for homogenizing chiral particulate composites,” *Physical Review E* **51** (6), 5701.
- Michielsen, Kristel, H De Raedt, and Doekele G Stavenga (2009), “Reflectivity of the gyroid biophotonic crystals in the ventral wing scales of the green hairstreak butterfly, *calophrys rubi*,” *Journal of the Royal Society Interface* **7** (46), 765–771.
- Michielsen, Kristel, and Doekele G Stavenga (2007), “Gyroid cuticular structures in butterfly wing scales: biological photonic crystals,” *Journal of The Royal Society Interface* **5** (18), 85–94.
- Mie, Gustav (1908), “Beiträge zur optik trüber medien, speziell kolloidaler metallösungen,” *Annalen der Physik* **330** (3), 377–445.
- Mirlin, AD, Yu V Fyodorov, A Mildenberger, and F Evers (2006), “Exact relations between multifractal exponents at the anderson transition,” *Physical Review Letters* **97** (4), 046803.
- Mishchenko, Michael I, Joop W Hovenier, and Larry D Travis (2000), “Light scattering by nonspherical particles: theory, measurements, and applications,”.
- Mokkapati, Sudha, and KR Catchpole (2012), “Nanophotonic light trapping in solar cells,” *Journal of Applied Physics* **112** (10), 101101.
- Moon, Jun Hyuk, G-R Yi, S-M Yang, David J Pine, and S Bin Park (2004), “Electrospray-assisted fabrication of uniform photonic balls,” *Advanced Materials* **16** (7), 605–609.
- Moyroud, Edwige, Tobias Wenzel, Rox Middleton, Paula J Rudall, Hannah Banks, Alison Reed, Greg Mellers, Patrick Killoran, M Murphy Westwood, Ullrich Steiner, *et al.* (2017), “Disorder in convergent floral nanostructures enhances signalling to bees,” *Nature* **550** (7677), 469–474.
- Muljarov, EA, and Wolfgang Langbein (2016), “Exact mode volume and purcell factor of open optical systems,” *Physical Review B* **94** (23), 235438.
- Muller, Nicolas, Jakub Haberk, Catherine Marichy, and Frank Scheffold (2013), “Silicon hyperuniform disordered photonic materials with a pronounced gap in the shortwave infrared,” *Adv. Opt. Mater.* **2** (2), 115–119.
- Muller, Nicolas, Jakub Haberk, Catherine Marichy, and Frank Scheffold (2017), “Photonic hyperuniform networks obtained by silicon double inversion of polymer templates,” *Optica* **4** (3), 361–366.
- Mupparapu, Rajeshkumar, Kevin Vynck, Tomas Svensson, Matteo Burresi, and Diederik S Wiersma (2015), “Path length enhancement in disordered media for increased absorption,” *Optics Express* **23** (24), A1472–A1484.
- Muskens, Otto L, Jaime Gómez Rivas, Rienk E Algra, Erik PAM Bakkers, and Ad Lagendijk (2008), “Design of light scattering in nanowire materials for photovoltaic applications,” *Nano Letters* **8** (9), 2638–2642.
- Nakayama, Tsuneyoshi, Kousuke Yakubo, and Raymond L Orbach (1994), “Dynamical properties of fractal networks: Scaling, numerical simulations, and physical realizations,” *Reviews of Modern Physics* **66** (2), 381.
- Naraghi, R Rezvani, S Sukhov, and A Dogariu (2016), “Disorder fingerprint: intensity distributions in the near field of random media,” *Physical Review B* **94** (17), 174205.
- Naraghi, R Rezvani, S Sukhov, JJ Sáenz, and A Dogariu (2015), “Near-field effects in mesoscopic light transport,” *Physical Review Letters* **115** (20), 203903.
- Naraghi, Roxana Rezvani, and Aristide Dogariu (2016), “Phase transitions in diffusion of light,” *Physical Review Letters* **117** (26), 263901.
- Nelson, Erik C, Neville L Dias, Kevin P Bassett, Simon N Dunham, Varun Verma, Masao Miyake, Pierre Wiltzius, John A Rogers, James J Coleman, Xiuling Li, *et al.* (2011), “Epitaxial growth of three-dimensionally architected optoelectronic devices,” *Nature Materials* **10** (9), 676–681.
- Noh, Heeso, Seng Fatt Liew, Vinodkumar Saranathan, Simon GJ Mochrie, Richard O Prum, Eric R Dufresne, and Hui Cao (2010), “How noniridescent colors are generated by quasi-ordered structures of bird feathers,” *Advanced Materials* **22** (26-27), 2871–2880.
- Noh, Heeso, Jin-Kyu Yang, Seng Fatt Liew, Michael J Rooks, Glenn S Solomon, and Hui Cao (2011), “Control of lasing in biomimetic structures with short-range order,” *Physical Review Letters* **106** (18), 183901.
- Nolan, John (2003), *Stable distributions: models for heavy-tailed data* (Birkhauser Boston).
- Novotny, Lukas, and Bert Hecht (2012), *Principles of nano-optics* (Cambridge University Press).
- O’Brien, Stephen, and John B Pendry (2002), “Photonic band-gap effects and magnetic activity in dielectric composites,” *Journal of Physics: Condensed Matter* **14** (15), 4035.
- Ohta, Noboru, and Alan Robertson (2006), *Colorimetry: fundamentals and applications* (John Wiley & Sons).
- Onelli, Olimpia D, Thomas van de Kamp, Jeremy N Skepper, Janet Powell, Tomy dos Santos Rolo, Tilo Baumbach, and Silvia Vignolini (2017), “Development of structural colour in leaf beetles,” *Scientific Reports* **7** (1), 1373.
- Onsager, Lars (1936), “Electric moments of molecules in liquids,” *Journal of the American Chemical Society* **58** (8), 1486–1493.
- Ornstein, L S, and F Zernike (1914), “Accidental deviations of density and opalescence at the critical point of a single substance,” *Proc. Akad. Sci.* **17**, 793.
- Oskooi, Ardavan, Pedro A Favuzzi, Yoshinori Tanaka, Hiroaki Shigeta, Yoichi Kawakami, and Susumu Noda (2012), “Partially disordered photonic-crystal thin films for enhanced and robust photovoltaics,” *Appl. Phys. Lett.* **100** (18), 181110.
- Parigi, Valentina, Elodie Perros, Guillaume Binard, Céline Bourdillon, Agnès Maître, Rémi Carminati, Valentina Krachmalnicoff, and Yannick De Wilde (2016), “Near-field to far-field characterization of speckle patterns generated by disordered nanomaterials,” *Optics Express* **24** (7), 7019–7027.
- Park, Jin-Gyu, Shin-Hyun Kim, Sofia Magkiriadou, Tae Min Choi, Young-Seok Kim, and Vinodhan N Manoharan (2014), “Full-spectrum photonic pigments with non-iridescent structural colors through colloidal assembly,” *Angewandte Chemie International Edition* **53** (11), 2899–2903.
- Pattelli, Lorenzo, Amos Egel, Uli Lemmer, and Diederik S Wiersma (2018), “Role of packing density and spatial correlations in strongly scattering 3d systems,” *Optica* **5** (9), 1037–1045.
- Pelton, Matthew (2015), “Modified spontaneous emission in nanophotonic structures,” *Nature Photonics* **9** (7), 427–435.
- Percus, Jerome K, and George J Yevick (1958), “Analysis of classical statistical mechanics by means of collective coor-

- dinates,” *Physical Review* **110** (1), 1.
- Pereira, Eduardo, José MG Martinho, and Mário N Berberan-Santos (2004), “Photon trajectories in incoherent atomic radiation trapping as lévy flights,” *Physical Review Letters* **93** (12), 120201.
- Peretti, Romain, Guillaume Gomard, Loïc Lalouat, Christian Seassal, and Emmanuel Drouard (2013), “Absorption control in pseudodisordered photonic-crystal thin films,” *Phys. Rev. A* **88** (5), 053835.
- Phillips, James C, Rosemary Braun, Wei Wang, James Gumbart, Emad Tajkhorshid, Elizabeth Villa, Christophe Chipot, Robert D Skeel, Laxmikant Kale, and Klaus Schulten (2005), “Scalable molecular dynamics with NAMD,” *Journal of Computational Chemistry* **26** (16), 1781–1802.
- Phillips, JC (1971), “Electronic structure and optical spectra of amorphous semiconductors,” *Physica Status Solidi* (b) **44** (1), K1–K4.
- Piechulla, Peter M, Lutz Muehlenbein, Ralf B Wehrspohn, Stefan Nanz, Aimi Abass, Carsten Rockstuhl, and Alexander Sprafke (2018), “Fabrication of nearly-hyperuniform substrates by tailored disorder for photonic applications,” *Advanced Optical Materials* **6** (7), 1701272.
- Pierrat, R, and R. Carminati (2007), “Threshold of random lasers in the incoherent transport regime,” *Physical Review A - Atomic, Molecular, and Optical Physics* **76** (2), 1–6.
- Pierrat, Romain, Philipp Ambichl, Sylvain Gigan, Alexander Haber, Rémi Carminati, and Stefan Rotter (2014), “Invariance property of wave scattering through disordered media,” *Proceedings of the National Academy of Sciences* **111** (50), 17765–17770.
- Plimpton, Steve (1995), “Fast parallel algorithms for short-range molecular dynamics,” *Journal of computational physics* **117** (1), 1–19.
- Poon, Wilson (2004), “Colloids as big atoms,” *Science* **304** (5672), 830–831.
- Pratesi, Filippo, Matteo Burrelli, Francesco Riboli, Kevin Vynck, and Diederik S Wiersma (2013), “Disordered photonic structures for light harvesting in solar cells,” *Opt. Express* **21** (103), A460–A468.
- Prum, Richard O, Eric R Dufresne, Tim Quinn, and Karla Waters (2009), “Development of colour-producing β -keratin nanostructures in avian feather barbs,” *Journal of the Royal Society Interface* **6** (suppl.2), S253–S265.
- Prum, Richard O, Tim Quinn, and Rodolfo H Torres (2006), “Anatomically diverse butterfly scales all produce structural colours by coherent scattering,” *Journal of Experimental Biology* **209** (4), 748–765.
- Prum, Richard O, and Rodolfo Torres (2003), “Structural colouration of avian skin: convergent evolution of coherently scattering dermal collagen arrays,” *Journal of Experimental Biology* **206** (14), 2409–2429.
- Prum, Richard O, and Rodolfo Torres (2004), “Structural colouration of mammalian skin: convergent evolution of coherently scattering dermal collagen arrays,” *Journal of Experimental Biology* **207** (12), 2157–2172.
- Prum, Richard O, Rodolfo H Torres, Scott Williamson, and Jan Dyck (1998), “Coherent light scattering by blue feather barbs,” *Nature* **396** (6706), 28.
- Pusey, Peter N, and W Van Megen (1986), “Phase behaviour of concentrated suspensions of nearly hard colloidal spheres,” *Nature* **320** (6060), 340.
- Pusey, PN (1987), “The effect of polydispersity on the crystallization of hard spherical colloids,” *Journal de Physique* **48** (5), 709–712.
- Pusey, PN (1991), “Liquids, freezing and the glass transition,”.
- Pusey, PN, W Van Megen, P Bartlett, BJ Ackerson, JG Rarity, and SM Underwood (1989), “Structure of crystals of hard colloidal spheres,” *Physical Review Letters* **63** (25), 2753.
- Rayleigh, Lord (1899), “Xxxiv. on the transmission of light through an atmosphere containing small particles in suspension, and on the origin of the blue of the sky,” *The London, Edinburgh, and Dublin Philosophical Magazine and Journal of Science* **47** (287), 375–384.
- Rechtsman, Mikael, Alexander Szameit, Felix Dreisow, Matthias Heinrich, Robert Keil, Stefan Nolte, and Mordechai Segev (2011), “Amorphous photonic lattices: band gaps, effective mass, and suppressed transport,” *Physical Review Letters* **106** (19), 193904.
- Rechtsman, Mikael C, Julia M Zeuner, Yonatan Plotnik, Yaakov Lumer, Daniel Podolsky, Felix Dreisow, Stefan Nolte, Mordechai Segev, and Alexander Szameit (2013), “Photonic floquet topological insulators,” *Nature* **496** (7444), 196–200.
- Redding, Brandon, Seng Fatt Liew, Raktim Sarma, and Hui Cao (2013), “Compact spectrometer based on a disordered photonic chip,” *Nature Photonics* **7** (9), 746.
- Rengarajan, Rajesh, Daniel Mittleman, Christopher Rich, and Vicki Colvin (2005), “Effect of disorder on the optical properties of colloidal crystals,” *Physical Review E* **71** (1), 016615.
- Renner, Michael, and Georg Von Freymann (2015), “Spatial correlations and optical properties in three-dimensional deterministic aperiodic structures,” *Scientific Reports* **5**, 13129.
- Reufer, Mathias, Luis Fernando Rojas-Ochoa, Stefanie Eiden, Juan José Sáenz, and Frank Scheffold (2007), “Transport of light in amorphous photonic materials,” *Applied Physics Letters* **91** (17), 171904.
- Riboli, F, P Barthelemy, S Vignolini, F Intonti, A De Rossi, S Combrie, and DS Wiersma (2011), “Anderson localization of near-visible light in two dimensions,” *Optics Letters* **36** (2), 127–129.
- Riboli, F, F Uccheddu, G Monaco, N Caselli, F Intonti, M Guirlioli, and SE Skipetrov (2017), “Tailoring correlations of the local density of states in disordered photonic materials,” *Physical Review Letters* **119** (4), 043902.
- Riboli, Francesco, Niccolò Caselli, Silvia Vignolini, Francesca Intonti, Kevin Vynck, Pierre Barthelemy, Annamaria Gerardino, Laurent Balet, Lianhe H Li, Andrea Fiore, *et al.* (2014), “Engineering of light confinement in strongly scattering disordered media,” *Nature materials* **13** (7), 720.
- Ricouvier, Joshua, Romain Pierrat, Rémi Carminati, Patrick Tabeling, and Pavel Yazhgur (2017), “Optimizing hyperuniformity in self-assembled bidisperse emulsions,” *Physical Review Letters* **119** (20), 208001.
- Ricouvier, Joshua, Patrick Tabeling, and Pavel Yazhgur (2019), “Foam as a self-assembling amorphous photonic band gap material,” *Proceedings of the National Academy of Sciences* **116** (19), 9202–9207.
- Rojas-Ochoa, Luis Fernando, JM Mendez-Alcaraz, JJ Sáenz, Peter Schurtenberger, and Frank Scheffold (2004), “Photonic properties of strongly correlated colloidal liquids,” *Physical Review Letters* **93** (7), 073903.
- van Rossum, MCW, and Th M Nieuwenhuizen (1999), “Multiple scattering of classical waves: microscopy, mesoscopy, and diffusion,” *Reviews of Modern Physics* **71** (1), 313.

- Rothmund, Paul WK (2006), “Folding dna to create nanoscale shapes and patterns,” *Nature* **440** (7082), 297.
- Rothemberger, Guido, Pascal Comte, and Michael Grätzel (1999), “A contribution to the optical design of dye-sensitized nanocrystalline solar cells,” *Solar Energy Materials and Solar Cells* **58** (3), 321–336.
- Rotter, Stefan, and Sylvain Gigan (2017), “Light fields in complex media: Mesoscopic scattering meets wave control,” *Reviews of Modern Physics* **89** (1), 015005.
- Ruppin, R (2000), “Evaluation of extended maxwell-garnett theories,” *Optics Communications* **182** (4-6), 273–279.
- Rustomji, Kaizad, Marc Dubois, Pierre Jomin, Stefan Enoch, Jérôme Wenger, C Martijn de Sterke, and Redha Abdeddaim (2021), “Complete electromagnetic dyadic green function characterization in a complex environment—resonant dipole-dipole interaction and cooperative effects,” *Physical Review X* **11** (2), 021004.
- Rytov, S M, Y. A. Kravtsov, and V. I. Tatarskii (1989), *Principles of Statistical Radiophysics*, Vol. 4 (Springer-Verlag, Berlin).
- Ryzhik, L, G. Papanicolaou, and J. B. Keller (1996), “Transport equations for elastic and other waves in random media,” *Wave Motion* **24**, 327.
- Ryzhov, Yu A, and VV Tamoikin (1970), “Radiation and propagation of electromagnetic waves in randomly inhomogeneous media,” *Radiophysics and Quantum Electronics* **13** (3), 273–300.
- Ryzhov, Yu A, VV Tamoikin, and VI Tatarskii (1965), “Spatial dispersion of inhomogeneous media,” *Soviet Phys. JETP* **21** (2), 433–438.
- Saito, Akira, Masaru Yonezawa, Junichi Murase, Saulius Juodkazis, Vygantas Mizeikis, Megumi Akai-Kasaya, and Yuji Kuwahara (2011), “Numerical analysis on the optical role of nano-randomness on the morpho butterfly’s scale,” *Journal of Nanoscience and Nanotechnology* **11** (4), 2785–2792.
- Salameh, Chrystelle, Flore Salviat, Elora Bessot, Miléna Lama, Jean-Marie Chassot, Elodie Mouloungui, Yan Wang, Marc Robin, Arnaud Bardouil, Mohamed Selmane, *et al.* (2020), “Origin of transparency in scattering biomimetic collagen materials,” *Proceedings of the National Academy of Sciences* **117** (22), 11947–11953.
- Salpeter, Edwin E, and Hans Albrecht Bethe (1951), “A relativistic equation for bound-state problems,” *Physical Review* **84** (6), 1232.
- Salvalaglio, Marco, Mohammed Bouabdellaoui, Monica Bolani, Abdennacer Benali, Luc Favre, Jean-Benoit Claude, Jerome Wenger, Pietro de Anna, Francesca Intonti, Axel Voigt, *et al.* (2020), “Hyperuniform monocrystalline structures by spinodal solid-state dewetting,” *Physical Review Letters* **125** (12), 126101.
- Salvarezza, RC, L Vázquez, H Miguez, R Mayoral, C López, and F Meseguer (1996), “Edward-wilkinson behavior of crystal surfaces grown by sedimentation of si o 2 nanospheres,” *Physical Review Letters* **77** (22), 4572.
- Sanders, Daniel P (2010), “Advances in patterning materials for 193 nm immersion lithography,” *Chemical Reviews* **110** (1), 321–360.
- Sapienza, R, P Bondareff, R Pierrat, B Habert, R Carminati, and NF Van Hulst (2011), “Long-tail statistics of the purcell factor in disordered media driven by near-field interactions,” *Physical Review Letters* **106** (16), 163902.
- Sapienza, R, PD García, J Bertolotti, MD Martin, A Blanco, L Vina, C López, and DS Wiersma (2007), “Observation of resonant behavior in the energy velocity of diffused light,” *Physical Review Letters* **99** (23), 233902.
- Sapienza, Riccardo (2019), “Determining random lasing action,” *Nature Reviews Physics* **1** (11), 690–695.
- Saranathan, Vinodkumar, Jason D Forster, Heeso Noh, Seng-Fatt Liew, Simon GJ Mochrie, Hui Cao, Eric R Dufresne, and Richard O Prum (2012), “Structure and optical function of amorphous photonic nanostructures from avian feather barbs: a comparative small angle x-ray scattering (saxs) analysis of 230 bird species,” *Journal of The Royal Society Interface* **9** (75), 2563–2580.
- Saulnier, PM, MP Zinkin, and GH Watson (1990), “Scatterer correlation effects on photon transport in dense random media,” *Physical Review B* **42** (4), 2621.
- Sauvan, Christophe, Jean-Paul Hugonin, Rémi Carminati, and Philippe Lalanne (2014), “Modal representation of spatial coherence in dissipative and resonant photonic systems,” *Physical Review A* **89** (4), 043825.
- Sauvan, Christophe, Jean-Paul Hugonin, IS Maksymov, and Philippe Lalanne (2013), “Theory of the spontaneous optical emission of nanosize photonic and plasmon resonators,” *Physical Review Letters* **110** (23), 237401.
- Savo, Romolo, Matteo Burrelli, Tomas Svensson, Kevin Vynck, and Diederik S Wiersma (2014), “Walk dimension for light in complex disordered media,” *Physical Review A* **90** (2), 023839.
- Savo, Romolo, Romain Pierrat, Ulysse Najar, Rémi Carminati, Stefan Rotter, and Sylvain Gigan (2017), “Observation of mean path length invariance in light-scattering media,” *Science* **358** (6364), 765–768.
- Scheffold, Frank, Ralf Lenke, Ralf Tweer, and Georg Maret (1999), “Localization or classical diffusion of light?” *Nature* **398** (6724), 206.
- Scheffold, Frank, and Georg Maret (1998), “Universal conductance fluctuations of light,” *Physical Review Letters* **81** (26), 5800.
- Scheffold, Frank, and TG Mason (2009), “Scattering from highly packed disordered colloids,” *Journal of Physics: Condensed Matter* **21** (33), 332102.
- Scheffold, Frank, and Diederik Wiersma (2013), “Inelastic scattering puts in question recent claims of anderson localization of light,” *Nature Photonics* **7** (12), 934–934.
- Schertel, Lukas, Gea T. van de Kerkhof, Gianni Jacucci, Laura Catón, Yu Ogawa, Bodo D. Wilts, Colin J. Ingham, Silvia Vignolini, and Villads E. Johansen (2020), “Complex photonic response reveals three-dimensional self-organization of structural coloured bacterial colonies,” *Journal of The Royal Society Interface* **17** (166), 20200196.
- Schertel, Lukas, Lukas Siedentop, Janne-Mieke Meijer, Peter Keim, Christof M Aegerter, Geoffroy J Aubry, and Georg Maret (2019a), “The structural colors of photonic glasses,” *Advanced Optical Materials*, 1900442.
- Schertel, Lukas, Ilona Wimmer, Patricia Besirski, Christof M Aegerter, Georg Maret, Sebastian Polarz, and Geoffroy J Aubry (2019b), “Tunable high-index photonic glasses,” *Physical Review Materials* **3** (1), 015203.
- Schöps, Oliver, Ulrike Woggon, Rajesh V Nair, *et al.* (2018), “Inhibited spontaneous emission using gaplike resonance in disordered photonic structures,” *Physical Review A* **98** (4), 043835.
- Schröder-Turk, Gerd E, S Wickham, Holger Averdunk, Frank Brink, JD Fitz Gerald, L Poladian, MCJ Large, and ST Hyde (2011), “The chiral structure of porous chitin within the wing-scales of *callophrys rubi*,” *Journal of Struc-*

- tural Biology **174** (2), 290–295.
- Schwartz, Tal, Guy Bartal, Shmuel Fishman, and Mordechai Segev (2007), “Transport and anderson localization in disordered two-dimensional photonic lattices,” *Nature* **446** (7131), 52–55.
- Seago, Ainsley E, Parrish Brady, Jean-Pol Vigneron, and Tom D Schultz (2008), “Gold bugs and beyond: a review of iridescence and structural colour mechanisms in beetles (coleoptera),” *Journal of the Royal Society Interface* **6** (suppl.2), S165–S184.
- Seal, Katayani, AK Sarychev, H Noh, DA Genov, Alexey Yamilov, VM Shalaev, ZC Ying, and Hui Cao (2005), “Near-field intensity correlations in semicontinuous metal-dielectric films,” *Physical Review Letters* **94** (22), 226101.
- Segev, Mordechai, Yaron Silberberg, and Demetrios N Christodoulides (2013), “Anderson localization of light,” *Nature Photonics* **7** (3), 197–204.
- Sellers, Steven R, Weining Man, Shervin Sahba, and Marian Florescu (2017), “Local self-uniformity in photonic networks,” *Nature Communications* **8**, 14439.
- Setälä, Tero, Kasimir Blomstedt, Matti Kaivola, and Ari T Friberg (2003), “Universality of electromagnetic-field correlations within homogeneous and isotropic sources,” *Physical Review E* **67** (2), 026613.
- Shalaev, Vladimir M (2002), *Optical properties of nanostructured random media*, Vol. 82 (Springer Science & Business Media).
- Shalaev, Vladimir M (2007), *Nonlinear optics of random media: fractal composites and metal-dielectric films*, Vol. 158 (Springer).
- Shang, Guoliang, Lukas Maiwald, Hagen Renner, Dirk Jalas, Maksym Dosta, Stefan Heinrich, Alexander Petrov, and Manfred Eich (2018), “Photonic glass for high contrast structural color,” *Scientific Reports* **8** (1), 1–9.
- Shapiro, B (1986), “Large intensity fluctuations for wave propagation in random media,” *Physical Review Letters* **57** (17), 2168.
- Shapiro, B (1999), “New type of intensity correlation in random media,” *Physical Review Letters* **83** (23), 4733.
- Sheng, Ping (2006), *Introduction to wave scattering, localization and mesoscopic phenomena*, Vol. 88 (Springer Science & Business Media).
- Sheremet, A, R Pierrat, and R Carminati (2020), “Absorption of scalar waves in correlated disordered media and its maximization using stealth hyperuniformity,” *Physical Review A* **101** (5), 053829.
- Shi, Lei, Yafeng Zhang, Biqin Dong, Tianrong Zhan, Xiaohan Liu, and Jian Zi (2013a), “Amorphous photonic crystals with only short-range order,” *Advanced Materials* **25** (37), 5314–5320.
- Shi, Lei, Yafeng Zhang, Biqin Dong, Tianrong Zhan, Xiaohan Liu, and Jian Zi (2013b), “Amorphous photonic crystals with only short-range order,” *Advanced Materials* **25** (37), 5314–5320.
- Siddique, Radwanul Hasan, Guillaume Gomard, and Hendrik Hölscher (2015), “The role of random nanostructures for the omnidirectional anti-reflection properties of the glasswing butterfly,” *Nature Communications* **6** (1), 1–8.
- Sigalas, MM, CM Soukoulis, C-T Chan, and D Turner (1996), “Localization of electromagnetic waves in two-dimensional disordered systems,” *Physical Review B* **53** (13), 8340.
- Skipetrov, SE, and John H Page (2016), “Red light for anderson localization,” *New Journal of Physics* **18** (2), 021001.
- Skipetrov, SE, and BA Van Tiggelen (2006), “Dynamics of anderson localization in open 3d media,” *Physical Review Letters* **96** (4), 043902.
- Skipetrov, Sergey E, and Igor M Sokolov (2014), “Absence of anderson localization of light in a random ensemble of point scatterers,” *Physical Review Letters* **112** (2), 023905.
- Skoge, Monica, Aleksandar Donev, Frank H. Stillinger, and Salvatore Torquato (2006), “Packing hyperspheres in high-dimensional euclidean spaces,” *Physical Review E* **74**, 041127.
- Smoluchowski, M v (1908), “Molekular-kinetische theorie der opaleszenz von gasen im kritischen zustande, sowie einiger verwandter erscheinungen,” *Annalen der Physik* **330** (2), 205–226.
- van Soest, Gijs, and Ad Lagendijk (2002), “ β factor in a random laser,” *Physical Review E* **65** (4), 047601.
- Solomon, TH, Eric R Weeks, and Harry L Swinney (1993), “Observation of anomalous diffusion and lévy flights in a two-dimensional rotating flow,” *Physical Review Letters* **71** (24), 3975.
- Soneira, Raymond M, and PJE Peebles (1977), “Is there evidence for a spatially homogeneous population of field galaxies,” *The Astrophysical Journal* **211**, 1–15.
- Song, Chaoming, Ping Wang, and Hernán A. Makse (2008), “A phase diagram for jammed matter,” *Nature* **453**, 629.
- Song, Dong-Po, Gianni Jacucci, Feyza Dundar, Aditi Naik, Hua-Feng Fei, Silvia Vignolini, and James J Watkins (2018), “Photonic resins: designing optical appearance via block copolymer self-assembly,” *Macromolecules* **51** (6), 2395–2400.
- Song, Dong-Po, Tianheng H Zhao, Giulia Guidetti, Silvia Vignolini, and Richard M Parker (2019), “Hierarchical photonic pigments via the confined self-assembly of bottlebrush block copolymers,” *ACS Nano* **13** (2), 1764–1771.
- Soukoulis, CM, S Datta, and EN Economou (1994), “Propagation of classical waves in random media,” *Physical Review B* **49** (6), 3800.
- Soukoulis, Costas M (2012), *Photonic crystals and light localization in the 21st century*, Vol. 563 (Springer Science & Business Media).
- Soukoulis, Costas M, and Martin Wegener (2011), “Past achievements and future challenges in the development of three-dimensional photonic metamaterials,” *Nature Photonics* **5** (9), 523.
- de Sousa, N, JJ Sáenz, Antonio García-Martín, Luis S Froufe-Pérez, and MI Marqués (2014), “Effect of long-range spatial correlations on the lifetime statistics of an emitter in a two-dimensional disordered lattice,” *Physical Review A* **89** (6), 063830.
- de Sousa, N, Juan José Sáenz, Frank Scheffold, A García-Martín, and Luis S Froufe-Pérez (2016), “Fluctuations of the electromagnetic local density of states as a probe for structural phase switching,” *Physical Review A* **94** (4), 043832.
- Sperling, Tilo, Wolfgang Buehrer, Christof M Aegerter, and Georg Maret (2013), “Direct determination of the transition to localization of light in three dimensions,” *Nature Photonics* **7** (1), 48–52.
- Spry, Robert J, and David J Kosan (1986), “Theoretical analysis of the crystalline colloidal array filter,” *Applied Spectroscopy* **40** (6), 782–784.
- Staudé, Isabelle, M Thiel, S Essig, C Wolff, K Busch, G Von Freymann, and M Wegener (2010), “Fabrication and characterization of silicon woodpile photonic crystals with a complete bandgap at telecom wavelengths,” *Optics*

- Letters **35** (7), 1094–1096.
- Stavenga, Doekele G, Jan Tinbergen, Hein L. Leertouwer, and Bodo D. Wilts (2011), “Kingfisher feathers – colouration by pigments, spongy nanostructures and thin films,” *Journal of Experimental Biology* **214** (23), 3960–3967.
- Stefik, Morgan, Stefan Guldin, Silvia Vignolini, Ulrich Wiesner, and Ullrich Steiner (2015), “Block copolymer self-assembly for nanophotonics,” *Chemical Society Reviews* **44** (15), 5076–5091.
- Stillinger, Frank H, and Thomas A Weber (1985), “Computer simulation of local order in condensed phases of silicon,” *Physical Review B* **31** (8), 5262.
- Stover, John C (1995), *Optical scattering: measurement and analysis*, Vol. 2 (SPIE optical engineering press Bellingham).
- Sullivan, Donald E, and JM Deutch (1976), “Local field models for light scattering and the dielectric constant of nonpolar fluids,” *The Journal of Chemical Physics* **64** (9), 3870–3878.
- Sun, Hong-Bo, Shigeki Matsuo, and Hiroaki Misawa (1999), “Three-dimensional photonic crystal structures achieved with two-photon-absorption photopolymerization of resin,” *Applied Physics Letters* **74** (6), 786–788.
- Svensson, Tomas, Kevin Vynck, Erik Adolfsson, Andrea Farina, Antonio Pifferi, and Diederik S Wiersma (2014), “Light diffusion in quenched disorder: Role of step correlations,” *Physical Review E* **89** (2), 022141.
- Svensson, Tomas, Kevin Vynck, Marco Grisi, Romolo Savo, Matteo Burrelli, and Diederik S Wiersma (2013), “Holey random walks: Optics of heterogeneous turbid composites,” *Physical Review E* **87** (2), 022120.
- Ta, Van Duong, Soraya Caixeiro, Dhruv Saxena, and Riccardo Sapienza (2021), “Biocompatible polymer and protein microspheres with inverse photonic glass structure for random micro-biolasers,” *Advanced Photonics Research*, 2100036.
- Taflove, Allen, and Susan C Hagness (2005), *Computational electrodynamics: the finite-difference time-domain method* (Artech house).
- Takeoka, Yukikazu (2012), “Angle-independent structural coloured amorphous arrays,” *Journal of Materials Chemistry* **22** (44), 23299–23309.
- Tarasov, Vasily E (2015), “Fractal electrodynamics via non-integer dimensional space approach,” *Physics Letters A* **379** (36), 2055–2061.
- Tétreault, Nicolas, Georg von Freymann, Markus Deubel, Martin Hermatschweiler, Fabian Pérez-Willard, Sajeev John, Martin Wegener, and Geoffrey A Ozin (2006), “New route to three-dimensional photonic bandgap materials: silicon double inversion of polymer templates,” *Advanced Materials* **18** (4), 457–460.
- Thorpe, MF (1973), “A note on band gaps in amorphous semiconductors (relation to structure),” *Journal of Physics C: Solid State Physics* **6** (4), L75.
- van Tiggelen, BA, and SE Skipetrov (2020), “Longitudinal modes in diffusion and localization of light,” *arXiv preprint arXiv:2012.11210*.
- van Tiggelen, Bart A, and Roger Maynard (1998), “Reciprocity and coherent backscattering of light,” in *Wave Propagation in Complex Media* (Springer) pp. 247–271.
- Toninelli, Costanza, Evangellos Vekris, Geoffrey A Ozin, Sajeev John, and Diederik S Wiersma (2008), “Exceptional reduction of the diffusion constant in partially disordered photonic crystals,” *Physical Review Letters* **101** (12), 123901.
- Torquato, Salvatore (2013), *Random heterogeneous materials: microstructure and macroscopic properties*, Vol. 16 (Springer Science & Business Media).
- Torquato, Salvatore (2018), “Hyperuniform states of matter,” *Physics Reports* **745**, 1–95.
- Torquato, Salvatore, and Jaeuk Kim (2021), “Nonlocal effective electromagnetic wave characteristics of composite media: beyond the quasistatic regime,” *Physical Review X* **11** (2), 021002.
- Torquato, Salvatore, and Frank H Stillinger (2003), “Local density fluctuations, hyperuniformity, and order metrics,” *Physical Review E* **68** (4), 041113.
- Torquato, Salvatore, Thomas M Truskett, and Pablo G Debenedetti (2000), “Is random close packing of spheres well defined?” *Physical Review Letters* **84** (10), 2064.
- Trompoukis, Christos, Inès Massiot, Valérie Depauw, Ounsi El Daif, Kidong Lee, Alexandre Dmitriev, Ivan Gordon, Robert Mertens, and Jef Poortmans (2016), “Disordered nanostructures by hole-mask colloidal lithography for advanced light trapping in silicon solar cells,” *Optics Express* **24** (2), A191–A201.
- Tsang, L, and J. A. Kong (2001), *Scattering of Electromagnetic Waves - Advanced Topics* (John Wiley and Sons, New-York).
- Tsang, L, and JA Kong (1980), “Multiple scattering of electromagnetic waves by random distributions of discrete scatterers with coherent potential and quantum mechanical formalism,” *Journal of Applied Physics* **51** (7), 3465–3485.
- Tsang, L, and JA Kong (1981), “Scattering of electromagnetic waves from random media with strong permittivity fluctuations,” *Radio Science* **16** (3), 303–320.
- Tsang, L, and JA Kong (1982), “Effective propagation constants for coherent electromagnetic wave propagation in media embedded with dielectric scatterers,” *Journal of Applied Physics* **53** (11), 7162–7173.
- Tsang, Leung, Chi-Te Chen, Alfred TC Chang, Jianjun Guo, and Kung-Hau Ding (2000), “Dense media radiative transfer theory based on quasicrystalline approximation with applications to passive microwave remote sensing of snow,” *Radio Science* **35** (3), 731–749.
- Tsang, Leung, and Akira Ishimaru (1984), “Backscattering enhancement of random discrete scatterers,” *JOSA A* **1** (8), 836–839.
- Tsang, Leung, Jin Au Kong, and Kung-Hau Ding (2004), *Scattering of electromagnetic waves: theories and applications*, Vol. 27 (John Wiley & Sons).
- Türeci, Hakan E, Li Ge, Stefan Rotter, and A Douglas Stone (2008), “Strong interactions in multimode random lasers,” *Science* **320** (5876), 643–646.
- Twersky, Victor (1964), “On propagation in random media of discrete scatterers,” in *Proc. Symp. Appl. Math.*, Vol. 16, pp. 84–116.
- Twersky, Victor (1975), “Transparency of pair-correlated, random distributions of small scatterers, with applications to the cornea,” *JOSA* **65** (5), 524–530.
- Uche, Obioma U, Frank H Stillinger, and Salvatore Torquato (2004), “Constraints on collective density variables: Two dimensions,” *Physical Review E* **70** (4), 046122.
- Uppu, Ravitej, and Sushil Mujumdar (2015), “Exponentially tempered lévy sums in random lasers,” *Physical Review Letters* **114** (18), 183903.
- Utel, Francesco, Lorenzo Cortese, Diederik S. Wiersma, and Lorenzo Pattelli (2019), “Optimized white reflectance in

- photonic-network structures,” *Advanced Optical Materials* **7** (18), 1900043.
- Van Albada, Meint P, and Ad Lagendijk (1985), “Observation of weak localization of light in a random medium,” *Physical Review Letters* **55** (24), 2692.
- Van Bladel, Jean, and J Van Bladel (1991), *Singular electromagnetic fields and sources* (Clarendon Press Oxford).
- Van Kranendonk, J, and JE Sipe (1977), “V foundations of the macroscopic electromagnetic theory of dielectric media,” in *Progress in Optics*, Vol. 15 (Elsevier) pp. 245–350.
- Van Tiggelen, BA, A Lagendijk, and DS Wiersma (2000), “Reflection and transmission of waves near the localization threshold,” *Physical Review Letters* **84** (19), 4333.
- Vignolini, Silvia, Thomas Gregory, Mathias Kolle, Alfie Lethbridge, Edwige Moyroud, Ullrich Steiner, Beverley J Glover, Peter Vukusic, and Paula J Rudall (2016), “Structural colour from helicoidal cell-wall architecture in fruits of *margaritaria nobilis*,” *Journal of The Royal Society Interface* **13** (124), 20160645.
- Vignolini, Silvia, Paula J Rudall, Alice V Rowland, Alison Reed, Edwige Moyroud, Robert B Faden, Jeremy J Baumberg, Beverley J Glover, and Ullrich Steiner (2012), “Pointillist structural color in pollia fruit,” *Proceedings of the National Academy of Sciences* **109** (39), 15712–15715.
- Vlasov, Yu A, VN Astratov, AV Baryshev, AA Kaplyanskii, OZ Karimov, and MF Limonov (2000), “Manifestation of intrinsic defects in optical properties of self-organized opal photonic crystals,” *Physical Review E* **61** (5), 5784.
- Vlasov, Yu A, MA Kaliteevski, and VV Nikolaev (1999), “Different regimes of light localization in a disordered photonic crystal,” *Physical Review B* **60** (3), 1555.
- Vogel, Nicolas, Stefanie Utech, Grant T England, Tanya Shirman, Katherine R Phillips, Natalie Koay, Ian B Burgess, Mathias Kolle, David A Weitz, and Joanna Aizenberg (2015), “Color from hierarchy: Diverse optical properties of micron-sized spherical colloidal assemblies,” *Proceedings of the National Academy of Sciences* **112** (35), 10845–10850.
- Vollhardt, Dieter, and P Wölffe (1982), “Scaling equations from a self-consistent theory of anderson localization,” *Physical Review Letters* **48** (10), 699.
- Vollhardt, Dieter, and Peter Wölffe (1980), “Diagrammatic, self-consistent treatment of the anderson localization problem in $d \leq 2$ dimensions,” *Physical Review B* **22** (10), 4666.
- Vukusic, Pete, Benny Hallam, and Joe Noyes (2007), “Brilliant whiteness in ultrathin beetle scales,” *Science* **315** (5810), 348–348.
- Vynck, Kevin, Matteo Burrelli, Francesco Riboli, and Diederik S Wiersma (2012), “Photon management in two-dimensional disordered media,” *Nature materials* **11** (12), 1017.
- Vynck, Kevin, Didier Felbacq, Emmanuel Centeno, AI Cuabuz, David Cassagne, and Brahim Guizal (2009), “All-dielectric rod-type metamaterials at optical frequencies,” *Physical Review Letters* **102** (13), 133901.
- Vynck, Kevin, Romain Pierrat, and Rémi Carminati (2014), “Polarization and spatial coherence of electromagnetic waves in uncorrelated disordered media,” *Physical Review A* **89** (1), 013842.
- Vynck, Kevin, Romain Pierrat, and Rémi Carminati (2016), “Multiple scattering of polarized light in disordered media exhibiting short-range structural correlations,” *Physical Review A* **94** (3), 033851.
- Wales, David J, and R Stephen Berry (1994), “Coexistence in finite systems,” *Physical Review Letters* **73** (21), 2875.
- Wan, Wenjie, Yidong Chong, Li Ge, Heeso Noh, A Douglas Stone, and Hui Cao (2011), “Time-reversed lasing and interferometric control of absorption,” *Science* **331** (6019), 889–892.
- Wang, BX, and CY Zhao (2018), “Achieving a strongly negative scattering asymmetry factor in random media composed of dual-dipolar particles,” *Physical Review A* **97** (2), 023836.
- Wang, BX, and CY Zhao (2020), “The dependent scattering effect on radiative properties of micro/nanoscale discrete disordered media,” *Annual Rev. Heat Transfer* **23**, 231–353.
- Wang, Jian-Sheng (2000), “Series expansion and computer simulation studies of random sequential adsorption,” *Colloids and Surfaces A: Physicochemical and Engineering Aspects* **165** (1), 325 – 343.
- Wang, Lihong, and Steven L Jacques (1992), “Monte carlo modeling of light transport in multi-layered tissues in standard c,” *The University of Texas, MD Anderson Cancer Center, Houston*, 4–11.
- Wang, Zhen-song, and Bao-wei Lu (1994), “The scattering of electromagnetic waves in fractal media,” *Waves in Random Media* **4**, 97–103.
- Watson, David F (1981), “Computing the n-dimensional delaunay tessellation with application to voronoi polytopes,” *The Computer Journal* **24** (2), 167–172.
- Weaire, D (1971), “Existence of a gap in the electronic density of states of a tetrahedrally bonded solid of arbitrary structure,” *Physical Review Letters* **26** (25), 1541.
- Weijs, Joost H, Raphaël Jeanneret, Rémi Dreyfus, and Denis Bartolo (2015), “Emergent hyperuniformity in periodically driven emulsions,” *Physical Review Letters* **115** (10), 108301.
- Weimann, Steffen, Manuel Kremer, Yonatan Plotnik, Yaakov Lumer, Stefan Nolte, Konstantinos G Makris, Mordechai Segev, Mikael C Rechtsman, and Alexander Szameit (2017), “Topologically protected bound states in photonic parity–time-symmetric crystals,” *Nature Materials* **16** (4), 433–438.
- Wertheim, MS (1963), “Exact solution of the percus-yevick integral equation for hard spheres,” *Physical Review Letters* **10** (8), 321.
- Wertheim, MS (1973), “Dielectric constant of non-polar fluids,” *Molecular Physics* **25** (1), 211–223.
- Whitney, Heather M, Mathias Kolle, Piers Andrew, Lars Chittka, Ullrich Steiner, and Beverley J Glover (2009), “Floral iridescence, produced by diffractive optics, acts as a cue for animal pollinators,” *Science* **323** (5910), 130–133.
- Widom, B (1966), “Random sequential addition of hard spheres to a volume,” *The Journal of Chemical Physics* **44** (10), 3888–3894.
- Wiersma, Diederik S (2008), “The physics and applications of random lasers,” *Nature Physics* **4** (5), 359.
- Wiersma, Diederik S (2013), “Disordered photonics,” *Nature Photonics* **7** (3), 188–196.
- Wiersma, Diederik S, Paolo Bartolini, Ad Lagendijk, and Roberto Righini (1997), “Localization of light in a disordered medium,” *Nature* **390** (6661), 671.
- Wiersma, Diederik S, and Ad Lagendijk (1996), “Light diffusion with gain and random lasers,” *Physical Review E* **54** (4), 4256.
- Wilts, Bodo D, Peta L Clode, Nipam H Patel, and Gerd E Schröder-Turk (2019), “Nature’s functional nanomaterials: Growth or self-assembly?” *MRS Bulletin* **44** (2), 106–112.

- Wilts, Bodo D, Kristel Michielsen, Hans De Raedt, and Doekele G Stavenga (2011), “Iridescence and spectral filtering of the gyroid-type photonic crystals in parides sesostris wing scales,” *Interface Focus* **2** (5), 681–687.
- Wilts, Bodo D, Kristel Michielsen, Hans De Raedt, and Doekele G Stavenga (2014), “Sparkling feather reflections of a bird-of-paradise explained by finite-difference time-domain modeling,” *Proceedings of the National Academy of Sciences* **111** (12), 4363–4368.
- Wilts, Bodo D, Kristel Michielsen, Jeroen Kuipers, Hans De Raedt, and Doekele G Stavenga (2012), “Brilliant camouflage: photonic crystals in the diamond weevil, *entimus imperialis*,” *Proceedings of the Royal Society B: Biological Sciences* **279** (1738), 2524–2530.
- Wilts, Bodo D, Xiaoyuan Sheng, Mirko Holler, Ana Diaz, Manuel Guizar-Sicairos, Jörg Raabe, Robert Hoppe, Shu-Hao Liu, Richard Langford, Olimpia D Onelli, *et al.* (2018a), “Evolutionary-optimized photonic network structure in white beetle wing scales,” *Advanced Materials* **30** (19), 1702057.
- Wilts, Bodo D, Xiaoyuan Sheng, Mirko Holler, Ana Diaz, Manuel Guizar-Sicairos, Jörg Raabe, Robert Hoppe, Shu-Hao Liu, Richard Langford, Olimpia D. Onelli, Duyu Chen, Salvatore Torquato, Ullrich Steiner, Christian G. Schroer, Silvia Vignolini, and Alessandro Sepe (2018b), “Evolutionary-optimized photonic network structure in white beetle wing scales,” *Advanced Materials* **30** (19), 1702057.
- Wilts, Bodo D, Benjamin Apeleo Zubiri, Michael A Klatt, Benjamin Butz, Michael G Fischer, Stephen T Kelly, Erdmann Spiecker, Ullrich Steiner, and Gerd E Schröder-Turk (2017), “Butterfly gyroid nanostructures as a time-frozen glimpse of intracellular membrane development,” *Science Advances* **3** (4), e1603119.
- Wolf, Pierre-Etienne, and Georg Maret (1985), “Weak localization and coherent backscattering of photons in disordered media,” *Physical Review Letters* **55** (24), 2696.
- Wooten, F, K Winer, and D Weaire (1985), “Computer generation of structural models of amorphous si and ge,” *Physical Review Letters* **54** (13), 1392.
- Wriedt, Thomas (1999), *Generalized multipole techniques for electromagnetic and light scattering* (Elsevier).
- Wright, AC, and MF Thorpe (2013), “Eighty years of random networks,” *Physica Status solidi (b)* **250** (5), 931–936.
- Yablonovitch, Eli (1982), “Statistical ray optics,” *JOSA* **72** (7), 899–907.
- Yablonovitch, Eli (1987), “Inhibited spontaneous emission in solid-state physics and electronics,” *Physical Review Letters* **58** (20), 2059.
- Yaghjian, Arthur D (1980), “Electric dyadic green’s functions in the source region,” *Proceedings of the IEEE* **68** (2), 248–263.
- Yamilov, Alexey G, Raktim Sarma, Brandon Redding, Ben Payne, Heeso Noh, and Hui Cao (2014), “Position-dependent diffusion of light in disordered waveguides,” *Physical Review Letters* **112** (2), 023904.
- Yan, Wei, Rémi Faggiani, and Philippe Lalanne (2018), “Rigorous modal analysis of plasmonic nanoresonators,” *Physical Review B* **97** (20), 205422.
- Yang, Jin-Kyu, Svetlana V Boriskina, Heeso Noh, Michael J Rooks, Glenn S Solomon, Luca Dal Negro, and Hui Cao (2010a), “Demonstration of laser action in a pseudorandom medium,” *Applied Physics Letters* **97** (22), 223101.
- Yang, Jin-Kyu, Heeso Noh, Seng Fatt Liew, Michael J Rooks, Glenn S Solomon, and Hui Cao (2011), “Lasing modes in polycrystalline and amorphous photonic structures,” *Physical Review A* **84** (3), 033820.
- Yang, Jin-Kyu, Carl Schreck, Heeso Noh, Seng-Fatt Liew, Mikhael I Guy, Corey S O’Hern, and Hui Cao (2010b), “Photonic-band-gap effects in two-dimensional polycrystalline and amorphous structures,” *Physical Review A* **82** (5), 053838.
- Yazhgur, Pavel, Geoffroy J Aubry, Luis S Froufe-Pérez, and Frank Scheffold (2021), “Light scattering from colloidal aggregates on a hierarchy of length scales,” *Optics Express* **29** (10), 14367–14383.
- Yeh, Pochi, *et al.* (1988), *Optical waves in layered media*, Vol. 95 (Wiley Online Library).
- Yi, Gi-Ra, Seog-Jin Jeon, Todd Thorsen, Vinodhan N Manoharan, Stephan R Quake, David J Pine, and Seung-Man Yang (2003), “Generation of uniform photonic balls by template-assisted colloidal crystallization,” *Synthetic Metals* **139** (3), 803–806.
- Yin, Haiwei, Biqin Dong, Xiaohan Liu, Tianrong Zhan, Lei Shi, Jian Zi, and Eli Yablonovitch (2012), “Amorphous diamond-structured photonic crystal in the feather barbs of the scarlet macaw,” *Proceedings of the National Academy of Sciences* **109** (27), 10798–10801.
- Yu, Sunkyu, Cheng-Wei Qiu, Yidong Chong, Salvatore Torquato, and Namkyoo Park (2020), “Engineered disorder in photonics,” *Nature Reviews Materials*, 1–18.
- Yu, Zongfu, Aaswath Raman, and Shanhui Fan (2010), “Fundamental limit of nanophotonic light trapping in solar cells,” *Proc. Natl. Acad. Sci. U.S.A.* **107** (41), 17491–17496.
- Yvon, Jacques (1937), *Recherches sur la théorie cinétique des liquides: fluctuations en densité et diffusion de la lumière* (Hermann et cie).
- Zaburdaev, V, S Denisov, and J Klafter (2015), “Lévy walks,” *Reviews of Modern Physics* **87** (2), 483.
- Zachary, Chase E, Yang Jiao, and Salvatore Torquato (2011), “Hyperuniform long-range correlations are a signature of disordered jammed hard-particle packings,” *Physical Review Letters* **106** (17), 178001.
- Zhang, Chi, Nicoletta Gnan, Thomas G Mason, Emanuela Zaccarelli, and Frank Scheffold (2016), “Dynamical and structural signatures of the glass transition in emulsions,” *Journal of Statistical Mechanics: Theory and Experiment* **2016** (9), 094003.
- Zhang, Fei, and Hao Yan (2017), “Dna self-assembly scaled up,”.
- Zhao, Tianheng H, Gianni Jacucci, Xi Chen, Dong-Po Song, Silvia Vignolini, and Richard M Parker (2020), “Angular-independent photonic pigments via the controlled micellization of amphiphilic bottlebrush block copolymers,” *Advanced Materials* **32** (47), 2002681.
- Zhu, Jixiang, Min Li, R Rogers, W Meyer, RH Ottewill, WB Russel, PM Chaikin, *et al.* (1997), “Crystallization of hard-sphere colloids in microgravity,” *Nature* **387** (6636), 883.
- Zito, Gianluigi, Giulia Rusciano, Giuseppe Pesce, Anna Malafronte, Rocco Di Girolamo, Giovanni Ausanio, Antonio Vecchione, and Antonio Sasso (2015), “Nanoscale engineering of two-dimensional disordered hyperuniform block-copolymer assemblies,” *Physical Review E* **92** (5), 050601.
- Zoorob, ME, MDB Charlton, GJ Parker, JJ Baumberg, and MC Netti (2000), “Complete photonic bandgaps in 12-fold symmetric quasicrystals,” *Nature* **404** (6779), 740.